

**ELECTROMYOGRAM INTERFERENCE REDUCTION IN
NEURAL SIGNAL RECORDING USING SIMPLE RC
COMPENSATION CIRCUITS**

Syeda Sabeeka Zehra

718747

A dissertation submitted in partial fulfilment of the
requirements for the degree of

Master of Philosophy

Supervisor: Prof. Andreas Demosthenous

April 2019



Department of Electronic and Electrical Engineering

University College London

Official Declaration

I, Syeda Sabeeka Zehra, confirm that the work presented in this dissertation is my own. References have been provided in the thesis, where information has been taken from other sources.

Abstract

Neuroprosthesis can partially restore lost motor functionalities of individuals such as bladder voiding using functional electrical stimulation (FES) techniques. FES involves applying pattern of electrical current pulses using implanted electrodes to trigger affected nerves that are damaged due to paralysis. A neural signal recorded using tripolar cuff electrodes is significantly contaminated due to the presence of EMG interference from the surrounding muscles. Conventional neural amplifiers are unable to remove such interferences and modifications to the design are required. The modification to the design of the Quasi-tripole (QT) amplifier is considered in this work to minimise the EMG interferences from neural signal recording. The analogy between this modified version of QT known as mQT and Wheatstone bridge claims to neutralise the EMG interference by adding compensation circuit to either end of the outer electrodes of the tripolar cuff and therefore balancing the bridge. In this work, we present simple 3 and 2 stage RC compensation circuits to minimise EMG interference in trying to balance the bridge in the neural frequency band of interest (500-10kHz). It is shown that simple RC compensation circuit in series reduces EMG interference only at the spot frequency rather than linearly in the entire frequency band of interest. However, two and three stages RC ladder compensation circuits mimicking electrode-electrolyte interface, can minimize the EMG interference linearly in the entire frequency band of interest, without requiring any readjustment to their components. The aim is to minimise EMG interference as close to null as possible. Invitro testing of about 20% imbalanced cuff electrode with proposed 3 and 2 stage RC ladder compensation circuits resulted in linear EMG interference reduction atleast by a factor of 6. On an average, this yielded an improvement of above 80% EMG minimisation, in contrast to above 90% observed in the optimisation results, when 1Ω transimpedance (EMG) was introduced into the setup. Further improvements to the setup and design can give more promising results in reliable neural signal recording for FES applications.

Table of Contents

ABSTRACT	II
TABLE OF CONTENTS	III
LIST OF FIGURES	VI
TABLE OF TABLES	VII
ACKNOWLEDGEMENTS	VIII
ABBREVIATIONS	X
CHAPTER ONE	1
1.1 INTRODUCTION	1
1.2 MOTIVATION	4
1.3 PROJECT AIMS	6
1.4 MAIN CONTRIBUTIONS.....	10
1.5 THESIS ORGANISATION	12
1.6 PUBLICATIONS.....	13
CHAPTER TWO	14
2.2 ANATOMY AND PHYSIOLOGY OF THE HUMAN SPINAL CORD	14
2.2.1 Basics of Anatomy	14
2.2.2 The Neuron Cell	15
2.2.3 The Action Potential	17
2.2.3.1 Natural and Artificial Nerve Stimuli	19
2.2.3.2 The propagation of nerve impulses	20
2.3 PATHOPHYSIOLOGY OF THE HUMAN SPINAL CORD INJURY	22
2.4 NEUROPROSTHESIS FOR SPINAL CORD INJURY TREATMENT	24
2.4.1 FUNCTIONAL ELECTRICAL STIMULATION	25
2.4.2 Neural Recording.....	27
2.4.2.1 Cuff Electrodes	29

Types of Cuff Electrodes.....	30
2.4.2.2 Imbalance	32
2.4.3 Amplifier configurations.....	33
2.4.3.1 The Quasi tripole (QT)	33
2.4.3.2 The True tripole (TT)	34
2.4.3.3 The Adaptive Tripole (AT)	35
2.4.3.4 Other methods and amplifier configuration.....	36
2.5 SPECIFICATIONS OF BIOELECTRIC POTENTIALS	37
2.6 ENG UNDERLYING RECORDING THEORY USING CUFF	38
2.7 EFFECT OF INTERFACE IMPEDANCE ON NEURAL SIGNAL RECORDING	40
2.7.1 Charge Transfer	41
2.7.1.1 The Double Layer	42
2.7.1.2 The Polarisation Impedance	43
2.7.1.2.1 The Constant Phase Element (CPE)	46
2.8 SUMMARY.....	47
CHAPTER THREE.....	48
THE NOVEL TECHNIQUE OF EMG REDUCTION FOR NEURAL SIGNAL RECORDING	48
3.1 INTRODUCTION	48
3.2 THE MODIFIED QT, MQT AND PASSIVE NEUTRALISATION	49
3.3 PRINCIPLE OF EMG REDUCTION USING SIMPLE RC COMPENSATION CIRCUITS AS Z_{TRIM}	51
3.4 EXPERIMENTAL SETUP AND METHOD.....	53
3.4.1 Electrodes Impedance Modelling	54
3.4.2 Interference Reduction Testing of Ztrim Compensation Circuits	57
3.5 EXPERIMENTAL RESULTS	62
3.5.1 Electrode impedance modelling of tripolar book electrode	62
3.5.2 Uncompensated Response of the Tripolar Book Electrode.....	64
3.5.3 Compensated Response of the Tripolar Book Electrode.....	65

3.5.3.1	RC as Ztrim.....	65
3.5.3.2	Simple 3-Stage RC Ladder Network as Compensation Circuit, Ztrim1.....	66
3.5.3.3	Simple 2-Stage RC Ladder Network as Compensation Circuit, Ztrim2.....	68
3.5.3.4	Performance Ratio, PR of Ztrim Compensation Circuits in dB.....	70
3.5.3.5	Sensitivity Analysis of R and C in the Compensation Circuit.....	72
3.5.4	Discussion of the Experimental Results.....	73
3.6	Possible Ways of Optimising Ztrim Component Parameters	76
3.6.1	Off- Chip Installation.....	76
3.6.2	Ztrim Impedance Scaling	77
3.7	NOISE DUE TO COMPENSATION CIRCUIT.....	80
3.8	SUMMARY.....	82
CHAPTER FOUR.....		83
CONCLUSION AND FUTURE WORK		83
4.1	SUMMARY.....	83
4.2	FUTURE WORK RECOMMENDATIONS.....	85
APPENDIX A		87
ZTRIM PARAMETERS DEDUCTION USING A MATHEMATICAL RELATION.....		87
INTRODUCTION.....		87
ANALYZATION OF BOOK ELECTRODE WITH ZTRIM CIRCUIT USING REPRESENTATIVE MODEL		88
	Regression analysis of the representative model RM	93
MATHEMATICAL RELATION BETWEEN CIRCUIT 1 AND CIRCUIT 2		97
DISCUSSION AND ANALYSIS		102
REFERENCES.....		109

List of Figures

1.1	Schematic diagram of the human spinal cord	2
1.2	Block diagram of conditional neural modulator	9
2.1	Typical structure of a neuron	16
2.2	Stages of an action potential in human spinal cord	18
2.3	Phases of action potential	21
2.4	Cyst formation after SCI	23
2.5	Flowchart of FES	24
2.6	The Cleveland FES Center's freehand system	26
2.7	Surface and Implanted electrodes	28
2.8	Cuff electrode implantation around the nerve of a rat	29
2.9	EMG and ENG potentials inside cuff	30
2.10	Types of cuff electrodes	31
2.11	Muscle activity produces differential-mode interference	32
2.12	The QT amplifier with tripolar cuff	34
2.13	The TT amplifier configuration	35
2.14	The AT amplifier configuration	36
2.15	EMG and ENG recorded signals	37
2.16	Action potential recording using cuff	40
2.17	Faradic and non-faradic charge transfer	41
2.18	The double layer capacitance	42
2.19	The Randles circuit model	44
2.20	The Cole circuit model	45
3.1	The electrodes of the QT amplifier seen as the Wheatstone Bridge	51
3.2	Phaser graphs for the bridge	52
3.3	Flowchart for performance evaluation of compensation circuits	54
3.4	Test setup for electrodes modelling	56
3.5	Tripolar cuff equivalent circuit model	58
3.6	Test setup for EMG minimisation	61
3.7	Modelling of electrode discs of tripolar cuff electrode model	63
3.8	EMG output from imbalanced cuff	64
3.9	Invitro and simulation results for RC Ztrim	66
3.10	EMG minimisation using 3 -stage RC Ztrim	67
3.11	EMG minimisation using 2-stage RC Ztrim	69
3.12	Comparison between simple Ztrim circuit.	70
3.13	Performance ratio of compensation circuits	71
3.14	Sensitivity analysis for compensation circuit	72
3.15	Capacitors scaling approach	78
3.16	Output comparison of scaled and unscaled compensation circuits	79
3.17	Noise response of a 3 stage RC compensation circuit	81

Table of Tables

Table 1 Circuit Parameters obtained from Impedance Modelling of Book Electrode..... 59

Table 2 Ztrim1 and Ztrim2 Circuit Parameters obtained from Optimization in Simulations 59

Acknowledgements

First, and foremost I would like to express my profound gratitude for Professor Andreas Demosthenous for his persistent assistance during my study, without whom it would not have been possible for me to submit my thesis.

Professor Andreas Demosthenous sincere and sustained support during the time of research motivated me enough to finally complete my work. I am thankful to him for always being available to assist and guide me whenever I needed him. His knowledgeable ideas always helped me in opening new doors for me in the research area and I have thankfully learnt a lot from him. Along, with providing me support in my research work, his emotional support is comparable to none, which served as a guiding light in the murky and zigzagged alleys of so many responsibilities and commitments in my personal life. His continuous motivation was my driving force and the vastness of his knowledge has always been an inspiration for me for aiming high enough to hit the mark. Having him as my mentor and supervisor for my study is not less than an endowment of God upon me. His empathy when I faced family problems not only helped me emotionally and morally but also motivated me to keep working for my study. I give all credit for the completion of my Mphil to Prof. Andreas, for his immense support and understanding during all this time. I can never thank him enough!

Dr. Clemens Eder for his insight and innovative ideas to begin my research work. I am sincerely thankful to him for guiding me and helping me during the first year of my study. The literature material he provided me helped me much in the area of my research and detailed discussions with him helped me a lot to learn from his valuable knowledge and experience.

I am thankful to my colleagues and friends at UCL for their support during the time of research. Specially, Dr. Majid Zamini for travelling abroad when I could not, to present my paper at the conference. My research colleagues to me are exactly what we regard as chip of the same block. They shared with me all the panic attacks, sleepless nights and stress induced restlessness. They were always there to count on. I thank all of them with all my heart.

Last but not the least comes the substantial support of my family. It being the building block of one's character and life plays a vital role in one's achievements and success. Although in the past few years, life has not been so kind to me but their countless prayers and support motivated me to continue my work. My husband for standing up for me when I lost the courage for my work completion in between. I thank all of them from the bottom of my heart.

Lastly, I hope that readers also find my work interesting as much as I found and it also helps the researchers in successful design of a neural transplant to restore lost motor functionalities of the victims of a spinal cord injury, so they could also enjoy normal life like us. I always wanted to utilise my knowledge and studies for the benefit of humanity and I am very thankful to UCL for giving me that opportunity. Thank you for reading this and I hope you enjoy reading my work.

Sabeeka S Zehra

London, April 2019

Abbreviations

AT Automatic- or Adaptive-Tripole

CNS Central Nervous System

CPE Constant Phase Element

EMG Electromyogram

ENG Electroneurogram

FES Functional Electrical Stimulation

IC Integrated Circuit

mQT Modified Quasi-Tripole

PNS Peripheral Nervous System

Pt Platinum

QT Quasi-Tripole

RC Resistor capacitor

SPI Spinal Cord Injury

SFAP Single Fibre Action Potential

TT True Tripole

Impact Statement

Acquisition of noise free neural information from peripheral nerves using Tripolar Cuff has been a challenging yet significantly important research topic in biomedical electronics, to mitigate against the effects of the Spinal Cord Injury (SCI), by bringing back the function of nerves to life that still remain after SCI. SCI affects an individual by not only causing physical influence to his life where his motor functions are drastically impaired or paralysed, but it also affects his psychological and social life to a greater extent.

The impact of this research in the advancement of acquiring and reusing neural information from the nerves is immense that is to return the SCI victim back to active and productive life. Neural signal recorded from the peripheral nerves is contaminated with the interferences from the surrounding muscles and hence it cannot be used to stimulate the nerves of a SCI victim. Unfortunately, not much work has been done in this area yet to record a reliable neural signal. This piece of research work is therefore focussed in the area of designing a cuff that could record an uncontaminated neural information. A novel technique has been presented in this piece of work that can record a micro-level neural signal by suppressing milli-level interferences. This interference neutralisation property of a recording cuff is highly important, and it is not limited to only one area of research. Once a cuff is designed that is capable of recording a reliable neural signal, it can be used not only in restoring motor functionalities of SCI patients such as bladder control, electro phrenic respiration, epilepsy or standing, stepping and grasping abilities but also in any medical application that requires efficient neural signal recording for the treatment of certain diseases.

This piece of research will also be helpful for the UCL Analogue and Biomedical Electronics group who are researching in the field of treating patients using electronic systems. It will also give an opportunity to the students who want to work in the medical field with an engineering background and would like to work for the humanity using their skills and knowledge. Nothing feels better than working for the benefit of humanity and this piece of work serves a minor contribution in the achievement of this goal.

CHAPTER ONE

1.1 Introduction

Spinal cord injury (SCI) is a distressing event that substantially affects the life of the victim at all scales especially young adults. According to the Spinal Research UK (last accessed 2018) more than 50 thousand people with SCIs are living in UK and Ireland, with the annual incidence recorded to be 1000 injuries at a treatment cost of £1 billion per annum. Statistics also reveal that approximately 80% of the cases received are of males with most occurrences among 15-38 years old. Accidental falls account for the largest percentage of SCIs are about 41.7%. Other major recorded causes of SCIs are due to road accidents of about 36.8%, sports of about 11.6% and the remaining minor causes of SCIs of about 10% are due to diseases, acts of violence and other unspecified cases. [1-5]

The motivation behind this work is to realise the true impact of spinal cord injury on the life of an individual that aside from causing the physical influence on his lifestyle, also affects his psychological and social well-being to the greater extent. It is no doubt a painful experience where personal freedom and dignity are often comprised, putting individuals under depression and anxiety with a feeling that things that were the basic source of their living such as walking, breathing, sexual response and bladder and bowel controls can never be the same as before the injury. Some positivity can be brought back in SCI victim by restoring his life that was prior to his injury. For many years treatment for SCI was very limited due to less understanding of everything that happens in the body after the point of injury. However, in the last two decades advancements in science and technology has given us a better understanding of everything that happens in the body after SCI and because of that that we now have more ideas about different treatment strategies that might be able to help the victim to reinstate his life back to normal. Apart from the improved care units available to the SCI patients, advancements

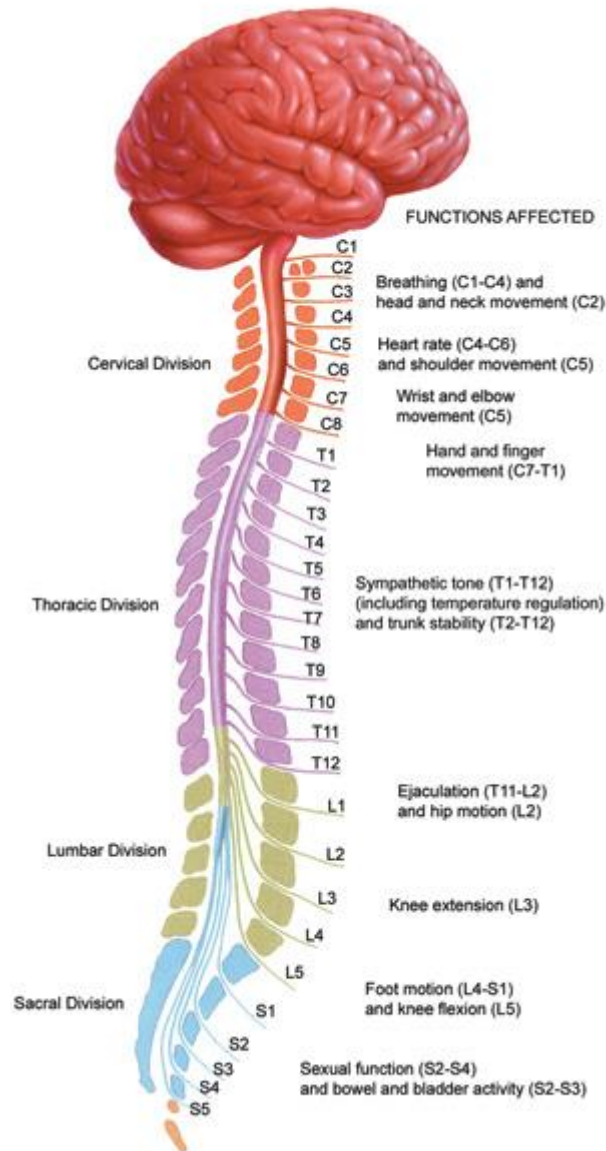


Fig. 1.1 Schematic diagram of the human spinal cord showing different divisions of spinal cord with reference to the vertebrae. 8 nerves emerging from cervical section responsible for the functions labelled in the graph, 10 from thoracic, 5 from lumbar and 5 from sacral division. [19]

in the medicine industry seem promising. Such as finding cures through the development of advance surgical methods and immune system modulation by spinal cord regeneration using stem cell transplants. Along with that advancements in the field of nanotechnology to find alternative solutions and intensive research in the field of microelectronics using implanted neuroprosthetic

devices to find aggressive physical rehabilitation also seems to be very promising in the future. [6-13]

According to National Institute of Neurological Disorders and Strokes a SCI is defined as the breakage or dislocation of vertebrae (fig. 1.1) protecting the spinal cord tissue, when it is exposed to forces greater than it can withstand. Once the spinal cord is bruised, crushed or torn, a lesion is formed affecting the flow of messages between the brain and the damaged area of the spinal cord. This interruption affects the body functions lower to the level of injury such as the mobility, sensory and autonomic functions of the body, causing temporary or permanent partial function and paralysis of the body muscles or organs. [6, 14-15]

After an injury, the damage to the body is determined by the location where it occurs on the spinal cord. In general injuries to the upper part of spinal cord are generally more severe, causing more loss of body functions than the lower part. A low level or back injury is often referred as paraplegia. With paraplegia a patient usually loses control over his lower body resulting in the loss of movement of limb and legs and intestinal bladder, and sexual dysfunction. Injuries that occur in the upper part of the spinal cord or neck region are generally referred as tetraplegia in which patient loses control over most of his body including both arms and legs movement and in extreme cases this may also affect his breathing that requires further treatment. [14-17] SCI can be further classified into complete and incomplete injuries. The nerves below the injury site are also affected because of spinal injury irrespective of the damage being traumatic or non-traumatic. Such an injury leads to a complete loss of motor function of the injured as well as the surrounding area. [18]

It is worth noting that spinal cord is not completely cut off in a complete injury rather an injury is said to be widespread when spinal cord has sustained enough damage across its complete width, resulting in no sensation or muscle control below the point of injury. Clearly, spinal cord injuries if they are complete have major impact on gross motor function of an individual. In contrast, an incomplete injury is to have some sensory preservation for motor function below the injury

site, with few unaffected nerve fibres known as peripheral nerves, still running up and down the body but not enough for the voluntary motor or sensational function of the muscles. These impaired body functions of the patient can then might be restored due to the presence of some undamaged nerves, to some extent using spinal cord rehabilitation techniques. [14-17] The detailed explanation of the anatomy and physiology of the human spinal cord along with the nature of the spinal injury is presented to the reader in the next chapter.

1.2 Motivation

Looking at the biological intricacy of spinal cord injuries, it is not a simple task to discover and formulate rehabilitative strategies which substantially lessen disabilities in a SCI victim. Hence, after a SCI, besides occupational therapy and conventional physiotherapy to restore lost motor functionalities of a patient, the most established method used is known as neuroprosthesis. In this method, a device that often uses functional electrical stimulation (FES) is surgically implanted to consolidate the nervous system. FES with the use of implanted electrodes produces short electrical pulses to produce contractions in the paralysed muscles or nerves, in a case when peripheral nerves are not damaged and hence repair impaired pathway between the brain and the effected site, after an injury. It not only offers a lower cost rehabilitation solution due to non-requirement of medicines and support equipment, but it also has no alarming side effects except when an implant fails or when there is a biological rejection from the body. [20-21, 28] A wide range of FES systems have been established including standing [25], walking [27], grasping [22, 23], cycling [26], as well as systems to regain respiratory control [29], hearing dysfunction [28] and bladder and bowel control [30] with patients suffering from some sort of incontinence after an injury.

To achieve better functionality of the neuroprosthesis implants, naturally occurring neural signal from the peripheral nerves can also be recorded as a feedback information in FES systems, that can be used as a command input to a stimulator. Bladder control implant is considered as a case study in this thesis and a potential application outcome for this particular piece of work. Dorsal

rhizotomy is a surgical procedure of cutting sacral roots, that is likely to increase bladder capacity and helps the patient from unwanted incontinence. However, due to risks involved after the surgery specially impaired reflexive erection in male patients, it is not a desirable choice for many SCI patients. Closed loop FES system in bladder control implant avoids the need of cutting dorsal sacral roots by either using artificial sensors on the bladder to record its pressure and volume or by recording sensory information from bladder afferents. The stimulator uses the recorded information to control undesired bladder contractions and in bladder voiding, hence regaining bladder continence and voiding without the need of risky surgical procedure of rhizotomy. [31-37]

General specifications to be considered in designing an implanted neural recording system includes the design of a suitable interface between the neural recorder/stimulator and nerve/tissue of interest. Suitable recording electrodes are to be selected in terms of material they are made of, site of implantation in the body and size and location of the target nerve. Certain type of electrodes also needs to be selected that could be used with an appropriate amplifier configuration of high gain, low noise, low power, etc., according to the requirement. It should also be noted that apart from the interference present inside the body, further interference will be added to the recorded neural information from the external recording system in the proximity of the implanted electrodes, that also needs to be removed. Where, metal electrodes are widely used to record neural formation in neuroprosthetic devices, it comes with many different types that are used with various amplifier configurations to record neural activity from the nerve. In this work, we are interested to use cuff electrodes for neural signal recording as they are not invasive to the nerve and do not penetrate inside it. Cuff electrodes have not only demonstrated to be reliable for long term neural recording but also offers the benefit of interference reduction when used in a tripolar configuration with an appropriate amplifier. Interference reduction is highly needed to extract an uncontaminated neural signal to be used in a neural recording system. If not reduced to a certain level, recorded neural information might not be useful at all for the intended purpose or results in a degraded performance. This is challenging as neural signal of microvolt level is embedded

behind the EMG interference of millivolt level and coming up with the design of a recording configuration that neutralises EMG interference and extracts unaffected neural signal to be used for patient rehabilitation is not a lightweight task. [38-47] Details of the neural recording system and EMG naturalisation technique are discussed in the next chapters for reader's interest.

1.3 Project Aims

The motivation behind this work is to rehabilitate spinal cord injury patients with the use of biomedical instrumentation, as discussed in the previous section of the chapter. The centre of interest is neuroprosthetic devices, which when used with a suitable amplifier configuration records a neural using implanted electrodes. The recorded signal is contaminated due to the presence of electromyogram EMG interference. Hence, the aim of this work is to present a new amplifier configuration with cuff electrode that could minimise the interference at the output of tripolar cuff electrode to an extent, so that an embedded electroneurogram ENG signal is extracted from it in an unaffected way. Bladder control implant which is a case study of this research works requires efficient recording of the neural signals from bladder afferents for appropriate neuromodulation. During bladder contraction, it has been shown in [48] that neural signals of about 0.1 μ V can be recorded in humans. These neural signals can be used to get information about the pressure and volume change of bladder and hence can be used in the stimulator for bladder control and voiding. However, the neural signals will be contaminated with presence of large EMG interference from surrounding muscles. Thus, an amplifier configuration with good EMG neutralisation is required that neutralises the interference not only at one frequency but in the entire frequency band of interest. Amplifier configuration should also be power efficient as device will be used by the patient with bladder incontinence throughout the day and rechargeable batteries will be powering the unit. Since the presentation of first amplifier configuration with tripolar electrodes in mid 70s, although research has been going on in this field, not many tripolar amplifier configurations have been introduced. The amplifier configuration with the above-mentioned characteristics is not yet available for reliable neural signal recording

from the peripheral nerves, which is something this research work will try to inscribe. Thus, coming up with the novel design of tripolar amplifier configuration offering EMG neutralisation in the entire frequency band of interest is not an easy task, as in this research work, the problem has been tried to tackle by adding a compensation circuit with discrete components to the output of tripolar cuff electrode, which forms the input of the amplifier. The idea of EMG interference neutralisation by this method has been demonstrated in invitro preparations before in [49] using a complicated non-uniform 20 stages RC ladder network at the output of tripolar cuff, that minimises EMG interference by a factor of 10 in the frequency bandwidth of interest. [50] The use of such large compensation circuit not only suffers from a bigger size which will not be feasible to be used with the bladder control implant required throughout the day but there is also a possibility of adding more noise to the neural signal due to the use of large number of resistors in the compensation circuit. In this research work, the idea of minimising EMG using compensation circuit with tripolar cuff electrode is carried forward, but the challenge is to minimise the EMG interference further and linearly in the frequency band of interest using simple compensation circuit with less discrete components. Thus, in this work, tripolar amplifier configuration with novel EMG neutralisation technique with simple compensation circuits has been presented and successfully evaluated in invitro preparations, being the aim of the project.

In terms of the practical use of the proposed EMG neutralisation compensation circuit in this research work, it can be used with the neural signal recorder of the implant device, such as with the conditional neuromodulator designed and tested by Donaldson et al., [51] to suppress unwanted bladder contraction or for bladder voiding. There are two main challenges required, one being the detection of noise free neural signals using recorder and other is the power efficiency of the device as it will be used by the patient throughout the day. For reliable neural signal recording, using compensation circuit with the tripolar electrode, preparatory work is required. Surface electrodes can be used to measure EMG interference from the muscles which can be injected into the book-electrode¹ [53] in an experimental setup through a transformer, after programming onto a waveform generator. [52] Equivalent circuit model of the book electrode with EMG

interference can then be constructed based on impedance profile of recording electrodes with impedance spectroscopy software to be used in simulation. Simulation results will provide the capacitors and resistors values required in the compensation circuit for EMG minimisation in the bandwidth of interest. Using this information, compensation circuit with discrete components will be constructed, which will be used as an off chip to the implant if capacitor sizes in the compensation circuit are bigger in size. In off-chip setup compensation circuit component values can also be varied using the knobs if required, for further EMG neutralisation. The neural signal will then be amplified in the implant and transmitted to external control unit for further processing. Fig. 1.2a., shows the signal pathway block diagram of the conditional neuromodulator designed, without the power supply arrangements while fig 1.2b., shows recording of EMG interference for finding component values of the compensation circuit, before it can be used in the implant device for EMG neutralisation. To meet the low power demand, the device must be battery powered but power would be used up not only by the recording part but by the other parts of the implant as well such an amplifier, microcontroller, signal convertors, internal signal communicator and external control unit. Microcontroller reconfigures the device and being the master transmits and receives data simultaneously between various parts of the device such as decoding commands using analogue to digital convertors for external

¹Book electrodes have clinical applications in nueroprosthesis for bladder control implants. It presents a tripolar electrodes arrangement in an array to make electrical connections with the nerve roots. Three rectangular platinum foils are fitted into a separate slot, inside a silicone rubber block. For neural signal detection, nerve roots are put into the slots. The centre electrode functions as a cathode, while the other two outer electrodes serve as anodes.

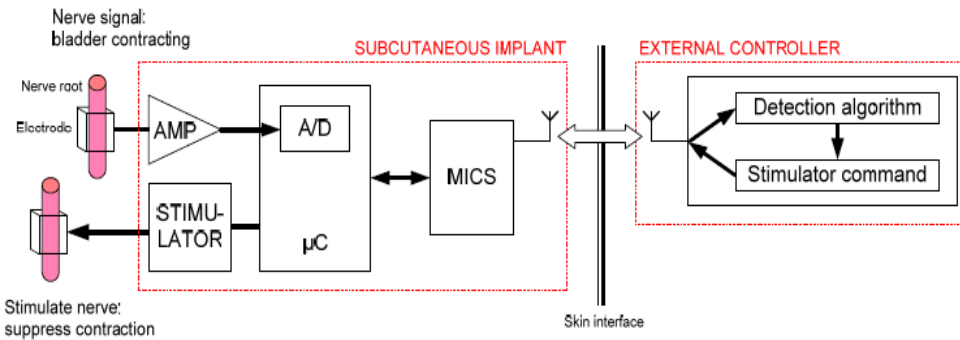


Fig. 1.2a. Block diagram showing the signal pathway between an implant and external controller for stimulating nerve and recording its signal in conditional neural modulator, reproduced from [51]

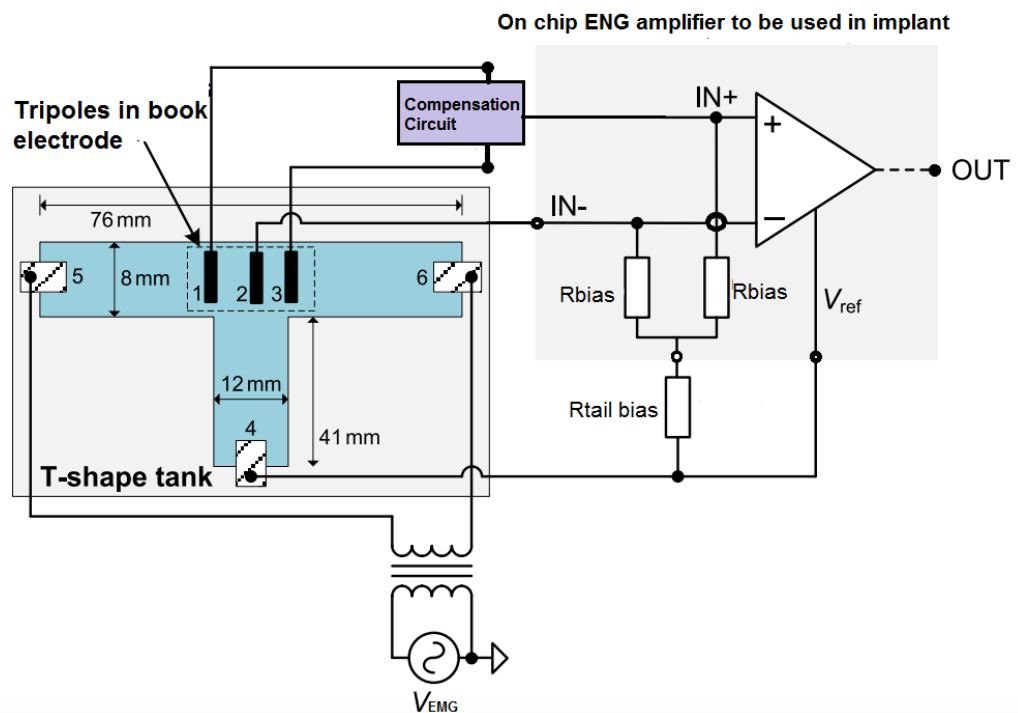


Fig. 1.2b. Experimental setup to introduce EMG interference into the book electrode to measure discrete component values for the compensation circuit to neutralise interference during preparatory task. Amplifier is not needed for this task but shown in the diagram to show connection of the book electrode with compensation circuit to it. After finding compensation circuit component values, it can be used with tripole of fig. 1.2a in the conditional neuromodulator design for bladder control and voiding. Figure modified from [52]

and internal use and performing ENG signal processing, including pulse and modulation settings for the stimulator, etc. Medical implant communication service (MICS) creates a two-way digital communication spectrum at 403MHz between the implant and the exterior control unit. The induction path also provides power to the stimulator along with a DC-DC convertor, setting suitable voltage level required for the stimulation. Same nerve roots are used for recording of the neural signal and for nerve stimulation for bladder voiding. The device can therefore be connected in a way so that three tripoles are used for stimulation and one for neural recording [51] Details of the power requirement and calculations of the conditional neuromodulator designed for bladder control can be found in [51] but to meet the power requirements, an under-mattress charger (UMC) has also been designed and tested to charge the device overnight for the day usage by the patient and finally the technique presented in this work for neural signal recording should ideally has lower power requirements.

1.4 Main contributions

This section briefly highlights the main contributions made in the trial of reaching the project objective; neutralization of EMG interference for the unaffected ENG neural signal detection by the recording amplifier.

- Measurement of individual electrodes impedances in a tripolar arrangement experimentally and creating its equivalent circuit model by accurately fitting experimental results on the output of the model.
- Creating equivalent circuit model of whole book electrode using electrode impedance profiles, capable of replicating similar EMG interference, that was introduced in the book electrode setup.
- Carrying out a series of in silico and invitro experiments to minimise EMG interference at a spot frequency, using simple RC circuit as a compensation circuit.

- Constant phase element (CPE) impedance representation using simple 3-stage RC ladder network.
- Presenting a novel technique of EMG neutralisation using simple 3 and 2 stage RC compensation circuits to minimise EMG interference linearly close to null and not only at the spot frequency but in the entire frequency band of interest, without any readjustment to the component values of the compensation circuit.
- Performing optimisation in simulations to find the component values for the compensation circuits to minimise EMG close to null.
- Invitro testing of imbalanced book electrode using compensation circuits with the circuit parameters values obtained in simulations to minimise EMG interference linearly and close to null.
- Identifying the redundant branch of a 3-stage RC compensation circuit for linear EMG minimisation beyond 100Hz. In silico and in vitro results were also obtained for 2-stage RC compensation circuit.
- Identifying the effect of scaling large capacitors of compensation circuit to reduce chip size and its effect on adding noise to the system because of resulting increased size of resistors.
- In silico estimation of interference (noise) added from the use of proposed compensation circuit into the book electrode.
- Performing critical review of the benefits and restraints of the approach used in EMG minimisation in this research work, possible ways of optimising Ztrim component values and presenting another approach (found in appendix A) to find realistic compensation circuit parameters without using optimisation in simulations.

1.5 Thesis Organisation

Chapter 1 is an introductory chapter highlighting the motivation and aims behind this research work. Brief account of remaining chapters of the thesis are described below.

Chapter 2 presents a literature review of the spinal cord injury and techniques used for the rehabilitation of the patients, setting foundation for the remaining chapters of the thesis. It explains the physiology of the spinal cord injury and basic mechanism of human nervous system in the context of neural signal recording such as propagation of action potential inside the nerve. It then talks about neuroprosthesis in detail, its mechanism and uses in improving the life of SCI victims which is the motivation of the work. The types of electrodes that can be used for neural signal recording from peripheral nerves are described with more emphasis on the use and importance of the implanted cuff electrodes. Various amplifier configurations are also presented along with their benefits and limitations for reliable neural signal recording from the nerves. The chapter ends with the discussion of challenges in neural signal recording with tripolar electrodes, how it can be tackled using various amplifier configurations and difficulties in using these configurations in the neural implant, along with the discussion on selection of neural bandwidth of interest used in this research work.

Chapter 3 forms the main chapter of the thesis. This chapter presents the novel technique of reliable neural signal recording using tripolar cuff electrodes. It begins with the introduction of the modified quasi tripole configuration and how the theory behind its neutralising principle is utilised to present a new compensation circuit to linearly minimise EMG interference in the bandwidth of interest. It demonstrates the performance and results of using this configuration in silico and in invitro preparations. Chapter ends with the discussion on the advantages and limitation of this design in terms of using it with the implant.

Finally, chapter 4 summarises the whole thesis along with the discussion on future work, to further improve the performance of the proposed novel technique for EMG neutralisation.

1.6 Publications

- 1- C. Eder, S.S. Zehra, M. Zamani and A. Demosthenous, "Suitable compensation circuits for on-chip interference reduction in neural tripolar recordings," 2013 IEEE 20th International Conference on Electronics, Circuits, and Systems (ICECS), pp. 241-244, December 2013.
- 2- Zehra S and Demosthenous A., "Simple Compensation Circuits Realisation for Interference Reduction in the Entire Band of Neural Tripolar Recordings," IEEE 37th Annual International Conference of Engineering in Medicine and Biology Society EMBC, August 2015.

CHAPTER TWO

Fundamentals of Neural Signal Recording

2.1 Introduction

This chapter introduces the basic concepts of neural signal recording after a spinal cord injury to restore life expectancies of an individual. It begins with the basics of anatomy and physiology of human spinal cord, description of the movement of neural signal inside human body and pathophysiology of the spinal cord injury. It then explains the treatments available, focusing on neuroprosthesis and principle behind it. Use of implanted electrodes for neural signal recording, different amplifier configurations being used for this task, along with their benefits and drawbacks are also discussed. The effect of interface impedance between electrodes and nerves on neural signal recording is also being explained along with the selection criteria of the bandwidth of interest used in this research work.

2.2 Anatomy and Physiology of the Human Spinal Cord

2.2.1 Basics of Anatomy

Spinal cord is a very important part of the central nervous system that controls and co-ordinate the activities of our bodies. It is a long cylindrical structure consisting bundles of nerve fibres that prolongs from the brain and runs down the back to the coxal known as hip bone. It provides two-way communication pathway between the brain and other parts of the body. It runs inside the spinal column surrounded by the hard rings of bones called vertebrae which are further surrounded by a protective membrane for its protection. Together the vertebrae and membrane make up the backbone that protects the spinal cord from the harmful injuries. Vertebrae are also joined together by softened cartilage discs for flexibility and cushioning to the soft spinal tissue inside the spinal cord. They

are uniformly organised and divided into five main sections with several spinal nerves coming out of them with specific motor and sensory functions. They are labelled with numbers and letters from head to tail bone according to their level of function and when injury occurs its location on these sections determines which body functions have been affected. [54-55]

The first region of the spinal cord chapter is known as a cervical region (chapter 1, fig. 1.1.) consisting of seven vertebrae with eight pairs of spinal nerves, controlling breathing and head, neck, arms and hands movement in the body. The next twelve vertebrae lie in the thoracic region that provides trunk stability and abdominal muscles control. The lumbar region has five vertebrae in the lower back after thoracic region where rib cage attaches to pelvis or hip bone and it controls legs movement. The sacral region with five vertebrae runs from the pelvis down the spinal cord and injury to this region causes bladder, bowel and sexual dysfunction. Generally, there is a direct relation between the injury location on the spinal cord and its effect on body functions. Thus, the higher the injury site the more body functions are compromised as communication between brain and spinal cord below the point of injury gets affected. [54-57]

2.2.2 The Neuron Cell

The human nervous system is broadly classified into central nervous system (CNS) and peripheral nervous system (PNS). The CNS consists of a brain and spinal cord, whereas the PNS consists of the nerves exiting through the spinal cord. Its sensory division consists of sensory nerves that transmit messages from the spinal cord to the brain and its motor division consists of motor nerves that carry information from brain to the particular muscle or organ, through spinal cord to generate a specific action. Neurons or nerve bundles are the communication cells in the spinal nerves that form the root of the central nervous system (CNS) at the cellular level. There are billions of neurons in the body that are responsible for receiving, processing and transmitting messages between the brain and spinal cord through the openings in the vertebrae. [55-56, 58-59]

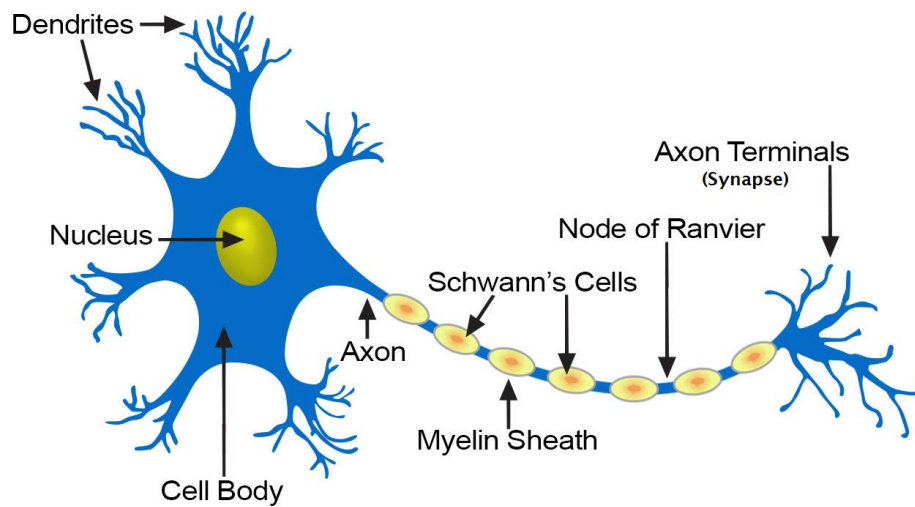


Fig. 2.1 Typical structure of a neuron showing dendrites that receive and pass signal information to the cell body, which processes it and pass it to synaptic/axon terminals through an axon to the target body. Diagram taken from [National Cancer Institute, SEER training modules]

A typical structure of a neuron (fig. 2.1) consists of a cell body, axon, dendrites and a synapse. Cell body consists of a nucleus that produces neurotransmitters when specialised branch like structures, surrounding the cell body known as dendrites receive action messages from other neurons and pass it to the cell body for assimilation. Cell body integrates the received signal and creates an output for a specific action. The information on the signal in the form of an impulse is then propagated through a tail like body of a neuron called axon to the synapse, which is the site of intracellular communication between the cell bodies. A message for a specific action is then transmitted from axon/synaptic terminal to the target cell, which can be another neuron or a muscle cell. [55-56, 58-60]

A neuron can be myelinated or unmyelinated. An unmyelinated neuron has no insulation around its axon and hence has a less conduction for electrical signals. Impulse travels faster in a myelinated neuron that has a myelin sheath around its axon. [58-61] The impulse that is transmitted from the cell body of a neuron to the

synaptic terminal to reach the target body is known as action potential, which is explained in detail in the next section.

2.2.3 The Action Potential

Nerve impulse is an electrical event on the plasma membrane of the neuron or muscle cells that last for a short time and is also known as Action Potential (fig. 2.2). Resting membrane potential is when neurons are at rest and illustrate non-uniform alignment of ions across the cell membrane. The difference in voltage across the sides of the cell membrane of the cell without any stimulation by the signal is called resting membrane potential. During this state more sodium ions are present outside the cell because of sodium-potassium channel pumping three sodium ions outside the cell for every two potassium ions that comes inside the cell. This turns the outside of cell more positive and the inside of the neuron more negative. The unequal distribution of ions across the membrane creates a potential difference of about -70mV , which means that cell exterior is now 70mV more positive than the inside of the cell. Ions have an innate ability to move from higher concentration to lower concentration in order to maintain equilibrium, but there is an impermeability of cell membrane to some of the across it. Leakage channels in plasma membrane are more permeable to potassium ions than other ions. Potassium ions move outside the cell membrane as a result of diffusion when leakage channels open up at rest thus turning inside of the cell more negative. This results in the formation of an electrical force of attraction between the inside and outside regions of the cell and sources potassium ions to move back inside the cell. Therefore, the resting potential of -70mV across the plasma membrane of the neuron is maintained with diffusion, electrical force and sodium-potassium pump when it is in its unstimulated state. [60-63]

When a neuron is triggered by a signal from another neuron or muscle cell, action potential occurs in the cell body of neuron down its axon, thus opening the gated ion channels in the cell membrane. The sodium ions flow from outside to the

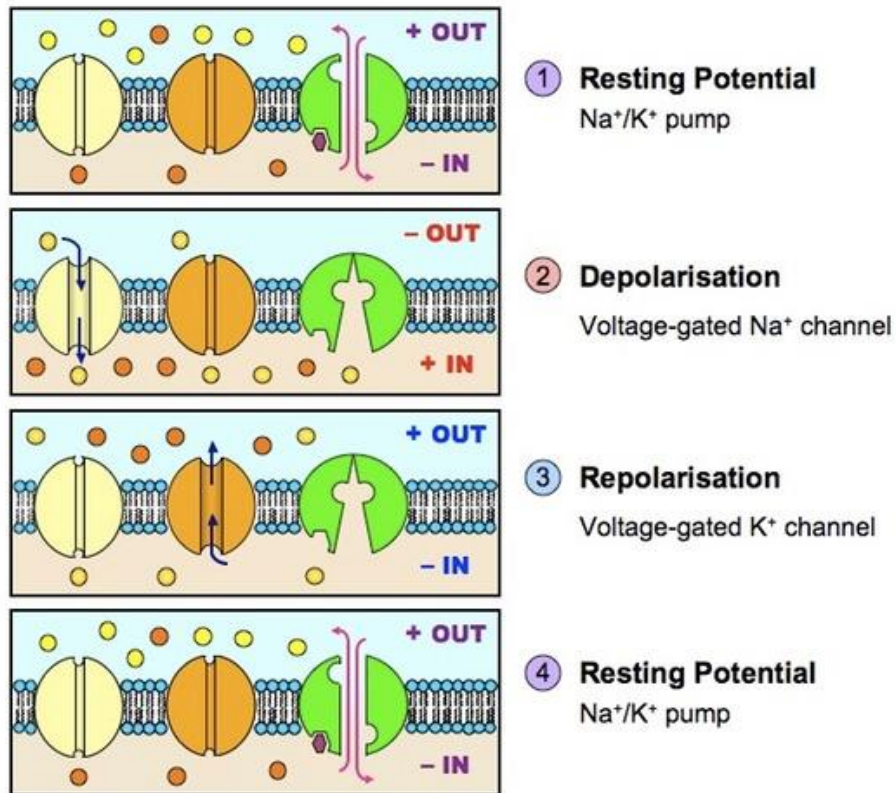


Fig. 2.2 showing the stages of an action potential in human spinal cord during the transmission of the neural signal. [64]

inside of the cell and the exterior of cell is now more negative than the inside due the presence of more positive ions inside the cell. This reversal of resting membrane potential charge is temporary and is known as local depolarisation of the cell membrane. The greater the stimulus, the larger local depolarisation occurs. This cause more gated ion channels to open and thus resulting in the formation of a chain reaction of electrical signals known as impulse, that get transferred down the axon of the neuron in one direction towards the end of the axon. An axon with a myelin sheath around it has a better conduction of the impulse because the small connections called as the Nodes of Ranvier between each myelin sheath becomes activated while transmitting action potential instead of activating every ion channel down the axon. The vesicles containing neurotransmitters from the cell body are released into the synaptic cleft to go to the target area as the impulse reaches the axon terminal. The local depolarisation also decreases with distance from the stimulus. However, if the stimulus is big

enough, depolarisation reaches to its threshold level of about 30mV. The sodium channels that opened up fast then become inactive again at this level, impeding the flow of sodium ions into the cell. This is then followed by with the opening of potassium gated ion channels that cause the movement of potassium ions out of the cell and hence decreasing the voltage of the cell. This state is called repolarisation when concentration of sodium ions inside the cell is more, and more potassium ions are present outside the cell. Now the cell is in a process of returning to its original resting state before the stimulus was received but when potassium ion gates close we end up at a position with more potassium ions present outside the cell than inside, and more sodium ions are present inside the cell than outside. Hence voltage slightly drops down further than resting potential and goes into the hyperpolarisation state. The cell now enters into refractory period when no action potential can be initiated, and sodium-potassium pump gets activated again along with diffusion and electrical forces to return sodium ions outside the cell and potassium ions inside the cell. Thus, this again establishes a resting potential of about 70mV across the plasma membrane of the neuron. [61-63]

2.2.3.1 Natural and Artificial Nerve Stimuli

Action potential can be induced either naturally or artificially. It is possible to induce it naturally for example by firing of another neuron or by a muscle stretch and artificially by passing a burst of current through electrodes e.g. by stimulus/ electrical pulse, that leads to size reduction of the resting potential hence causing it to 'fire'. However, the amount of current i.e. stimulus intensity or strength, doesn't dictate the amplitude of an action potential as its generation is not dependant on the current that produced it. Moreover, the activation threshold for an action potential 'firing' and refractory period are not same for each nerve fibre, but the conduction velocity, shape and magnitude remain constant across the axon's length. This is only applicable when external conditions e.g. temperature and ionic conditions remain constant on a uniform length axon. The range of resting potential falls between -60 to -95 mV always, while the peak potential of the spike lies in the range of +20 to +50 mV. [65] All types of excitable tissues,

with differences in the shapes and duration of action potential, show similar behaviours in terms of amplitudes of the resting and action potential. [64-66]

2.2.3.2 The propagation of nerve impulses

For further understanding of the generation of the nerve impulses unmyelinated and myelinated nerve fibres should be considered differently from one another. In unmyelinated nerve fibres myelin sheath is not present so whole length of the axon can be involved in nerve impulse generation.

The complete mechanism of nerve impulse generation can be summed up in the following three stages: [62-63, 67]

- The concentration of positively charged sodium ions being more positive outside the cell makes the interior of the neuron negatively charged, known as the resting stage.
- The sodium ions move into the neuron on opening of sodium channels. As a result, the interior of the cell becomes more positive than the exterior and this is referred as a depolarisation stage.
- Potassium channels now open but sodium channels remain close and hence flushing potassium ions into the cell. They are also positively charged; hence the resting potential is reached again which is the final stage of the whole process.

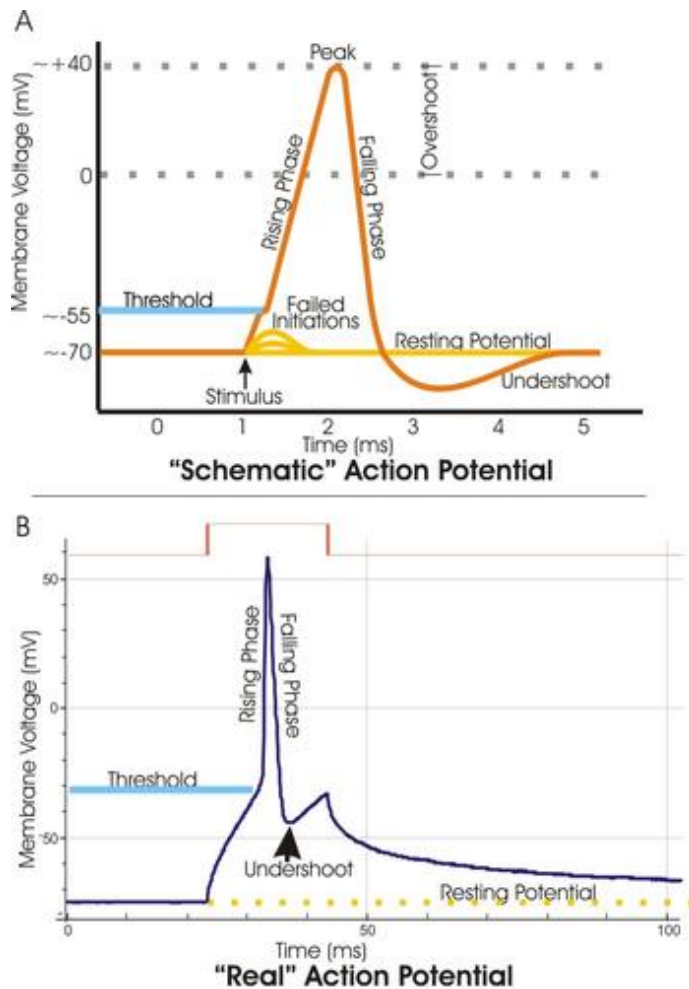


Fig. 2.3. (A) showing phases of an ideal action potential and (B) showing phases of a real action potential. Distortion in (B) is because of the recording techniques used. Hyperpolarisation is the curve below resting potential point in (A) where no nerve impulse is generated. [68]

These three stages occur one after the other and capture the active zone that lies in between a zone which has not been stimulated yet and the other where repolarisation has just taken place. This sandwiched zone known as the active region in the area is where the nerve impulse information is being transferred. For a short span of time after the closing of potassium channels, the potential goes below the resting potential therefore no new nerve impulse can be generated despite of the presence of any stimulus. This phase is known as hyperpolarization after potential and is shown in fig 2.3. Contrary to this, if an axon segment does not undergo the hyperpolarizing after-potential phase, it can

be stimulated into the depolarisation stage for the generation of a nerve impulse. Hence the polarisation and depolarisation process can without being attenuated. The distinctive feature between unmyelinated and myelinated membranes is that the depolarization can occur all along the length of unmyelinated nerve fibres whereas for the latter it occurs only at nodes of Ranvier. [61-63, 67]

2.3 Pathophysiology of the Human Spinal Cord Injury

The spinal cord injuries affect the ascending and descending axonal pathways and not just that, cellular destruction and demyelination also cause inflammation (fig. 2.4) therefore, causing loss of movement, sensation and autonomic control below and at the level of the lesion. According to recent clinical methodologies high doses of Methylprednisolone is used for the treatment of SCI to limit the spinal cord injury. They are beneficial to some extent but for the potential healing a lot research is required for discovering and inventing interventions and therapies potent enough to deal with the complications of pathophysiology of SCI. Some discoveries have been made at the preclinical level that aims both at decreasing the secondary damage and optimizing working of the remaining neural systems of the body besides stimulating regeneration and repair. Neuronal and glial cells are damaged because of traumatic SCI both at the site of injury and around it. The body's response system has 3 stages that take place immediately after SCI, are listed below.

Acute Phase

Acute phase includes the time of injury and following first few days, during which many pathophysiological processes begin simultaneously. Initially soon after injury damage to soft tissue blood vessels and neuronal cells occur resulting in cell death or necrosis due to ischemia. Such damage is termed as mechanical damage. Effects of contusion injury are more prominent in the grey matter of the spinal cord. However white matter is preserved in the form of a ring at the site of

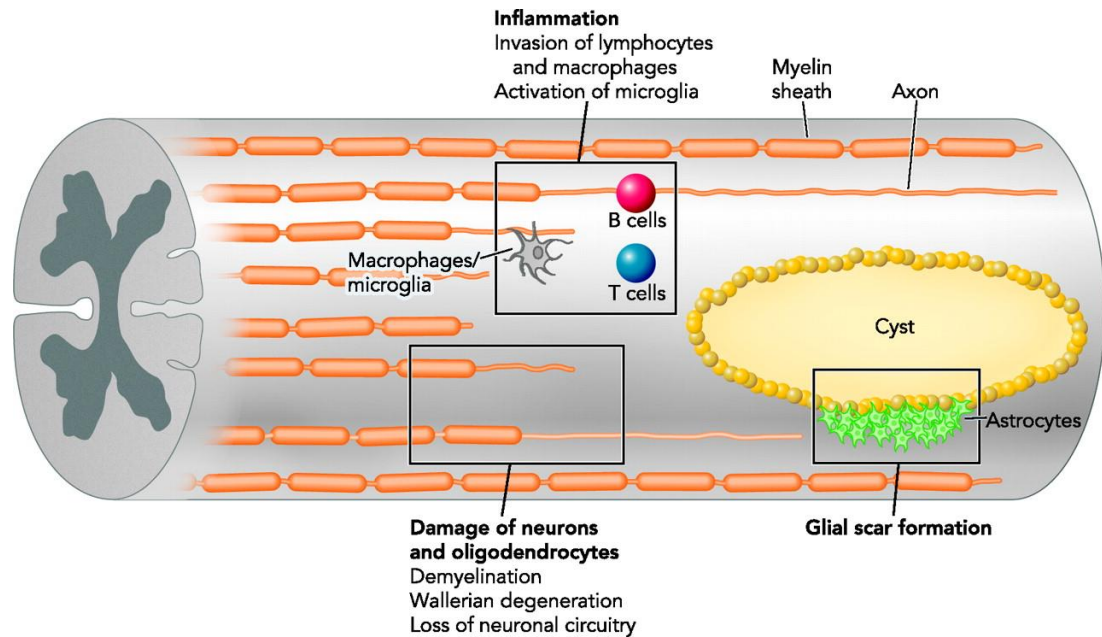


Fig. 2.4. showing effect of spinal cord injury. Many neurons die immediately after SCI. After an injury, cysts may be formed resulting in glial scar formation due to astrocytes. This results in the disruption of neural pathway of many axons in the neurons resulting in Wallerian degeneration. Figure taken from American Physiological Society (2008).

injury. Right after few minutes generation of trauma induced action potentials takes place along with electrolytic shifts of sodium, potassium and calcium ions. Intracellular levels of sodium and calcium ions rise, and extracellular levels of potassium ions rises to unbearable levels leading to a failure of neural functionality and resulting in a spinal injury. This state continues for the next 24 hours and depicts a generalized failure of CNS and PNS. Haemorrhage with localized edema, thrombosis, vasospasm and loss of autoregulation of the vasculature aggravates the whole situation. Vertebral displacement along with edema leads to spinal cord compression, as even in the best circumstances the time to admission after SCI is approximately three hours and the acute trauma processes do not let the clinical interventions work better.

Secondary and chronic injury process

Unlike acute phase of SCI, the secondary and chronic injury processes are much more favourable targets for the therapeutic interventions because they occur

hours to weeks after the trauma. Furthermore, due to secondary injury to the spinal column, the axons also become demyelinated. [69-75]

2.4 Neuroprosthesis for Spinal Cord Injury Treatment

Neuroprosthetics is a discipline that deals with connection of neuroscience and biomedical engineering to improve life functionalities of people suffering from spinal cord injury, with the use of implantable devices known as Neuroprosthesis. In the recent years, a lot of work is being established in this field to restore motor functions of the disabled persons. The concept behind using neuroprosthesis is the restoration of sensory, motor and autonomic functions using the interface between technology and human nervous system which could be chemical, mechanical or electrical. Typically, it is an active device under subjects control that triggers the affected muscle or nerve by sending electrical pulses to it and hence re-establishes neural pathway between the brain and affected part. Fig 2.5 shows a typical neuroprosthesis in which some command input such as a switch is required to trigger the system. The stimulator then sends the controlled electrical pulses using electrodes around the nerves to the neural structures for the regeneration of the required action potential. Studies show that a lot of impaired functions due to Spinal Cord Injury (SCI) can be restored by correctly

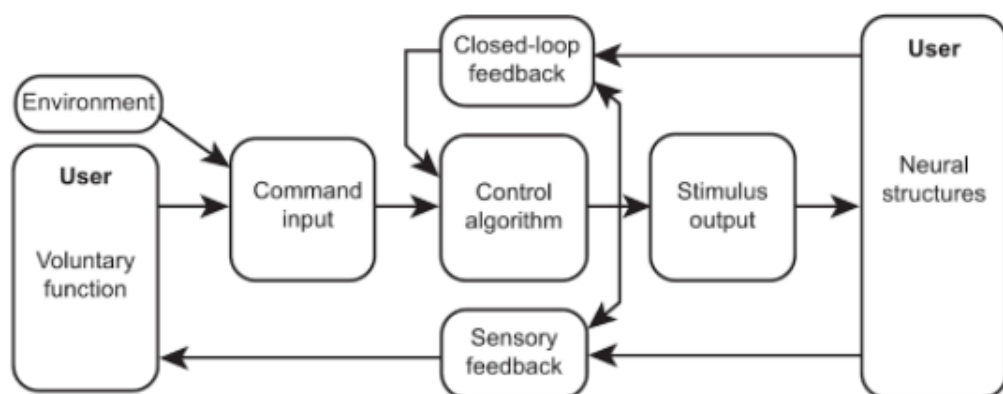


Fig. 2.5 Typical flowchart showing various stages of neuroprosthesis between device (user input) and neural interface to restore motor movements after an SCI. [83]

stimulating the nervous system in this way, as most peripheral nerves are unaffected even after the injury. It also offers the benefit of being a non-invasive implant, using cuff electrodes around the nerves for recording and stimulation, which makes them even more attractive for the treatment of SCI patients. Neuroprosthesis also needs to be designed according to the patient's requirements as every sufferer would have a different physiology and different needs according to the injury. For example, bladder neuroprosthesis are meant to improve bladder incontinence and control of an SCI victim according to his own unique needs and drop-foot prosthesis can be used to treat the drop foot syndrome and helps in foot lifting and movement in accordance with the requirements. In terms of its physical design, it is desirable to make neuroprostheses devices portable and power efficient, to be used anytime in the day when required and small, so they can also be implanted in congested body areas. Care must also be taken during implantation as any damage to peripheral nerves increases the chance of not restoring the body function as required. [76-82, 90] The details of the technique used by neuroprosthesis and signal recording are explained in the following sections of the chapter.

2.4.1 Functional Electrical Stimulation

Functional electrical stimulation (FES) is a method used by neuroprosthesis that uses implanted electrodes to apply small electrical pulses to stimulate the neurons in the peripheral nerves. The triggering of the nerves includes both the efferent nerves (motor nerves) that run from the central nervous system to the muscles and the afferent nerves (sensory nerves) running from the organs to the central nervous system. This generates contractions in the paralyzed muscles or organ of an SCI patient, helping to restore movement after an injury. For correct stimulation, pulses are desired to be symmetrical and biphasic and a detailed attention is also required in the selection and design of implanted electrodes. Fig 2.6 shows a first-generation freehand system, reported in mid 1980s using FES, for the restoration of the hand movement after an injury. A patient cannot grasp

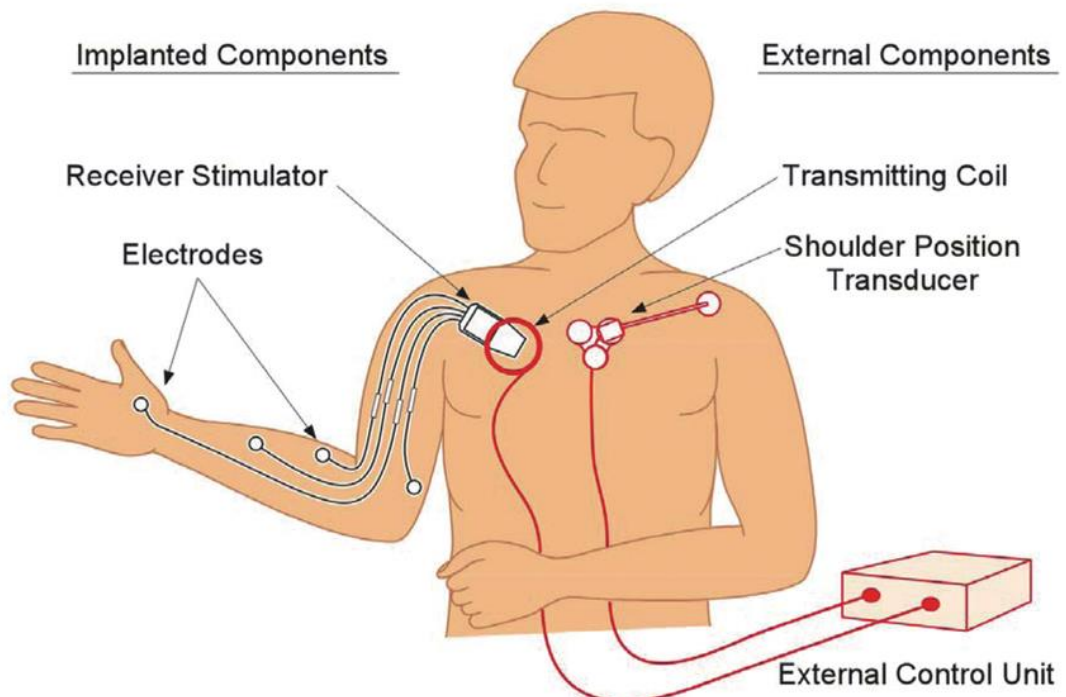


Fig. 2.6. shows FES system in use to restore hand grasping and elbow movement. Transducer sends a signal to control unit on shoulder movement, which sends pulses to the effected nerves using implanted electrodes to produce muscle contractions for hand and elbow movement. [88]

objects or extend his elbow without it. When a patient moves or retracts his left shoulder as an input to the system, implanted electrodes on a command from external control unit sends series of small electrical pulses producing contractions in the effected muscles and hence helps in hand grasping and elbow extension. [83-92]

Both open and closed-loop FES systems can be used depending on the function to be restored however, there is more focus on the closed-loop system research nowadays. Closed loop system offers an advantage of automatic control (less user interaction) without the use of an additional external artificial sensors by recording neural activity and using it as a control input to the stimulator. It

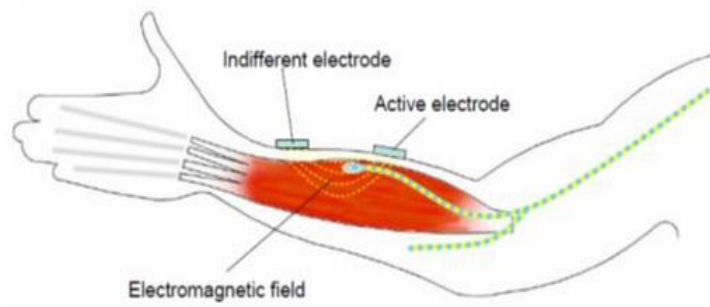
improves the system performance by monitoring the output and adjusting the input according to it, using a feedback control loop. [93-95]

2.4.2 Neural Recording

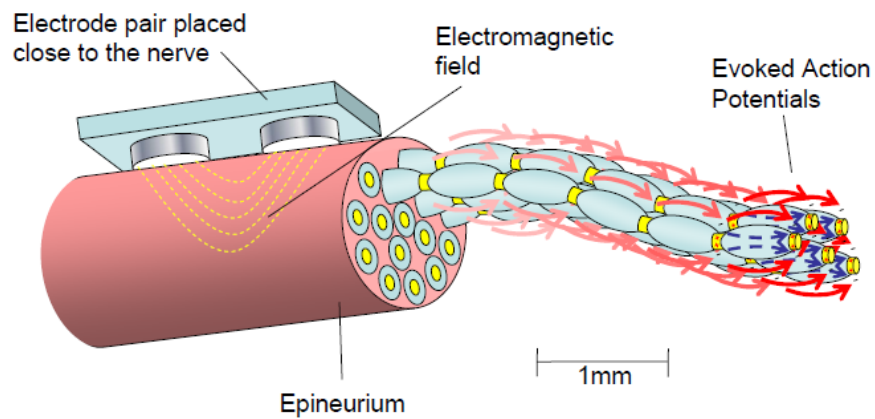
Closed-loop FES system uses recorded neural signal to be sent to a stimulator to improve systems performance. Electrodes can be used to record neural activity from the nerves. Electrodes are of many types and designs but categorically they are divided into two main categories (fig. 2.6.). One is the transcutaneous electrodes, that are surface electrodes, typically placed on the patient's skin. The other type is subcutaneous electrodes which are further divided into two types i.e. percutaneous and implanted electrodes. Percutaneous electrodes are needle electrodes that are invasive to the nerves; injected into the nerve and are used for short-time neural recording in FES systems. Implanted electrodes, which can be intrafascicular or cuff type; non-invasively encapsulates the nerve and are mostly used for neural signal recording. [96-100]

Although, surface electrodes are non-invasive and simple to use, but they suffer from various disadvantages when used with FES systems. In order to overcome high electrical impedance of the skin, bigger electrodes are required to provide higher stimulating voltage for the generation of appropriate tissue currents. The bulky design of neuroprosthesis due to large stimulating electrodes and heavy batteries is not user friendly. It not only requires more power to run, making it difficult to be used throughout the day for example for bladder voiding implant, but it also offers difficulty to patient in terms of its recalibration every time it is needed to be used. Current dispersal in the tissue can also not be predicted, which can be dangerous for the tissue areas with more electrical conductance. It is recorded that because of the shape of volume impedance of metal surface electrodes, current density is less in the middle and more at their corners. These concerns are somewhat mitigated by improving the design and material of surface electrodes for example rubber electrodes and hydrogel electrodes, but they also cannot be used for the nerves that are deep inside the body which, cannot be stimulated from the surface. In contrast, implanted cuff electrodes are a subject of more attention for neural signal recording, being non-invasive to the

nerve and covers the bundle of nerve fibres and hence provide long term chronic recording of neural activity from the nerve. [98-99, 101-102]



(a)



(b)

Fig. 2.7. Types of electrodes that are used in FES systems to record neural signal. (a) Surface electrodes, (b) Implanted electrodes [103]

2.4.2.1 Cuff Electrodes

The cuff-electrode encapsulates the whole circumference of a nerve, with openings at both ends and the nerve passing longitudinally through it, for neural signal recording (fig. 2.8). It comprises of two basic parts, one is the cuff itself and the other the electrodes as actual electrical interface to the nerve. It is typically made of an insulating material silicon with electrodes fitted inside it in relation to the target nerve. Electroneurogram signals, ENG were first recorded from peripheral nerves in mid 1970s by Hoffer [41] and Stein [38] using cuff electrodes. It offers an important benefit in neural signal recording by acting as an insulator, which separates a defined volume of constant diameter from outside. This lessens the volume of the tissue for the ENG signals in which currents flow and thereby increasing the action potential inside the cuff. It also shields the inner volume from external interferences surrounding the cuff-electrode. Since external interferences can enter the cuff only at its ends, the gradient of the resulting interference inside the cuff is constant, shown in figure 2.9. It provides an additional benefit of long-term neural signal recording from peripheral nerves



Fig. 2.8. Figure showing implantation of cuff electrode in rat's nerve, demonstrated by Raspopovic, (2010).

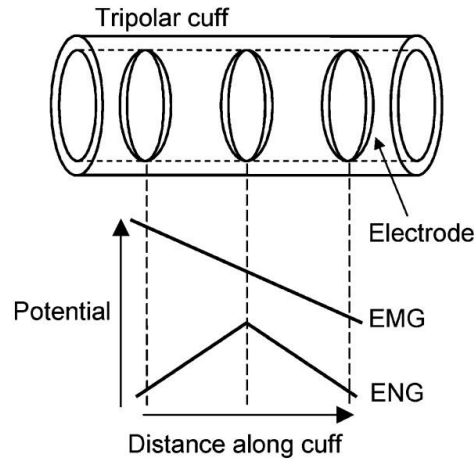


Fig. 2.9. ENG and EMG potentials shown inside the cuff electrode for neural signal recording. [49]

without causing harm to the nerve and surrounding tissue. Recalibration is also not required, every time it needs to be used by the patient, thus making it a better candidate for neural signal recording. [46-48, 103-107]

Types of Cuff Electrodes

Arrangement of the electrodes inside the implanted cuff electrode divides it into three main types (fig.2.9), described as follow.

(a) Monopolar cuff

Monopolar cuff has a single electrode inside the centre of it and a neural recording is recorded between this centre electrode and a reference electrode, which is positioned outside the cuff. In order to maximise the recorded neural signal, electrode has to be positioned to the middle of the cuff, hence a smaller sized cuff can be made in a mono polar arrangement. [108]

(b) Bipolar cuff

Bipolar cuff has two rings of electrodes one on each side of the cuff. The neural recording is performed by taking differential measurements between the two end electrodes. The recording quality directly relates to the distance between them that is, greater the separation between the electrodes greater will be the

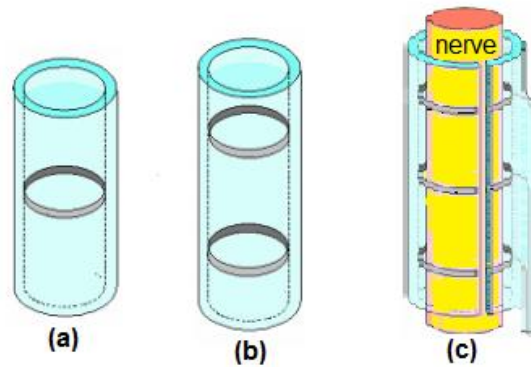


Fig. 2.10 Types of cuff electrodes. (a) monopolar cuff electrode with one ring electrode (b) bipolar cuff electrode with two electrode rings (c) tripolar cuff electrode encapsulating a nerve with three ring electrodes. Figure revised from Pachnis PhD. dissertation, 2010

amplitude of the recorded signal. It is shown that the amplitude of the recorded neural signal drops due to effect of external surroundings on it, when electrodes are moved at the end of the cuff. [109-110]

(a) Tripolar cuff

This is the most commonly used cuff among its types and offer several advantages. A typical tripolar cuff consists of three ring electrodes that are placed from an equal distance from each other inside the cuff. The neural recording is taken between the centre and the outer electrodes, whose quality is also dependent on the positioning of the end electrodes. The further the end electrodes are positioned in the cuff; the better-quality signal can be recorded. Under ideal conditions, the potential differences between symmetrically positioned end electrodes are equal and opposite in magnitude and hence, can be cancelled out using suitable amplifier configuration. On contrary, action potential is maximum at the middle electrode due to same potential differences between the two pair of electrodes (fig. 2.8). These two mechanisms, interference rejection and ENG amplification both are essential for reliable ENG recording. In contrast, to monopolar and bipolar cuffs, the tripolar cuff also offers the advantage of higher external interference reduction due to high signal-to-noise ratio, when connected with suitable amplifier configuration. [45-47, 111, 123-124]

2.4.2.2 Imbalance

Symmetry of the electrodes inside the tripolar cuff is very crucial for complete EMG interference rejection. Asymmetry of the end electrodes with respect to central electrode exploits the linearizing property of the cuff, due to increased tissue impedance between the pair of electrodes, resulting in a higher potential drop between them that are further apart. The interferences measured by both electrode pair are now unequal and cannot be cancelled out completely. The same effect can be observed if the tissue impedance inside the cuff changes or electrode impedance at the interface changes, due to inhomogeneous formation of tissue around the cuff with time. Rahal [110] introduced further imbalances in the cuff and named them “end-effects” (fig. 2.11). The field that field linearity inside the cuff is affected due its finite length which, causes amplitude drop of the neural signal at the end of the cuff. Triantis related this outcome to the orientation and proximity of the external source of interference with respect to the cuff. Even though imbalances reported effect the cuff property of EMG cancellation, but it does not affect the recording of ENG as with a suitable amplifier configuration these interferences can be rejected for efficient neural signal recording from the nerves. [112-113]

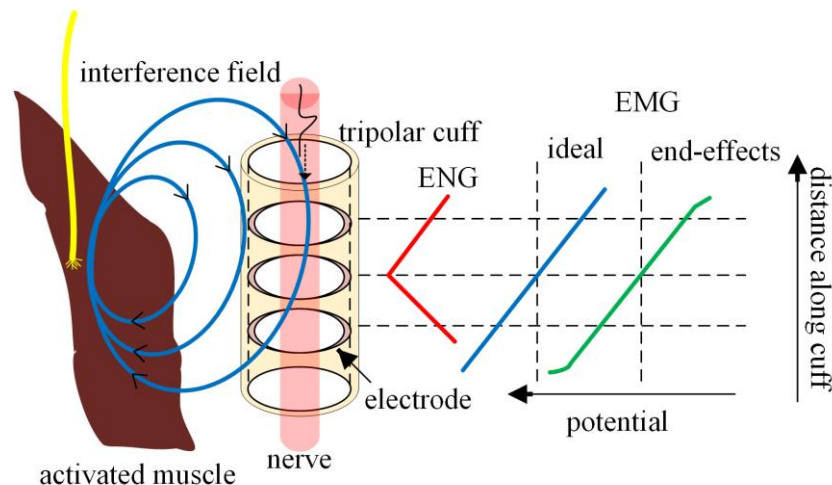


Fig. 2.11 ENG and EMG potential under ideal and real conditions. Muscle activity producing differential-mode interference causing voltage drop in tissue resistance. End-effects exploit cuff linearizing property making EMG unequal between the electrodes and does not result in its complete removal. [114]

2.4.3 Amplifier configurations

Tripolar cuff electrodes when used with a suitable amplifier configuration, can neutralize the interferences, giving a reliable ENG signal at the output. Quasi-tripole, QT and True-tripole, TT are the most common amplifier configurations tested with the tripolar cuff. A bigger and less power efficient amplifier might not be suitable to be used in the neuroprosthesis implant. In this section some amplifier configurations to be used with tripolar cuff are discussed briefly to understand the advantages and disadvantages they offer in terms of reliable ENG recording from the nerve.

2.4.3.1 The Quasi tripole (QT)

The QT configuration is the most known configuration that is used with the tripolar cuff to record neural information and EMG minimisation. It was first introduced and tested by Stein [38] in 1975. In this configuration (fig. 2.12), the two end electrodes of the tripolar cuff are short circuited, forming one end of an amplifier and offering an advantageous property of “screening-effect”. EMG current passes through the short-circuited electrodes instead of the tissue inside the cuff, reducing potential gradient of the interference in the tissue between outer electrodes. ENG forms the peak at the middle electrode that forms another input of the amplifier. The linearizing property of the configuration is due to cuff being a very good insulator. However, due to the imbalances reported under real conditions, the screening-effect and linearizing property both get affected. Some of the EMG current still passes through the cuff exploiting its screening-effect and linearizing property is also exploited with EMG potential inside the cuff not being completely equal and opposite, resulting in only partial cancellation of EMG. Unfortunately, QT does not offer any way to readjust the balance to remove interference completely [109, 112], but it offers the benefit of lower current consumption, due to the use of only one amplifier in the design as compared to other configurations.

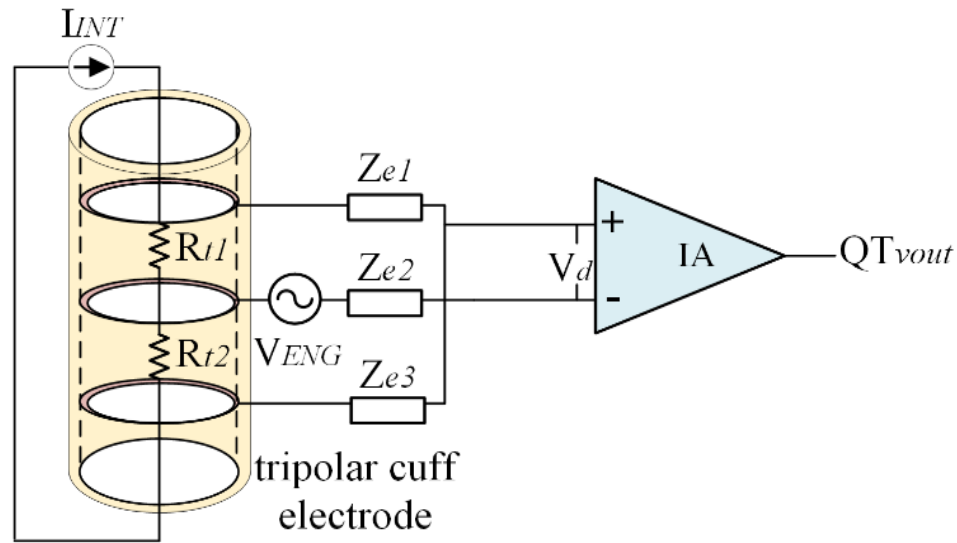


Fig. 2.12 The QT amplifier configuration with tripolar cuff electrode. EMG appears at R_{t1} , Z_{e1} and R_{t2} , Z_{e3} , while ENG forms peak at the middle electrode.

2.4.3.2 The True tripole (TT)

The TT amplifier configuration is another known configuration to be used with the tripolar cuff to record reliable neural signals with EMG minimisation. It was first introduced by Pflaum [111] in 1995 and consists of three differential amplifiers in the design. Electrodes of the tripolar cuff go as a pair in each amplifier and the output of these forms the input of the third amplifier (fig. 2.13). There are several advantages of this arrangement as compared to the QT. TT is insensitive to cuff electrode impedance mismatches due to high impedance at the amplifier's inputs. Although, it is more sensitive to cuff imbalance, but EMG interference can be rejected by adjusting the gain of the two differential amplifiers positioned in the 1st stage, equalizing the EMG in both sides and cancelling it out in the 2nd stage of the configuration. Recorded EMG signal is also double using TT. Hence, it is possible to cancel out EMG interference using TT configuration, but it also consumes a larger amount of current as compared to QT, making it unfavourable to be used in battery powered implants with low power requirements.

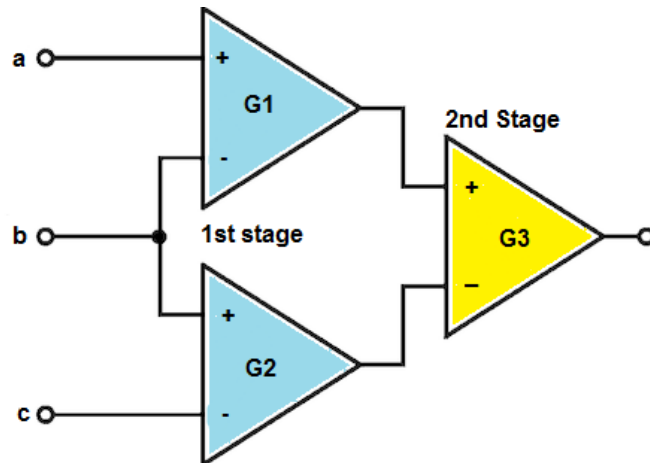


Fig. 2.13. The TT amplifier configuration, a, b and c points are linked to the electrodes in the cuff, EMG is removed but at the expense of more current consumption.

2.4.3.3 The Adaptive Tripole (AT)

The adaptive tripole is a modification to the design of TT that automatically adapts itself to adjust the cuff errors. It was proposed by Rahal [115] in 1999 and tested by Demosthenous and Traintis [118] in 2005. The adjustment of the first stage amplifier gains in TT can be made automatic by the AT (fig. 2.14). Automatic feedback gain adjustment of two variable gain amplifiers (G_1 and G_2) compensates the cuff imbalance, which are controlled by the feedback voltages α and $-\alpha$. The system amplifies the difference between the absolute values of the two variable gain amplifiers (first stage) in G_3 by comparing the amplitudes of their output and rectifying them. The output then goes into a long time constant integrator, producing potentials α and $-\alpha$, which are the feedback signals to G_1 and G_2 . Based on this information, G_1 and G_2 adjust themselves to make EMG equal and opposite to be cancelled out automatically at the output. [120] This amplifier configuration causes a further increase of the current consumption and therefore has the same drawbacks but more pronounced as a TT when integrated to an implant.

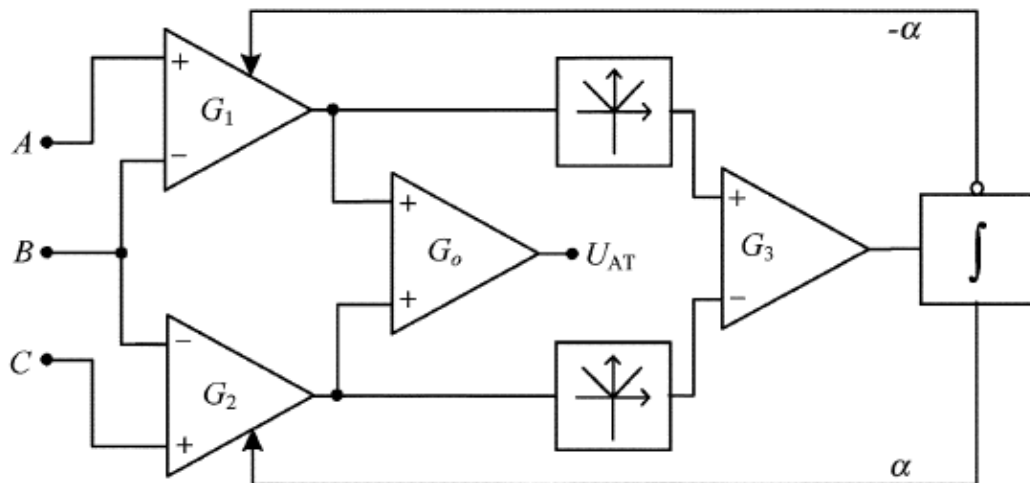


Fig. 2.14 Schematic of the Adaptive-Tripole for EMG minimisation and ENG recording. [112]

2.4.3.4 Other methods and amplifier configuration

There are other amplifier configurations as well that can be used to remove EMG interferences to detect an unaffected neural signal from the nerve. One of them is the screened-tripole (ST) [115] which, is derived from the TT configuration. This configuration also has three amplifiers like TT but with an additional pathway to bypass the current, so that less currents causing interference passes through inside the cuff. This path is provided by putting two electrodes at the ends of the cuff and short circuiting them. The signal-noise performance as compared to QT and TT configuration is better but at the expense of higher power requirements and bigger size which is not suitable to be used with battery powered implants. Other techniques that can be considered to record neural activity from the nerves by removing EMG interference are using high order analogue/digital filters to extract ENG signal from the EMG or by using other complex algorithms and artificial neural networks, but they all are not only systematically complicated [45, 115] but also require more power to be used at an implant level and hence, cannot be used as a favourable choice for neural signal recording with EMG neutralisation. [112, 125-128]

2.5 Specifications of Bioelectric Potentials

The recorded magnitude of naturally occurring neural ENG signals with the use of tripolar cuff is found to be in few microvolt range, typically between 3 to 10 μ V (fig 2.15a), in a bandwidth of 500Hz to 10kHz and maximum power below 3kHz, as shown in fig. 2.15a. Mechanically-evoked ENG signal in the figure is due to the firing of action potentials by several nerves at the same time. The difficulty in recording this small amplitude ENG signal is the presence of EMG interference from surrounding muscles. EMG is in millivolt range (fig. 2.15b), typically between 1 to 100mV, with frequency varying from 1Hz to 3Khz and most of the power concentrated at about 250Hz. [40, 95, 106]

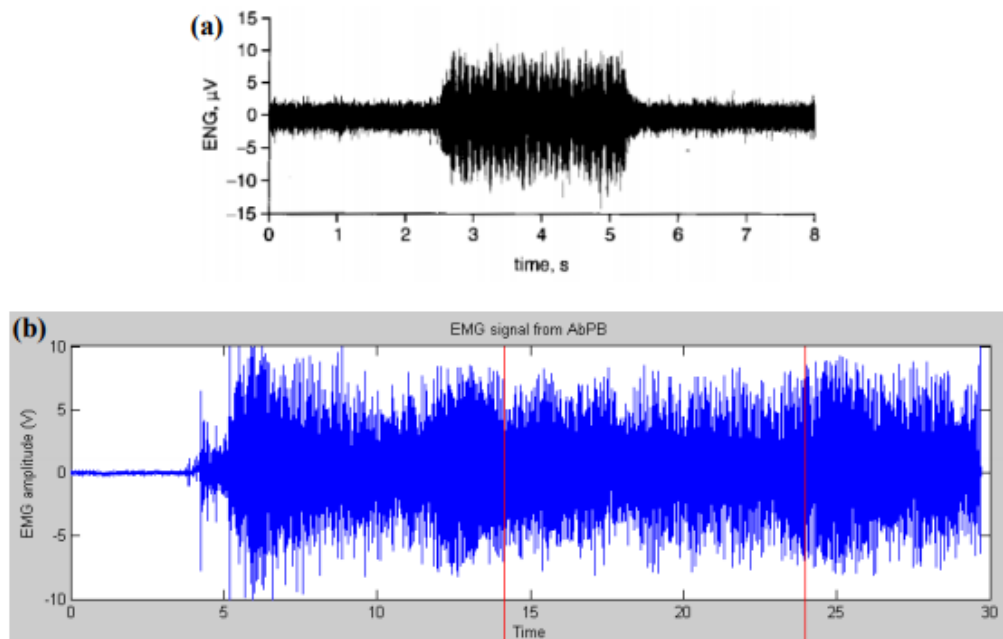


Fig. 2.15 (a) Mechanically ENG spectrum recorded from pig's sacral nerve using tripolar cuff electrode. Trace from Donaldson et al., 2003 (b) EMG spectrum showing amplitude in mV, recorded for about 30s, from the right-hand muscle of a female adult. Graph taken in courtesy from Implanted devices group, UCL.

This makes the extraction of the unaffected neural signal challenging as the required microvolt ENG signal is embedded behind the millivolt EMG interference. In order to record neural information reliably from the nerve, EMG

interference must be neutralised to an extent so that a clean ENG signal is extracted out for further processing.

The typical frequency range lies between 1-10 kHz for neural recording measurements of few μV using tripolar cuff, however this can be optimised for better neural measurements recording. For example, for the bladder control, Mathers [56] explained that with respect to nerve impulse propagation, within the immediate vicinity of the bladder, nerve impulses travel at speeds neighbouring 60 m/s near the roots where the nerve cells have diameters ranging from 7 to 14 μm . This means that more nerve activity can be observed at higher frequencies where the diameter of the nerve is large as well. Also, neural measurements at lower frequencies will not be picked up by the electrodes due to their design limitations and due to less activity in the smaller part of the nerve. [66] Therefore, the bandwidth of interest is selected to be between 500Hz to 10 kHz for this project, to detect reliable ENG signals by neutralizing or removing EMG interferences in that range.

2.6 ENG underlying Recording Theory using Cuff

The nerve root or a single nerve fibre can be used to record neural ENG signal by placing cuff around it. For an active nerve root source, the potential of the extracellular field inside the nerve root is because of the sum of the total electric field of each active fibre. [96] Single-fibre action potential (SFAP) is when one fibre is active and compound action potential (CAP) is when most or all nerve fibres become simultaneously active. Naturally occurring ENG has a smaller amplitude than CAP due to the simultaneous firing of many neurons. [47, 109] As a tradition, cuffs are designed on the basis of SFAP amplitude optimisation so in applications where CAP is of an interest rather than SFAP, the obtained results are linked to the root mean square value of the neural signal. [130] However, in literature [109] ENG measurement using cuff electrodes advances in terms of SFAP measurement for both myelinated and unmyelinated nerve fibres. It should also be noted that apart from interference, the amplitude of ENG signal, when recorded, also depends on cuff dimensions, its positioning around the nerve and number of electrodes inside it. [45, 130-131]

Many models have been presented to show neural signal registration from a myelinated nerve fibre using cuff electrodes, however here only one example is presented for readers understanding. Fig. 2.16 shows the schematic representation of how action potential is constructed inside the cuff. It is seen that the shape of single fibre action potential (SFAP) is highly influenced by the cuff dimension. [130-131] Similar action currents are generated by each node of Ranvier when an action potential passes through a nerve fibre. Each action potential is postponed by the time of propagation it takes to travel from a node to the next. The delayed t_d from one node to the next is the internodal distance over the conduction velocity in meter per second. The action current changes with the diameter of the nerve fibre linearly. This is because of the direct relationship between the area of the node of Ranvier and diameter of the fibre. [127, 130-131] As action potential moves in the nerve fibre, it reaches each respective node at a specific time. This results in production of an action current because of the activation of current sources and the same signal now appearing at differing times are conducted by the electrodes installed within the cuff. This expansion of an action potential will now activate many nodes of Ranvier at once and hence, the single fibre action potential recorded by cuff is due to the superposition of all same but delayed action currents. The SFAP at its peak in the centre of the cuff can be calculated by the following equation [130], where $i_{ac}(t - k.t_d)$ is the action current that is delayed, and H_k is the network function relating each point of node k to the electrode in the cuff.

$$\text{Single fibre action potential, } SFAP(t) = \sum_{K=1}^{\text{no.of nodes}} (i_{ac}(t - k.t_d) \otimes H_K(t))$$

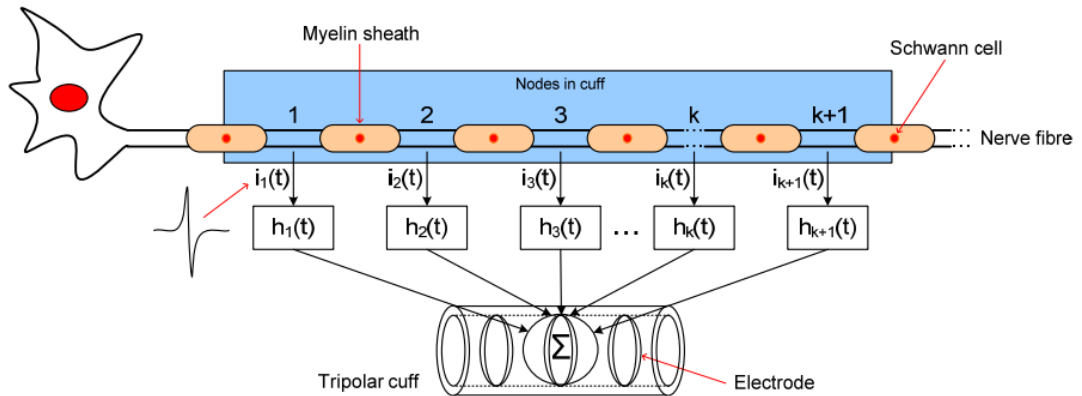


Fig. 2.16 Illustration of SFAP recorded using cuff electrode, due to addition of current sources at each node of Ranvier, delayed by the time t_d with respect to node k . [figure taken from (Andreasen 1997)].

The transfer function is almost negligible for nodes outside the cuff, hence making prominent contribution by the nodes inside to the single fibre action potential (i.e., ENG). Therefore, this is how SFAP is recorded by the nerve cuff electrodes when action current passes through the nerve. [130]

2.7 Effect of Interface Impedance on Neural Signal Recording

Impedance characterisation of electrode-electrolyte interface is important in neural signal recording due to the occurrence of undesirable electrochemical reactions at the interface and its effect on minimising EMG interference during neural signal recording. In the following sections, the electrode-electrolyte interface impedance is briefly explained and how it can be represented with some equivalent circuit models, which will be used later for EMG minimisation using tripolar cuff electrodes.

2.7.1 Charge Transfer

Stimulation and sensing of nerve fibres by cuff electrodes is based on the charge transfer across the interface between the tissue and electrode. For in vitro investigations this interface is often represented by a contact between metal surface and saline [132-135]. The Faradic and non-Faradic mechanisms are mainly involved in the charge transfer at the electrode-electrolyte interface. Non-Faradic charge transfer involves capacitive charge and no electrons move between electrode and electrolyte. This is due to the rearrangement of the charged chemical species in the electrolyte and their adsorption and desorption at the electrode surface. Faradic charge transfer whereas, involves the transfer of electrons at the interface of electrode and electrolyte due to the occurrence of redox reactions at the electrode. [136]

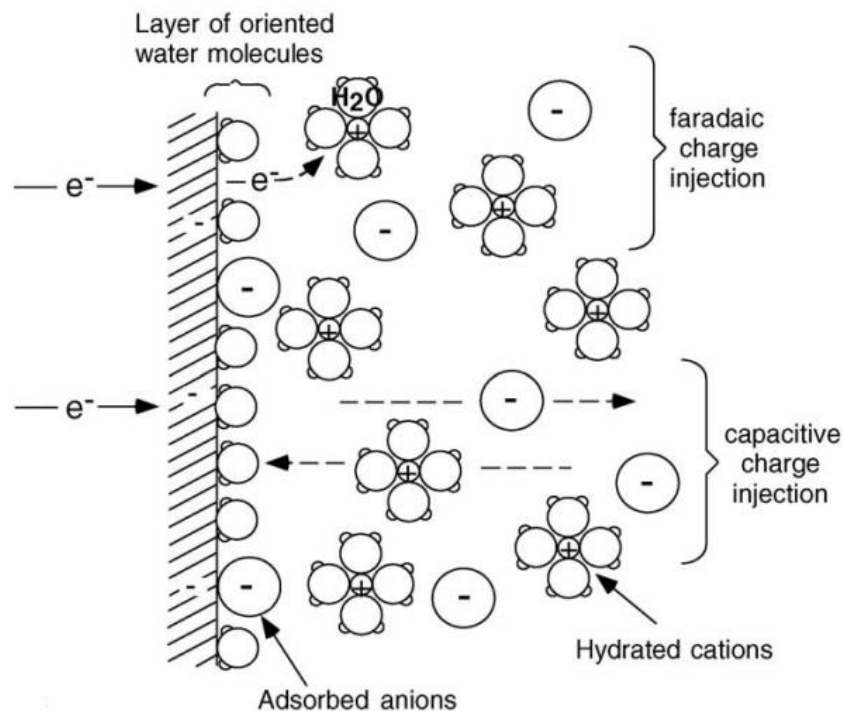


Fig. 2.17 Faradic and non-Faradic charge transfer at electrode electrolyte interface.

[136]

2.7.1.1 The Double Layer

The transfer of charges at the electrode-electrolyte interface results in the formation of a double layer, in a non-faradic charge transfer. This can be modelled by a simple capacitor known as double layer capacitor, C_{dl}. The formation of C_{dl} is due to various physical phenomenon, whose in-depth details are beyond the scope of this writing but can be found in [137-141]. When a negative metal electrode is placed in an electrolyte, charge distribution occurs between the electrode-electrolyte ions. The positive charged ions move from the electrolyte towards the negatively charged electrode. This results in the formation of a rigid layer of opposite charges near the electrode, separated by the solvent layer hence acting as a dielectric. At this point, the negatively charged ions on the electrode and positively charged ions are electrically neutral at the interface, due to being equal and opposite. The opposite process occurs at the other electrode and the ions exchange process is also reversible if the voltage polarity

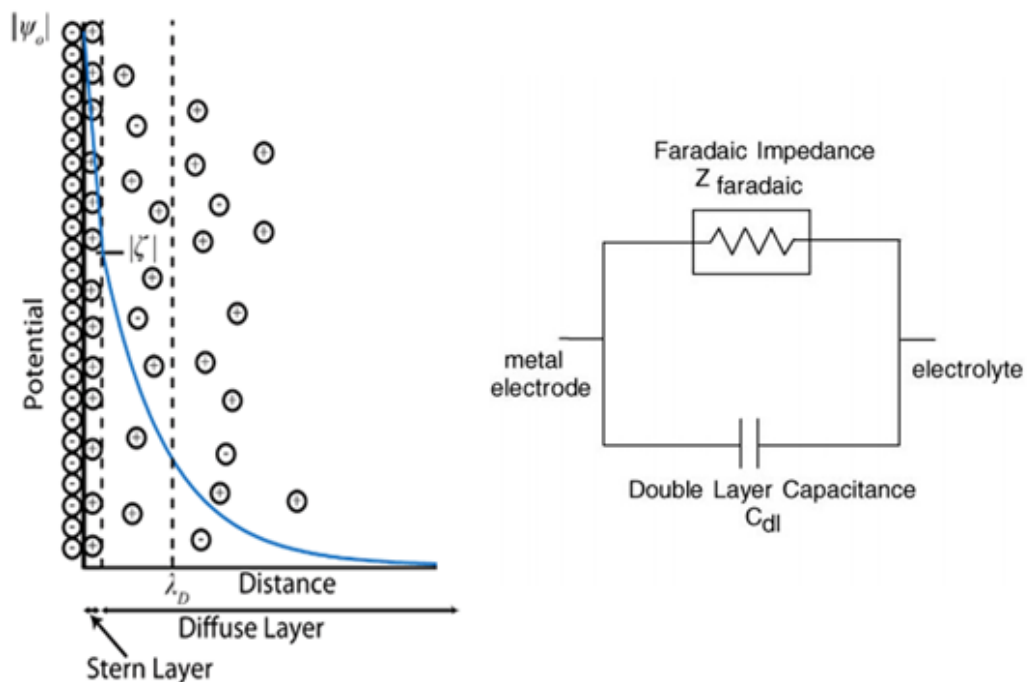


Fig. 2.18 Left figure showing the double layer model by Stern and the right figure shows the equivalent circuit model due to transfer of electrons at equilibrium (Stern layer). [136]

at the electrodes are changed. However, even at the resting stage when voltage

is not applied externally, constant exchange of electrons [141] occurs due to electrochemical reactions across the energy barrier. This movement of electrons faces a resistance known as a charge transfer resistance, R_{ct} . Hence, the total interface impedance due to the double layer can be modelled by a parallel combination of a capacitor a resistor of leakage resistance. [136, 142] This model represents the process of charge transfer at the so called pseudo-capacitive (due to being frequency and potential dependent) electrode-electrolyte interface. Thus, it can be concluded that in neural signal recording, the interface impedance between cuff and nerve cannot be modelled by a simple R and C and they have pseudocapacitive impedance behaviour at the interface.

2.7.1.2 The Polarisation Impedance

Many equivalent circuit representations have been proposed to mimic the interface impedance. Warburg [147] in 1989, represented the interface impedance with a polarisation resistor in series with a polarisation capacitor, the magnitude of which is indirectly proportional to the square root of frequency while the phase angle is frequency independent, with a fixed value of 45° . However, it was later found that this model was inconsistent to represent electrode-electrolyte interface impedance at low frequencies because of its impedance not varying inversely with the frequency and specially when there is also a high direct current resistance at an interface. This led to further research and development of better electrode-electrolyte impedance models in which polarisation impedance of different electrodes at the interface was observed for a wider frequency range. [133, 135] The two well-known models for describing electrode-electrolyte impedance are the Randles and Cole circuit models.

Randles [148] circuit model proposed in 1947, is shown in fig. 2.19. It consists of an active electrolyte resistance (R_{access}) in series with the double layer capacitance, C_{dl} which in turn is parallel to the impedance of a faradic reaction. Impedance of a faradic reaction consists of a resistor due to active charge transfer at the interface in series with a specific electrochemical element called Warburg element, representing diffusion process at the interface. R_{ct} is due to

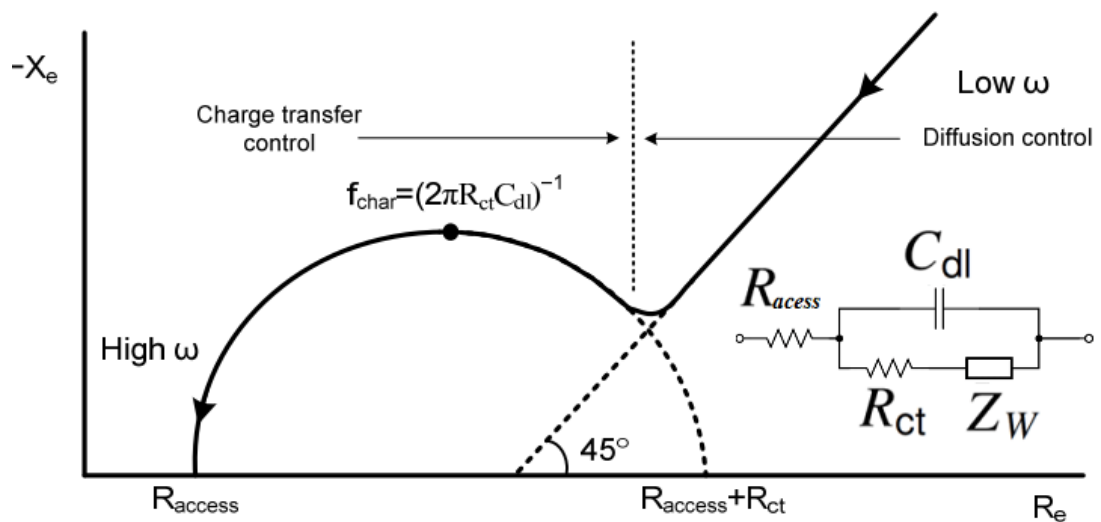


Fig. 2.19 Randles equivalent circuit model on the right. R_{access} is active electrolyte resistance, R_{ct} charge transfer resistance, Z_W Warburg element. Nyquist plot using Randles model, showing impedance characteristics at high and low frequencies. Bulk resistance is dominating at high frequencies, and ions diffusion process at lower frequencies due to C_{dl} dominance. Nyquist plot reproduced from [143]

charge transfer resistance at the interface, while R_{access} is the active electrolyte resistance depending on the electrode geometry. It is frequency independent over a larger frequency range, including frequencies that are of interest in human physiological applications. [144] Randle model shows that at high frequencies, the access resistance dominates due to short circuiting of the capacitance, while at lower frequencies, Warburg element dominates resulting in ions diffusion process from electrolyte to the interface. (fig 2.19).

Cole [143] model proposed in 1940, shown in fig 2.20a. It replaced double layer capacitance, C_{dl} with a new impedance element known as constant phase element (CPE). It has a simpler model than Randles and consists of a parallel network of charge transfer resistance, R_{ct} and constant phase element (CPE), which are in series with an active electrolyte resistance, R_{access} . It can be described with the following equation, proposed by Cole to explain the complicated impedance contours observed at the tissue-electrode interfaces. [143]

$$Z = R_{\infty} + (R_0 - R_{\infty}) / [1 + (j\omega/\omega_0)^{\alpha}] \quad (2.2)$$

Where ω_0 , is the angular frequency, R_{∞} is the access resistance dominating at higher frequencies, R_0 is the resistance seen at lower frequencies and α lying in the range of 0-1 is a numerical constant with no dimensions. Simulating this relation gives a circular arc as shown in fig 2.20b, from which resistance values can be calculated as CPE phase, ϕ_{CPE} allows the circulation of α from low to high frequencies.

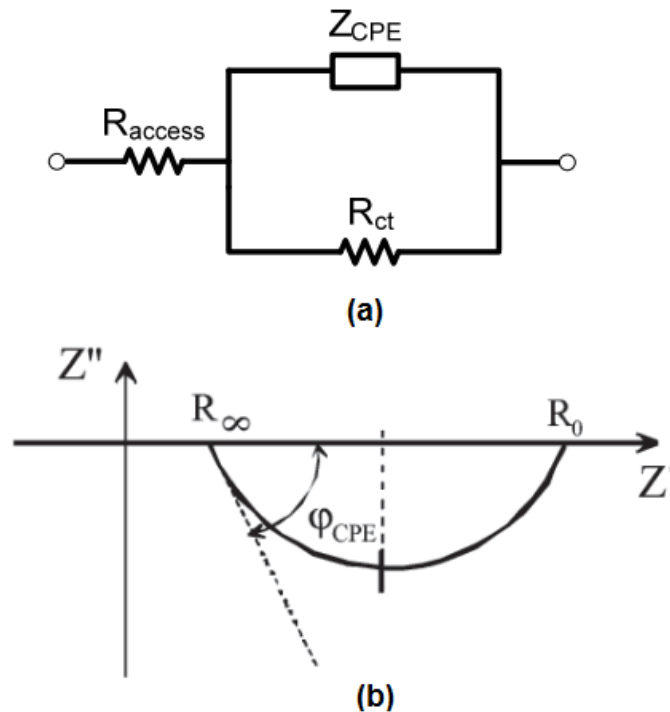


Fig. 2.20 (a) Cole model in which Cdl is equated to Z_{CPE} . (b) Impedance loci of Cole model, R_{∞} showing resistance at high frequencies and R_0 showing resistance at low frequencies. Dotted line shows Z_{CPE} and ϕ_{CPE} is an angle of CPE. Loci model graph reproduced from [146].

2.7.1.2.1 The Constant Phase Element (CPE)

In Cole model, double layer capacitance, C_{dl} is equated to polarisation capacitor, Z_{CPE} . CPE represents the double layer capacitance in the presence of the surface irregularities and chemical reactions at the interface. It hence, gives a measurement of the impedance due to non-faradic charge transfer at the interface and is defined by an equation,

$$Z_{CPE} = K(j\omega)^{-\alpha}$$

Where, K is the magnitude of Z_{CPE} independent of angular frequency, ω , and phase depending on the constant α , due to which this impedance is being named as CPE. Z_{CPE} is purely capacitive for $\alpha = 1$ and purely resistive for $\alpha=0$ and typically lies between 0.5 and 1 for ideally polarizable electrodes. [145] For $\alpha=0.5$, CPE represents Warburg but both models represent different interfacial reactions at electrode-electrolyte interface. [133, 149] Unlike Warburg, at decreasing frequencies CPE element shows no transition from extensive to intensive behaviour because of the exclusion of diffusion process, that was not to be seen at concerned frequencies in many physiological applications. Due to this, studies also revealed that CPE can be the best model to represent the polarisation impedance loci observed at the both biological and electrochemical interfaces. [150-156] The metal electrodes also showed a constant phase angle at lower frequencies and hence Cole model with less parameters as compared to Randles model seems a better choice to represent electrode-electrolyte interface impedance using cuff electrodes. [150-151, 156] Cuff electrodes have a polarisation impedance that does not change with frequency like simple RC. It has a pseudocapacitive impedance at the electrode-nerve tissue interface and CPE can be used to successfully mimic such impedance. Generally, there are two approaches to model CPE at the interface. One is to construct a circuit mimicking the frequency behaviour of the electrodes and the other is by the geometrical or topological structure of the electrodes [146, 154]. However, CPE cannot be realized accurately with discrete passive elements and many models that are available, they can only approximate the properties of CPE. [150-155] How helpful the realisation of electrode-electrolyte interface with circuit model

using CPE can be in EMG neutralisation, will be explained with results in the next chapter.

2.8 Summary

This chapter provided a literature review of the human spinal cord injury and neuroprosthesis before going into the details of neural signal recording. It first explained the spinal cord injury and its effect on the nervous system followed by the discussion of different techniques that can help in restoring the life functionalities of the SCI victims. Neuroprosthesis and its use in improving the life of SCI patients is explained. Closed loop techniques particularly functional electrical stimulation, FES is discussed as they provide automatic adjustment without requiring external sensors. Major emphasis is laid on the type of electrodes that can be used by FES systems in recording neural information from the nerves. Advantages and drawbacks of using surface and implanted electrodes are discussed and cuff electrodes being non-invasive and suitable for long term neural recording are favoured. The required ENG signal to be recorded is embedded behind the interferences from the surrounding muscles so different amplifier configurations to be used with cuff electrodes are discussed to record neural signal by removing interferences from it. Imbalances are reported in real using cuff electrodes hence different amplifier configurations were discussed specially in terms of their size and power requirements for imbalances neutralization. QT is simple with less power requirement but offers no way to adjust imbalances externally. TT and AT can neutral interference by adjusting their gains but suffer from high power requirements that are not suitable to be used with battery-powered implants. A brief literature review is also provided on the effect of interface impedance on neural signal recording using electrodes, whose further details will be provided in the next chapter, where a novel technique of minimising EMG interference is shown by simulations and in vitro verifications.

CHAPTER THREE

The Novel Technique of EMG Reduction for Neural Signal Recording

3.1 Introduction

The neural signal that is recorded using tripolar cuff electrodes is contaminated with the myoelectric interference, which appears at the output of the amplifier. This chapter presents a new technique of EMG minimisation and demonstrates its efficacy by saline-bath experiments. As discussed in the previous chapter, Quasi-tripole (QT) with tripolar cuff electrodes, is beneficial as it has a screening effect and only used one differential amplifier. However, it has a drawback as it offers no way to adjust the balance [109. 112] to remove interference. True-tripole (TT) is insensitive to electrode interface impedance and gives approximately double ENG signal but suffers from the presence of two front end amplifiers; doubling current consumption as compared to QT. [111] Similarly, adaptive-tripole (AT) automatically adjusts the cuff errors but suffers from high power requirements than TT and QT as it utilizes six operational amplifiers (two variable gain amplifiers, three differential amplifiers, one feedback amplifier), a comparator, two rectifiers and an integrator. [118] Battery powered implants faces the challenge of achieving low power consumption, making QT favourable to use. Its modified version known as modified-quasi tripole (mQT) allows the conventional arrangement of QT to remove interference by using a simple passive technique. [49]

Here, the reader is first introduced to the theory of mQT and passive EMG minimisation technique, followed by the proposal of a new passive technique of reducing EMG, using simple compensation circuits with it. The ability to neutralise interference is demonstrated through number of silico and invitro preparations.

The benefits and the limitations of the technique are also discussed in terms of improving the quality of recorded neural signal in neuroprosthesis. Lastly, the effects of optimisation of discrete components of compensation circuit in terms of power requirement using scaling are also discussed, along with the highlight on the possibility of using a new method, general idea of which is presented in appendix 1 of the thesis.

3.2 The Modified QT, mQT and Passive Neutralisation

Struijk and Thomsen [46] in 1995 presented a modified version of the conventional QT, by recognizing that imbalance in the cuff causes EMG interference. To test this, they connected potentiometer to the outer to allow adjustment. A small improvement was found to be possible using manual trimming in experiments. Imbalance can be due to tissue resistance, R_{t1} and R_{t2} or due to electrode impedances Z_{e1} and Z_{e3} . In order to reach null EMG breakthrough using QT, the ratio of the two tissue resistances must be equal to the ratio between the two electrode impedances at the amplifier output, which is not seen under real conditions. Interference current, EMG (labelled I_{INT}) flows through Z_{e1} and Z_{e3} that needs neutralisation, whereas Z_{e2} only forms the input of the amplifier with high input impedance, where ENG signal appears. [50]

Pachnis et al. [50] proposed that QT is analogous to Wheatstone bridge. The two tissue resistances, R_{t1} and R_{t2} between the electrodes forms one side of the bridge while the two electrodes impedances, Z_{e1} and Z_{e3} forms the other side of the bridge (fig 3.1). Any imbalance in the cuff appears at the output of the bridge, V_d , that forms the differential input to the QT amplifier. The V_{INT} is a voltage source for the EMG that sends the interference current, I_{INT} into the cuff, resulting in a drop of potential across its end electrodes. Thus, the EMG output (V_d) at the input of the QT amplifier is:

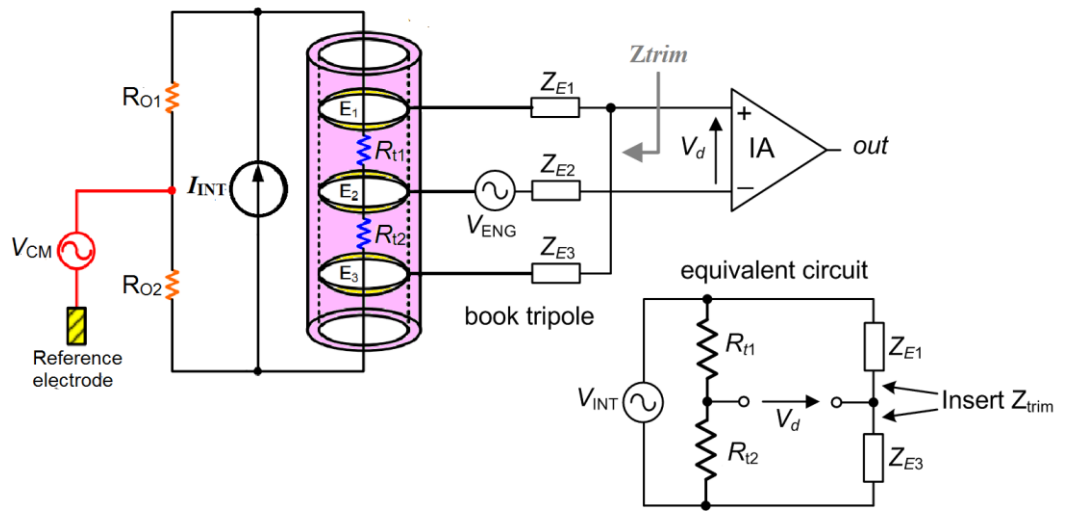


Fig. 3.1. Tripolar cuff electrode model attached to the QT arrangement. It shows three electrode impedances and two tissue resistances. Two tissue resistances and two end electrodes impedances form the analogy of Wheatstone bridge, EMG appears here that needs to be cancelled out, while ENG appears at the middle electrode. Balancing the bridge by inserting Z_{trim} to either end of outer electrodes is equivalent to EMG cancellation at the amplifiers input. V_{CM} is a common mode interference, that can be removed [157] by adjusting the potentiometer so that source resistances seen by the amplifier becomes equal and cancels out.

$$V_d = \left(\frac{R_{t2}}{R_{t1} + R_{t2}} - \frac{Z_{E3}}{Z_{E1} + Z_{E3}} \right) V_{INT} \quad (3.1)$$

which shows that the bridge is balanced when the ratios between the two resistances and the two impedances become equal ($R_{t1}Z_{E3} = R_{t2}Z_{E1}$). [49, 160] This causes the output V_d to become zero and hence no EMG interference appears at the input of the amplifier. Balancing is achievable by adding a compensation circuit to either end of the outer electrodes. However, unfortunately experimental results revealed that when bridge was tried to be balanced using simple RC filter, EMG interference was not completely neutralised. It was only minimised at the spot frequencies and not linearly in the entire frequency bandwidth of interest. This shed the light on the fact that simple RC filters cannot be used to balance the bridge as electrodes impedance does not behave like a parallel RC [117] and electrode-electrolyte interface needs to be considered. The

electrode-electrolyte interface can be represented by the constant phase element (CPE) as discussed in the previous chapter. Also, as the EMG interference minimisation at the spot frequency is of little importance for reliable neural signal recording, CPE behaviour of the recording electrodes was considered, to be used as a Ztrim with mQT. Experimental results yielded EMG reduction by a factor of 10 at all frequencies but with the use of large 20 stages non- uniform RC ladder network [50] that might not be suitable to be used with an implant with less power and smaller size requirements. Thus, in this work, the approach of balancing the bridge using CPE is carried forward, with the proposal of new simple compensation circuits, explained in the next section.

3.3 Principle of EMG Reduction using Simple RC Compensation Circuits as Z_{trim}

In this section, principle of EMG minimisation using simple RC compensation circuits as a Z_{trim} with mQT is presented, followed by the experimental method, simulation and experimental results. In the previous chapter, effect of electrode-electrolyte interface on neural signal recording and its chemical nature were discussed. Models that better resemble complex chemical interface of recording electrodes, when used as a Z_{trim} can improve the EMG minimisation linearly without requiring tuning, in the entire frequency band of interest [117], as series or parallel RC circuits are too simple to mimic the impedance at the interface and hence do not linearly minimise EMG. This is because for equal phase angles, a

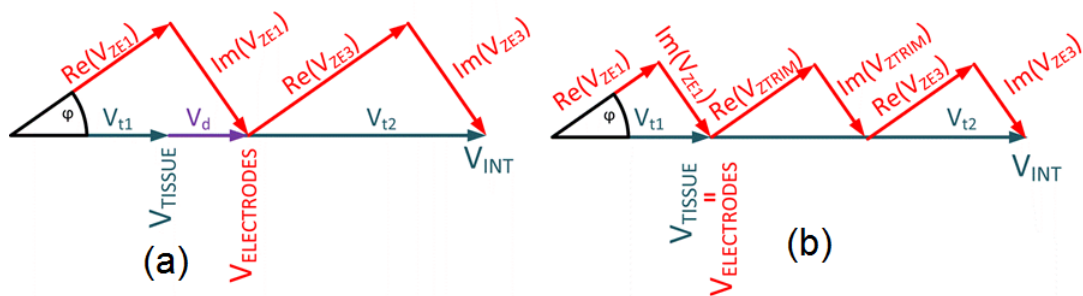


Fig. 3.2. Figure showing phasor representation for bridge of fig. 3.1. (a) $R_1 \gg R_2$ but $Z_{E1} = Z_{E3}$, the source voltage follows the current through electrodes by phase difference $\phi_{ZE1} = \phi_{ZE3}$. (b) Z_{trim} added to balance the bridge that has the phase with phase difference at that frequency, $\phi_{ZTRIM} = \phi_{ZE1} = \phi_{ZE3}$. Figure updated from [164]

small Ztrim with same phase angle can null the interference at a single frequency, however impedance with unequal phase angles require a Ztrim with phase difference at that frequency, as shown in the phaser diagram fig 3.2.

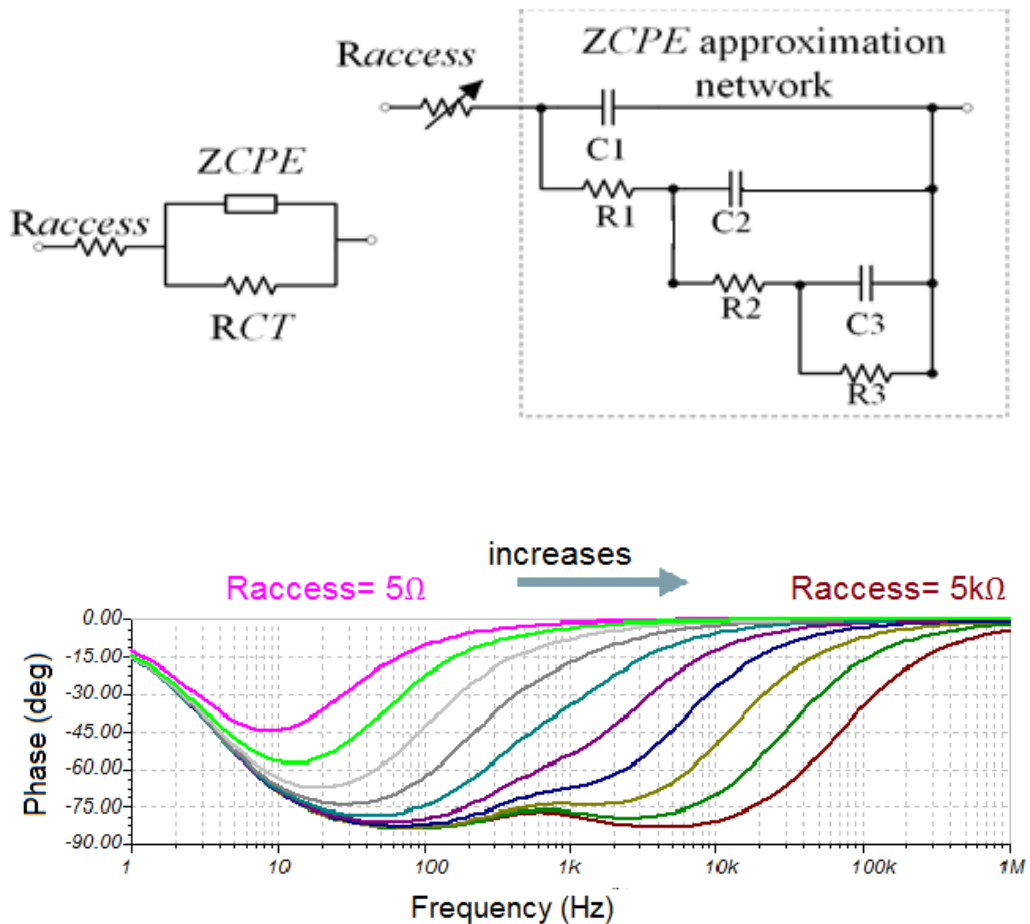


Fig. 3.2. Top figure showing model used for CPE of recording electrode. Bottom phase graph shows, how forcing Ztrim to behave like CPE is achieved using 3 stage RC network by varying active electrolyte bulk resistance, R_{access} from 5Ω to $5k\Omega$. Brown line represent phase output using $5k\Omega$ and pink line shows for 5Ω . Forcing Ztrim to behave like CPE is likely to remove interference irrespective of the frequency.

Hence, as described the motivation is based on the fact that models replicating the interface impedance of the recording electrodes should be considered to neutralise the EMG interference at the bridge output. The recording electrodes impedance can be realistically modelled by a CPE and where more complicated

forms of CPE are available [144], we proposed that impedance profile of our platinum recording electrodes can be realistically modelled (method shown in the next section), with a CPE in series with active electrolyte (access) resistance [163], leading to a simpler 3 stages RC ladder network (fig. 3.3). This RC ladder network forces Ztrim to behave like CPE and balances the bridge by neutralizing EMG linearly in the entire frequency band of interest.

Ideally, EMG interference must be nullified completely to record reliable neural signals, however in reality complete rejection of EMG is challenging due to noise being added from external sources other than EMG and due to discrepancies expected between the simulations and experimental results of CPE evaluation. Therefore, the optimum target to reduce EMG interference by balancing mQT(bridge) as close to the null as possible, so that ENG signal is obtainable without being overlapped with the EMG interference.

3.4 Experimental Setup and Method

There are two major test scenarios to be tested to see the effect of our proposed Ztrim compensation circuits for EMG reduction. The first was the impedance modelling of the tripolar electrodes and the second was the determination of the interference rejection behaviour of the whole cuff electrode. The steps taken to evaluate the performance of EMG minimisation using proposed Ztrim compensation networks in this work, are summarised in the flowchart below (fig. 3.3).

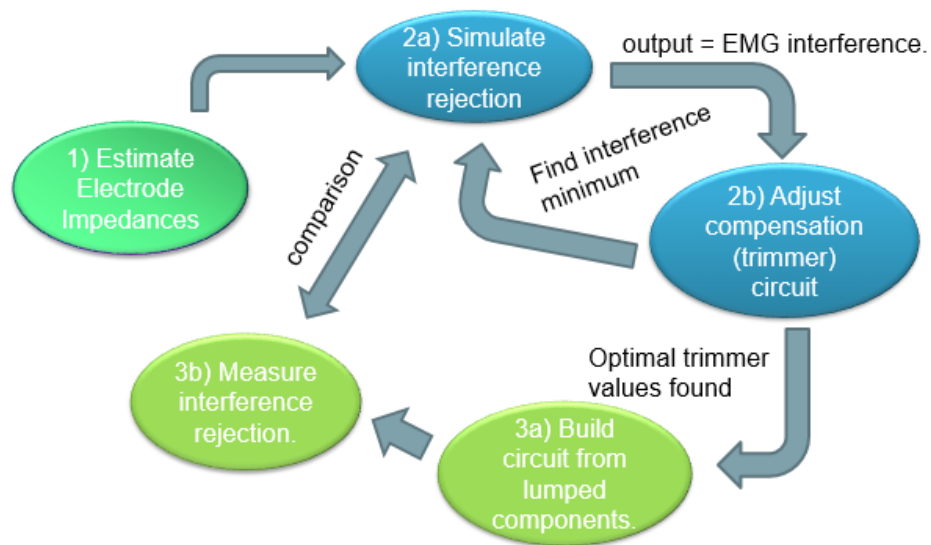


Fig. 3.3 Steps taken to evaluate performance of proposed simple RC networks to be used as Ztrim with mQT.

3.4.1 Electrodes Impedance Modelling

The most important property of the electrodes model was that it reproduces the impedance behaviour of the tripolar cuff, using which equivalent circuit model of the tripolar cuff could be established for the simulations. There are three different approaches to do impedance modelling. [165] First is to make a complete distinction between all processes contributing to the impedance behaviour and integrating them separately. This approach establishes a model as complex as the process itself. Second is to identify the processes that make the largest contribution to the charge transfer, finding the simplest electrical equivalent that comprises all these structures. Third is to review the impedance interface as a black box, making extensive measurements and finding the electrical circuit that matches the electrical behaviour. We opted for the black box approach as it was simple and more suitable to achieve the aims of an equivalent circuit which meets the impedance behaviour. The development of the equivalent circuit shown in fig 3.2 was based on the assumption that there has to be one capacitive path and one purely resistive path of charge transfer from active electrolyte (R_{access}) to

the electrode metal. The capacitive path was meant to represent the non-faradic charge transfer of double layer and sorption (capacitor and a resistor in parallel) while the resistive path should model the contributions of faradic charge transfer. The decision for the equivalent circuit of CPE built up from three capacitors and three resistors was a trade-off between complexity of the model and achieved quality of experimental electrode impedance fitted data on it.

For this purpose, a test set up was first needed to build to record impedance profile of the recording electrodes in invitro preparations. The test setup used for impedance modelling of electrodes is shown in fig 3.4. It consists of a T-shaped Perspex tank with a capacity of about 20ml for the electrolyte. The book-electrode was used to represent platinum foil electrodes in tripolar configuration. It was fixed to the bottom of the tank using a silicone sealant, to avoid its movement during experiments. The middle electrode in the book was intentionally made offset with respect to the outer electrodes of the book, so that EMG current when passing through it produces a differential input to amplifier (distance between electrode 1 and 2 was made more than the distance between 2 and 3). EMG current passes through the book through the two outer stainless-steel electrodes installed opposite to each other on the tank corners, while the third electrode installed on the tank's perpendicular arm was used as a reference electrode (connected to the mains earth). Measurements should be carried out in the conditions that could be adapted to the actual ambient conditions in the body, so a saline matching conductivity of human cerebrospinal fluid was added at a room temperature into the tank. This conductivity was reported to be of 15.95mS/cm in the frequency range of 0-10kHz. [166] Before conducting an experiment, the setup was thoroughly cleaned with deionized water and EMG electrodes and reference electrode with isopropyl alcohol, to avoid any contamination during experiment. It was made sure that no bubbles appear during verifications because of the possibility of electrolysis in the tank.

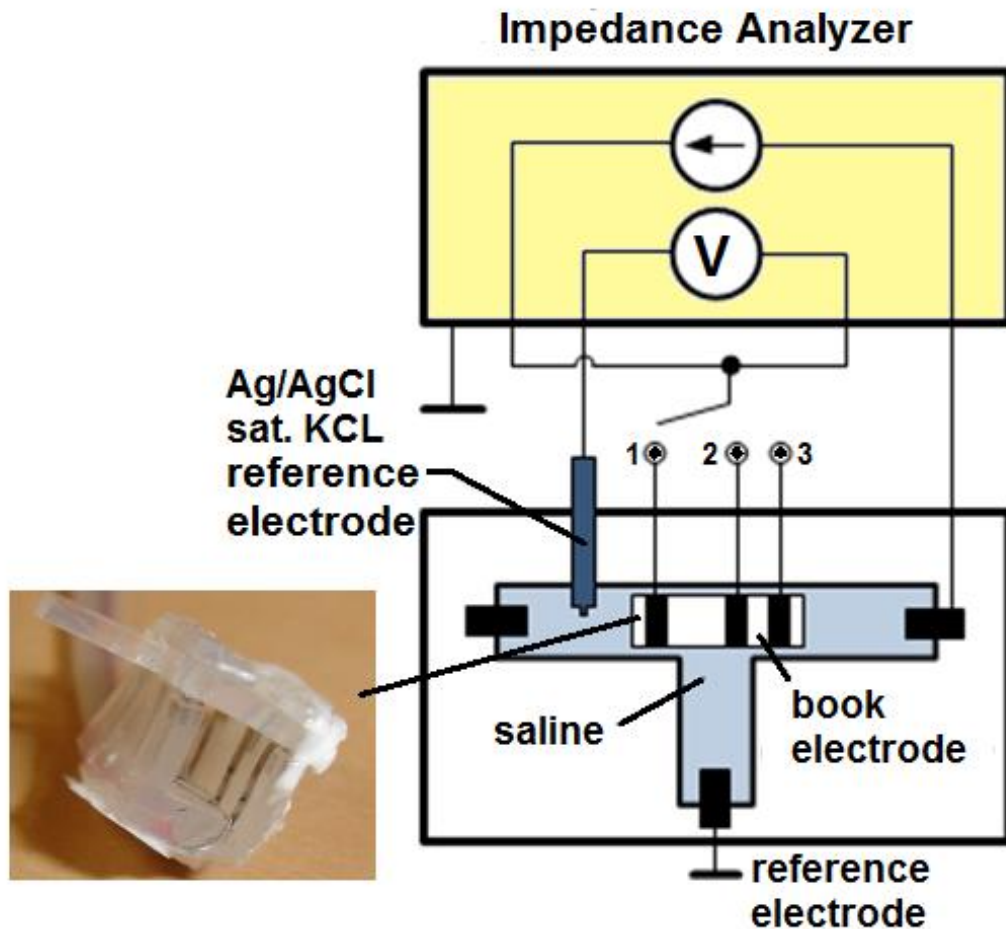


Fig. 3.4 Test apparatus used to measure impedance of electrodes in the book arranged in tripolar configuration (middle electrode offset). Ag/AgCl sat. KCl was used as a reference electrode and transimpedance was recorded for each electrode using impedance analyser. Picture on the left shows the real book electrode used in the tank.

For recording impedance profile of individual electrodes in the book, another reference electrode Ag/AgCl sat. KCl was used, that was placed between the book electrode and the working electrode. The electrodes impedance measurements were carried out using an impedance analyzer (Wayne Kerr, series 6500b), in the frequency range of 500- 10kHz. The lowest adjustable current value of 200uA of the machine was used as a drive current (EMG) and the resulting differential voltages were recorded between the reference electrode and the chosen book electrode, in the frequency range of interest. Experimental data of each electrode in the book was then imported into the impedance data fitting software EC-Lab (Bio-Logic, Science Instruments), which varied the RC

parameters of a given equivalent circuit of CPE (fig. 3.2) to optimally fit on the experimental results. Using discrete component values obtained through this impedance data fitting software, an equivalent circuit model of whole tripolar cuff electrode (in the form of book) was constructed to be used later in the simulations (fig 3.5).

3.4.2 Interference Reduction Testing of Ztrim Compensation Circuits

The tripolar book model simulated in Cadence IC6 circuit simulator is shown in fig. 3.5. The compensation circuits to be used with the model as Ztrim are simple RC, 3-stage RC ladder network (Ztrim1) and its even simplified version 2- stage RC ladder network (Ztrim2). The values of the compensation circuits were found by global optimization procedure in the software. RC components in the proposed CPE model are dependent on each other in a recursive pattern in each step, hence only the first R and C parameters of the Ztrim compensation circuits were varied, while the rest being dependent on them, in same ratios as in the sole impedance model of the recording electrode. The R and C components were varied until the EMG interference at the output voltages was minimised as close to null as possible, with a benefit of tweaking compensation circuit impedance for further EMG adjustment if required. The circuit parameters used in creating a cuff model from measured individual electrode impedances are shown in table 1 and values obtained for Ztrim compensation circuits are shown in table 2.

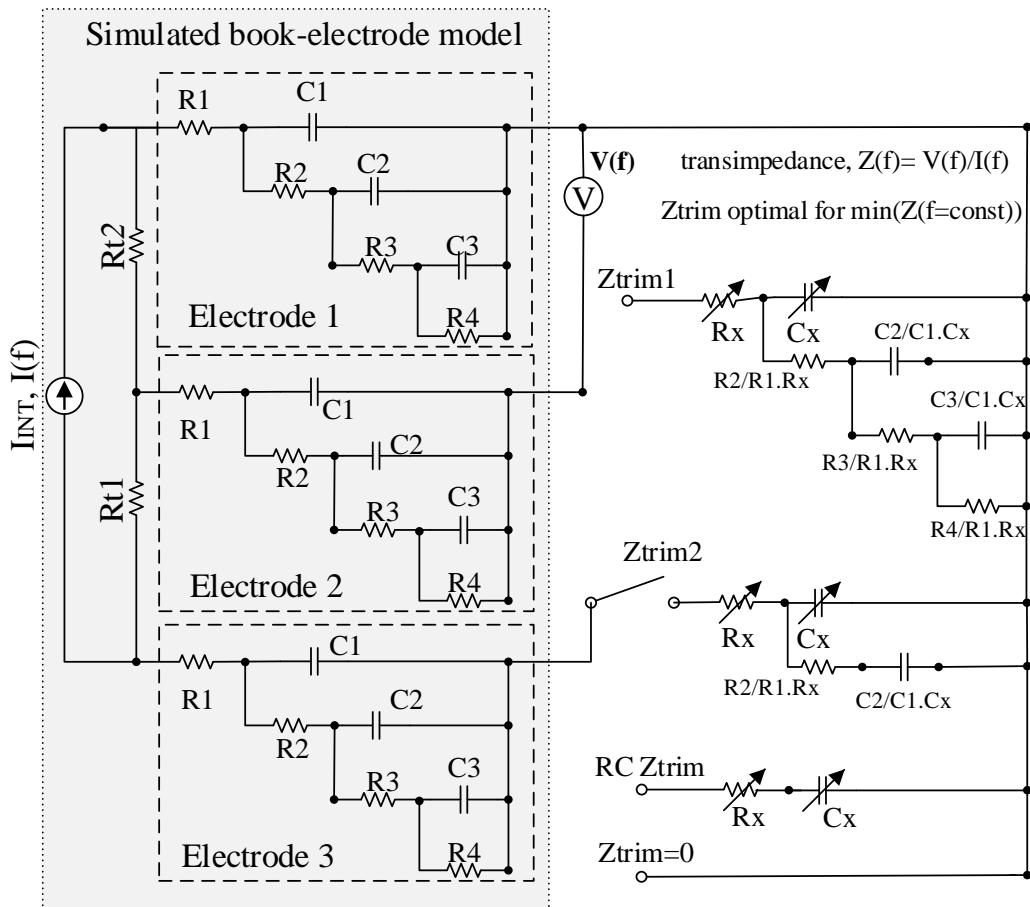


Fig. 3.5 Simulation model of a book electrode with and without Ztrim compensation circuits. Electrodes are represented from impedance modelling of recording electrodes in the book and Ztrim impedances are found by optimization in simulations. Compensation circuits are simple RC trim, Ztrim1 (3 stage RC ladder network) and Ztrim2 (2 stage RC ladder network). Electrode 1 and 3 are short circuited to which Ztrim/ Ztrim=0 attaches using a switch. R1 and C1 of Ztrim1 and Ztrim2 are the circuit parameters that are varied to find EMG minimum while rest of them being recursively dependent in CPE were varied in the ratios format as shown. Resulting transimpedance is measured between electrode 2 and short-circuited electrode 1 and 3, that will form the differential input of the amplifier. Electrode 1, 2 and 3 are Z_{e1} , Z_{e2} and Z_{e3} measured from impedance modelling of electrodes in the book.

Table 1 Circuit Parameters obtained from Impedance Modelling of Book Electrode

Electrode (Ze)	R1/Ω	R2/Ω	R3/Ω	R4/Ω	C1/F	C2/F	C3/F
1	44.4	149.7	1.36K	3.53K	3.9u	3.1u	4.3u
2	48.7	304.9	2.32K	2.65K	2.7u	1.8u	4.1u
3	35.5	365.4	2.26K	3.38K	3.2u	2.1u	3.3u

Table 2 Ztrim1 and Ztrim2 Circuit Parameters obtained from Optimization in Simulations

Parameter	ZTRIM1	ZTRIM2
Values		
C1	2.0 u/ F	2.0 u/ F
C2	2.1 u/ F	2.1 u/ F
C3	1.2 u/ F	-
R1	35.5 Ω	35.5 Ω
R2	365.4 Ω	365.4 Ω
R3	2.3 k Ω	-
R4	3.4 k Ω	-

In vitro preparations involve the demonstration of the effectiveness of our proposed Ztrim compensation circuits in EMG reduction. The circuit parameters obtained in simulations were used for Ztrim compensation circuit components. Setup shown in fig 3.4 was now rearranged to the one shown in fig 3.6. The Ztrim compensation circuit was attached to either end of the outer electrodes of the book. Same experimental conditions were kept as before. The minimum available EMG current of 200uA was passed through the book electrode from the two opposite corner electrodes in the tank, using Wayne Kerr (6500b) impedance analyser. As the book electrode was intentionally made offset in the setup, output voltage measurement without Ztrim was expected to be higher than null. The amount of imbalance in the book electrode was approximately calculated by measuring, axial resistances (R_{t1} and R_{t2}), giving an imbalance of about 20%² in the book electrode. To observe the effect of Ztrim compensation circuits on EMG minimisation, the voltage differences were then recorded between the short-circuited outer electrodes of the book and the middle electrode, in the frequency range of 500-10kHz, with and without Ztrim circuits. Output voltages were recorded in terms of the input current, giving transimpedance (EMG) of about 1Ω, whose performance ratio PR was defined as follows. This was just to observe the EMG minimisation improvement on a different scale.

$$PR_{dB} = 20\log_{10} \left(\frac{Z_{12} (Z_{trim}=0)}{Z_{12} (Z_{trim} \neq 0)} \right) \quad (3.2)$$

2 $R_{t1} = 22\Omega$ and $R_{t2}=9.6\Omega$ and $Z_{e1}=Z_{e3}$, corresponds to 50% imbalance of electrode impedance and about 30% imbalance for the tissue resistance. The overall percentage imbalance being the difference of the two ratios, can be calculated as
 $||[R_{t2}/(R_{t1}+R_{t2})]*100-[Z_{e1}/(Z_{e1}+Z_{e3})]*100|=|(9.6/31.6)*100-(1/2)*100|\approx 20\%$

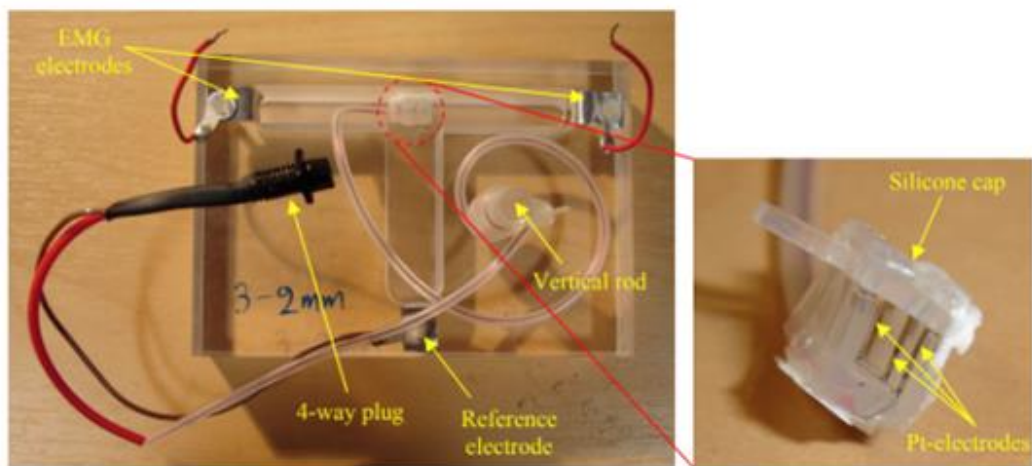
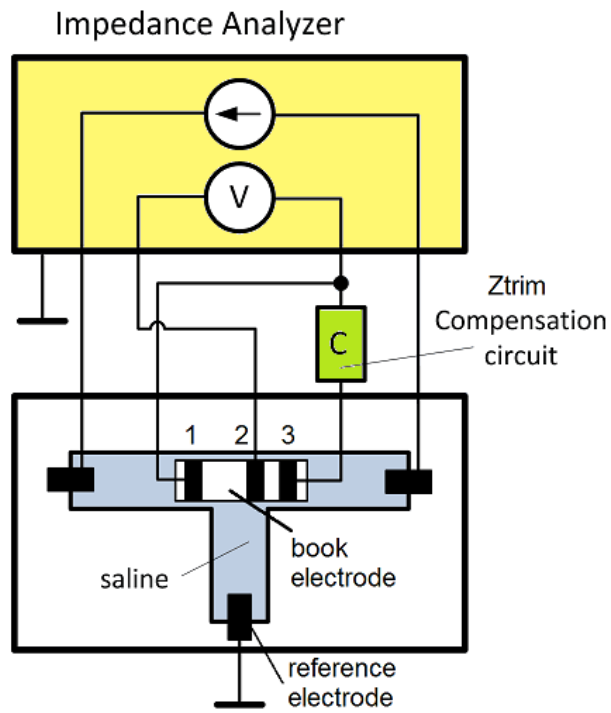


Fig. 3.5 Top figure showing custom setup built to measure the effect of using Ztrim with book electrode for EMG minimisation. Bottom figure shows the picture of actual T-shaped tank used in invitro testings.

3.5 Experimental Results

3.5.1 Electrode impedance modelling of tripolar book electrode

The impedance data obtained in invitro preparations of each book electrode were compared with the output of impedance spectroscopy software used, that varied the RC parameters of a given equivalent circuit of CPE (fig. 3.2) to optimally fit on the experimental results. Simulations and invitro results obtained for each electrode disc of book electrode are shown in figure 3.7. A simple 3-stage RC ladder network was proposed for CPE modelling of electrode impedance measurements, as discussed earlier in section 3.4.1, and the results obtained for each electrode disc confirm that it can be used for this task, showing a close correlation between invitro and simulation results of both transimpedance and phase.

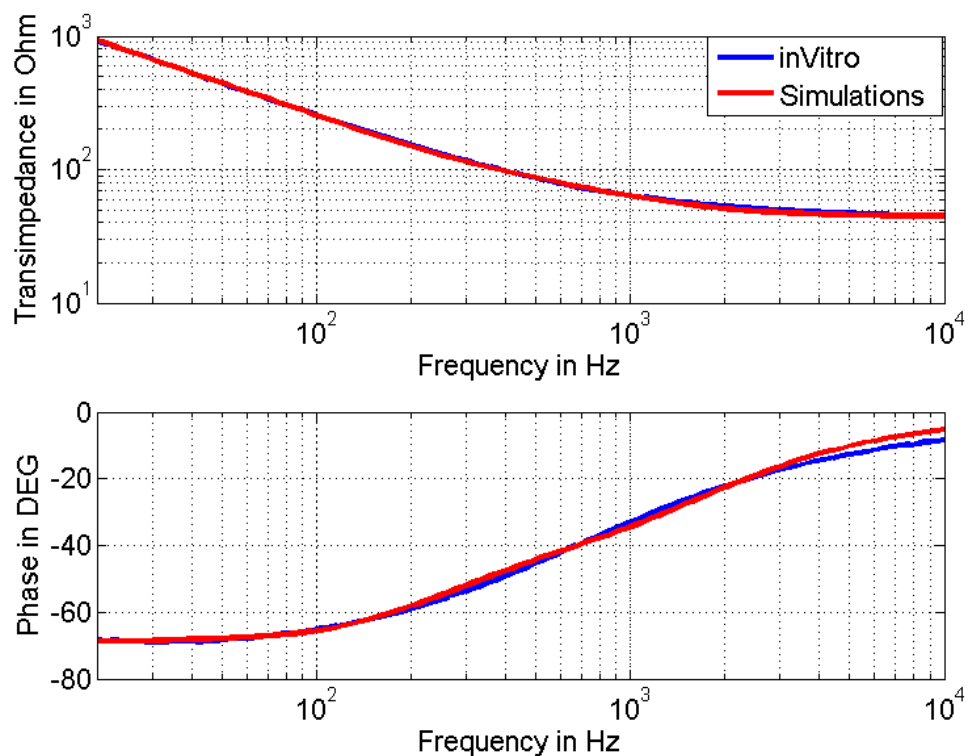
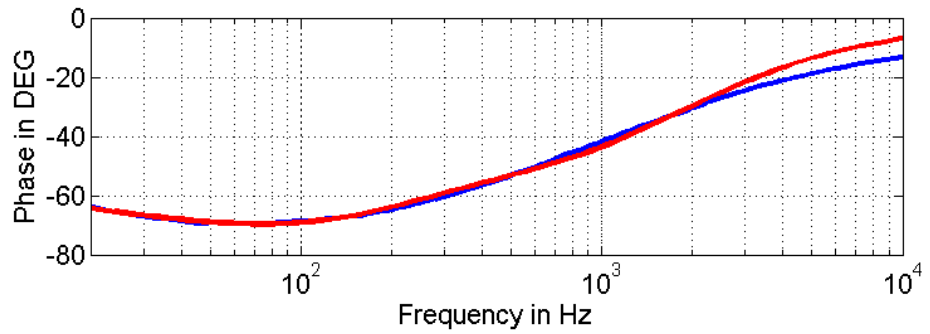
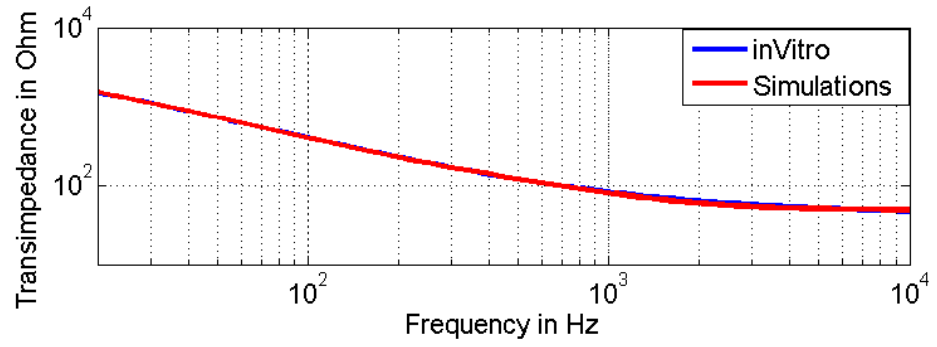
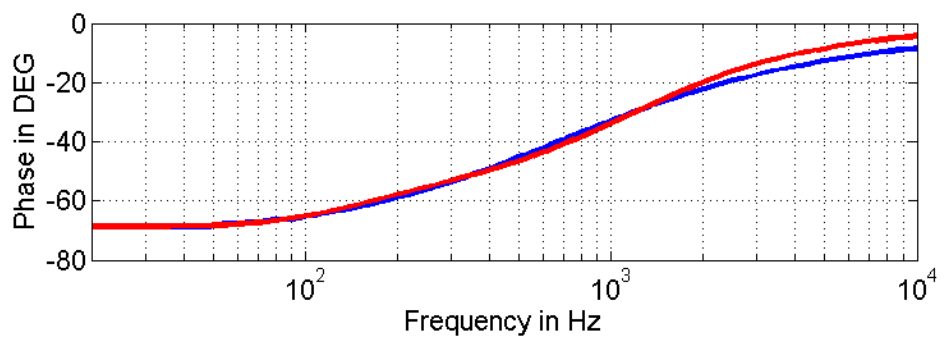
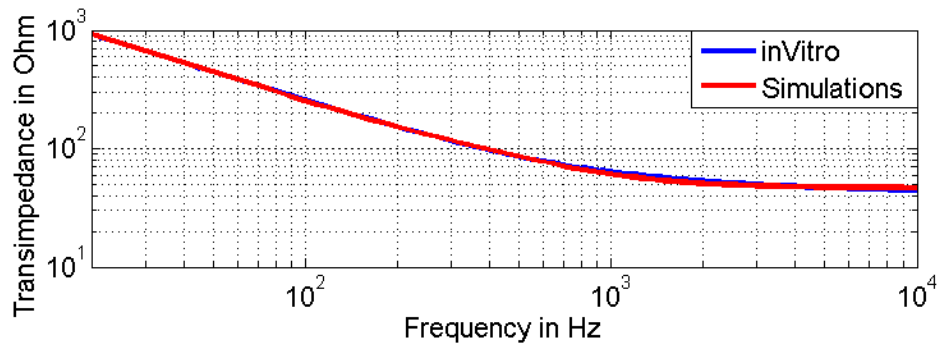


Fig 3.7 (a) Electrode impedance modelling of electrode disc 1 (Ze1) of book electrode, showing good correlation of proposed 3 stage RC ladder network CPE with experimental results.



(b)



(c)

Fig 3.7 (b) Electrode impedance modelling of electrode disc 2 (Ze2) and (c) electrode disc 3 (Ze3) of the book electrode, showing good correlation of proposed 3 stage RC ladder network CPE with the experimental results.

3.5.2 Uncompensated Response of the Tripolar Book Electrode

Uncompensated response shows the amount of interference, EMG present at the output of the cuff, that needs to be neutralised. The response of the uncompensated tripolar book electrode examined over the frequency range of interest is shown in fig. 3.8. Invitro results show the presence of varying interference in the form of transimpedance output, while simulation results obtained by using models of electrode impedance show a close correlation with measured interference. Both shows almost same degree of imbalance in the book electrode, a higher impedance at lower frequencies and a lower at higher frequencies with a roll-off of less than 20dB per decade in the frequency range. Results confirm that proposed 3 stage RC ladder network used to mimic electrode

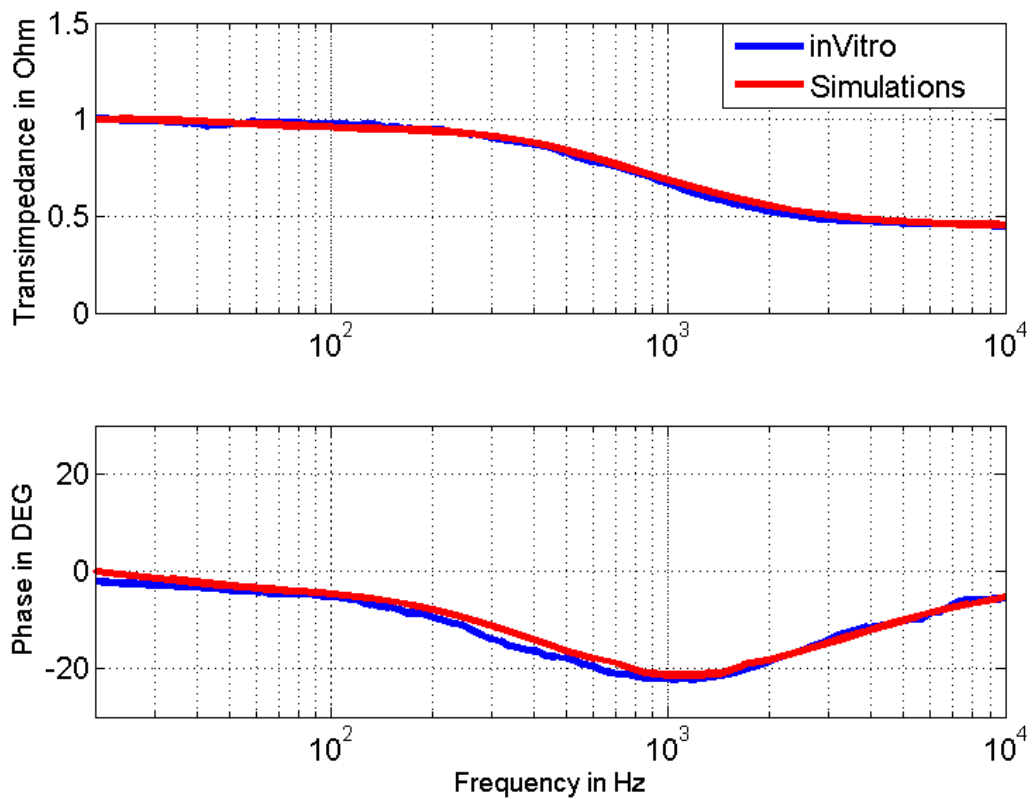


Fig. 3.8. Figure showing the transimpedance spectrum (EMG interference) of imbalanced tripolar book electrode. Simulating book electrode using electrode impedance model shows a close correlation of magnitude and phase with the invitro results, confirming that this book electrode model can now be used in simulation to find Ztrim compensation circuit parameters for EMG minimisation.

impedance modelling is appropriate to replicate the values of the book electrode

under experimental conditions and can now be used in simulations to find accurate components values for the Ztrim compensation circuits to be used later in balancing the bridge under lab conditions.

3.5.3 Compensated Response of the Tripolar Book Electrode

3.5.3.1 RC as Ztrim

Fig. 3.9 illustrates the comparison between simulation and invitro results when simple RC compensation circuit was used as a Ztrim with the tripolar book electrode to minimise EMG interference. Result shows that simple RC is capable of minimizing EMG interference only at the spot frequency rather than in the entire frequency band of interest, due to the electrode-electrolyte interface nature not being like simple RC. In a 20% imbalanced book electrode, simulation results show the nulling of EMG interference up to about 5 mΩ from ~1.0 (V/I) at 100Hz which, is about improvement of 99%, in contrast to nulling up to about 0.15 Ω, which is about 85% improvement achieved during the invitro verification of EMG minimisation, where improvement of 100% means that EMG has been completely nullified at that particular frequency. The results in the lab for simple RC were obtained by adjusting the potentiometer around the R and C component values that were obtained in the simulations using optimization procedure described in the method section. The discrepancy observed between the simulations and in invitro results is due to interference added to the results from external sources that could be improved by improving the experimental setup. However, EMG minimisation at the spot frequency rather than in the entire frequency band of interest is of less interest as interference at other frequencies will be convoluting the neural signal. Hence results confirm that simple RC not mimicking electrode-electrolyte interface impedance, when used as a compensation circuit with cuff electrode can minimise EMG interference only at the spot frequency.

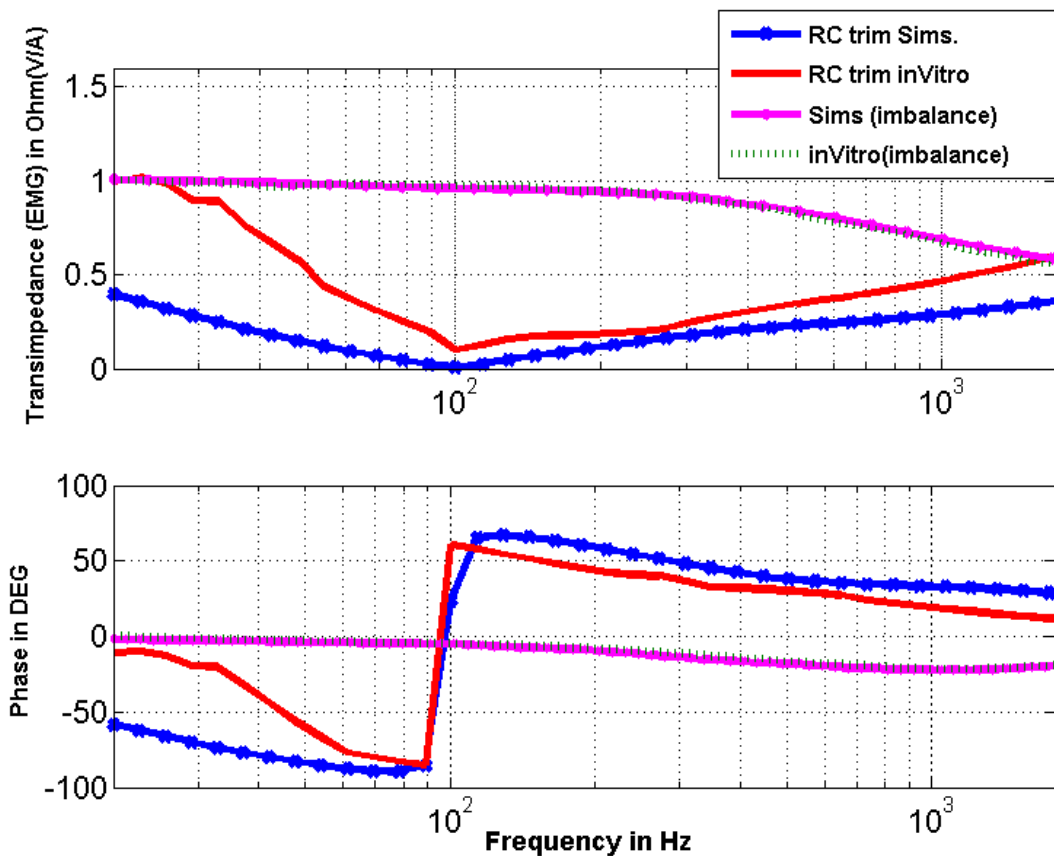


Fig. 3.9. Comparison graph showing EMG minimisation using simple RC as a Ztrim at 100Hz. RC compensation circuit parameters found in simulations (blue line) shows its correlation with invitro results (red line) by minimising EMG (20% imbalance in the book, ~1 V/I interference) by a factor of 10 in invitro in contrast to reduction by a factor of almost 200 in simulations. Results confirm that simple RC when used as a Ztrim is capable of minimising EMG only at the spot frequency.

3.5.3.2 Simple 3-Stage RC Ladder Network as Compensation Circuit, Ztrim1

Figure 3.10 shows the results obtained for EMG minimisation when 3-stage RC ladder network called Ztrim1 was used as compensation circuit with imbalanced book electrode. It can be clearly seen that EMG interference at around 1Ω is now reduced linearly at all frequencies. On an average, the simulation results yielded the notable performance of about 97% EMG minimisation (from 1Ω to 30mΩ) and

in invitro verification showed an improvement of about 86% (from 1Ω to 0.15Ω) in EMG minimisation, linearly in the entire frequency band of interest. It should also be noted that parameters obtained from optimisation in simulations were used as component values of the compensation circuits during in invitro testing and no readjustment were made to them. Good correlation in simulation and invitro testing results also confirm that circuit parameters obtained in simulations are capable of minimising EMG interference linearly under lab conditions too, where further improvement to the results may be possible by tweaking only first R and C parameters in the compensation circuit while others being dependent in terms of their ratios with them.

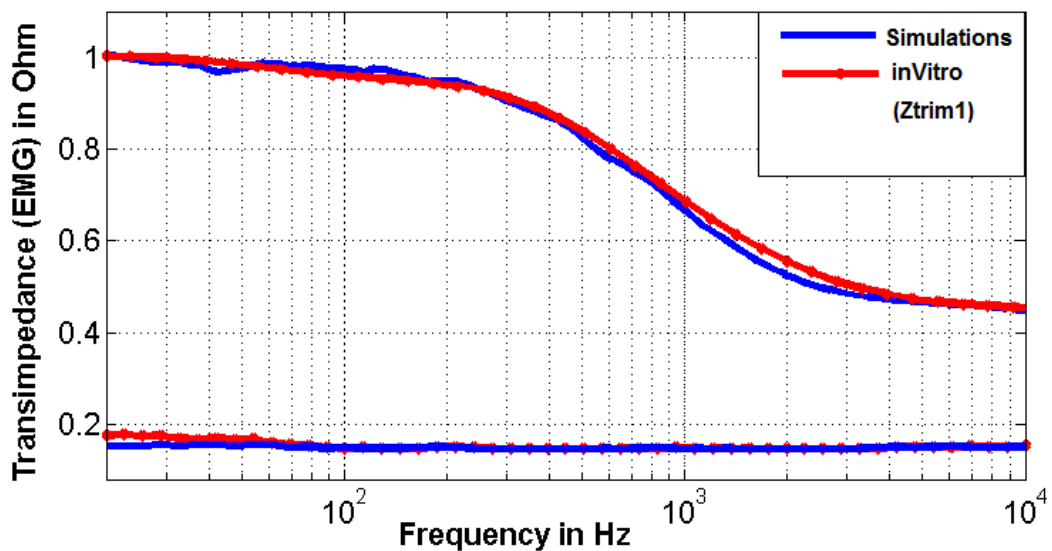


Fig. 3.10 EMG minimisation from $\sim 1\Omega$ interference to about 0.15Ω (8 times reduction approx..) in invitro verification in contrast to minimisation to about $30m\Omega$ (about 37 times reduction) observed in simulations. Using 3-stage RC ladder network as a Ztrim, EMG is now linearly minimised in the entire frequency range rather than at one spot frequency, hence frequency independent. Results also show very good correlation between the simulations and invitro results of the Ztrim1 circuit, with a slight difference at frequencies lower than 100Hz. Thus, circuit parameters obtained in simulations using optimisation method by varying only first resistor and capacitor, gives similar EMG minimisation in invitro verification, reducing imbalance in the book electrode from 20% to about 3%.

3.5.3.3 Simple 2-Stage RC Ladder Network as Compensation Circuit, Ztrim2

The 2-stage RC compensation circuit, Ztrim2 was obtained by identifying the redundant stages in 3-stage RC ladder network, which might be enough in obtaining the appropriate ENG signal recording during in-vivo verification and hence it will also provide the benefit of consuming less power, less noise and less space in the neuroprosthesis implant. Figure 3.11 shows the results obtained for EMG minimisation when 2-stage RC ladder network called Ztrim2 was used as compensation circuit with imbalanced book electrode. This configuration of Ztrim resulted in EMG minimisation linearly from about 1Ω to about $81\text{m}\Omega$ (improvement of about 93%) when observed at 100Hz, in contrast to minimisation from about 1Ω to about 0.17Ω i.e., an improvement of about 85% being observed. However, it can also be seen in figure 3.12 that Ztrim2 has a slightly lower tendency of minimising EMG interference at frequencies below 1 kHz as compared Ztrim1, with both becoming identical at frequencies beyond 1 kHz. The invitro testing although show larger interference (transimpedance) observed than the simulation results, yet it illustrates an almost linear trend of being frequency in the bandwidth of interest.

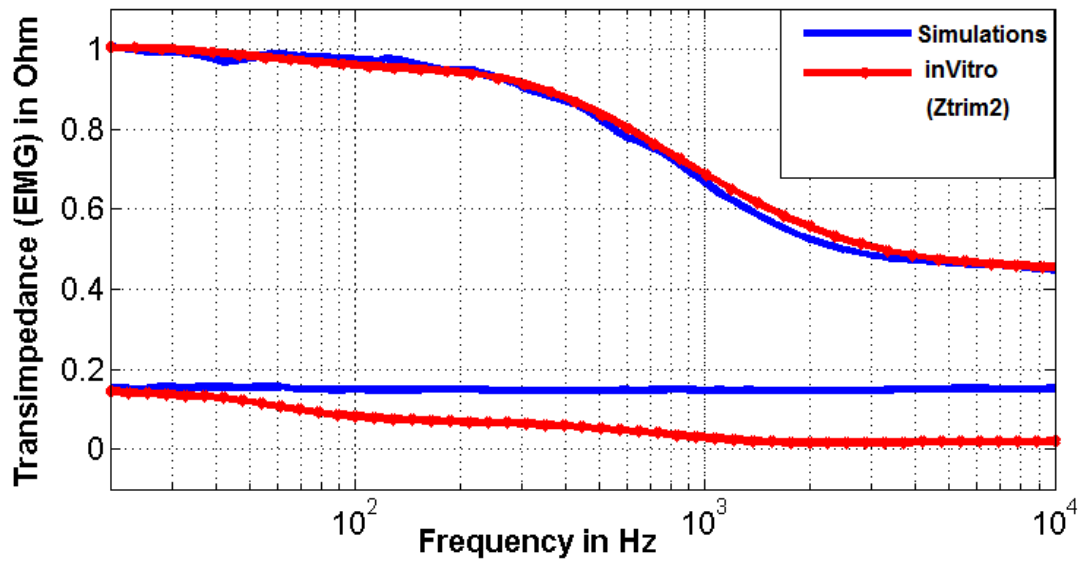


Fig. 3.11 EMG minimisation from $\sim 1\Omega$ interference to about 0.17Ω (7 times reduction approx..) in invitro verification in contrast to minimisation to about $81m\Omega$ (about 14 times reduction) observed in simulations at 100Hz. Although slightly less correlation between simulations and invitro testing of Ztrim2, yet it is capable of minimising EMG almost linearly in the entire frequency of interest (becoming more linear at higher frequencies, with the use of less circuit parameters in the compensation circuit).

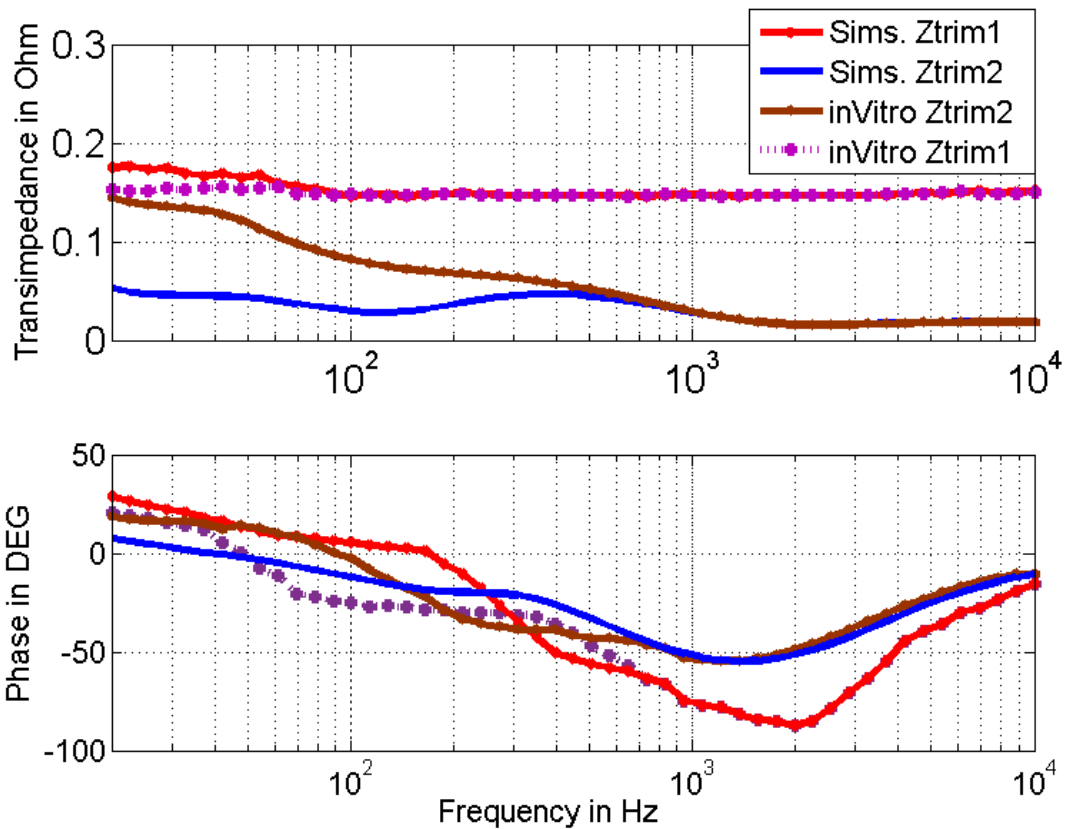


Fig. 3.12 Graph showing magnitude and phase comparison of EMG minimisation using 3-stage RC ladder compensation circuit (Ztrim1) and 2 stage RC ladder compensation circuit (Ztrim2), both in simulations and invitro verifications. First it can be seen that all are capable of minimising EMG linearly in the entire frequency bandwidth. The difference between EMG minimisation using Ztrim1 and Ztrim2 in invitro testing is about 20mΩ at lower frequencies which becomes equal again at frequencies beyond 1kHz (blue and brown lines) This difference of less EMG minimisation using Ztrim2 is also observed in simulations at lower frequencies (red and purple lines). The less EMG minimisation observed using both compensation circuits under experimental conditions is due to more interference added to the setup from external sources, which can be improved along with further improvement by tweaking first RC values in the compensation circuit.

3.5.3.4 Performance Ratio, PR of Ztrim Compensation Circuits in dB

The performance of the compensation circuits on EMG minimisation can also be analysed on a better scale instead of seeing the absolute transimpedance values shown in the results above. For this, the relation introduced as equation 3.2 in method section was used. The performance ratio, PR of each compensation circuit was calculated in dB, with and without using it with the book electrode. Fig. 3.13 displays the graph obtained for each compensation circuit using

performance ratio relation. It is evident from the graph that simple RC results in a distinguished peak at the frequency for which it was nulled. It reaches to a noticeable performance of about 102 dB at 100 Hz in simulations in contrast to about 46 dB in invitro testing. 3 and 2 stage RC ladder networks showed an almost linear EMG minimisation in the entire frequency bandwidth, hence flatter response was observed in performance ratio calculation. When observed at 100Hz, the 3- stage RC ladder compensation circuit reaches to about 70 dB improvement in simulations in contrast to about 50dB in the 2-stage RC compensation circuit. Similarly, invitro verification of 3-stage RC compensation circuit demonstrated an improvement of about 38 dB in contrast to about 36 dB with the use of 2-stage RC compensation circuit with the book electrode. This 2 dB difference was observed to diminish at higher frequencies.

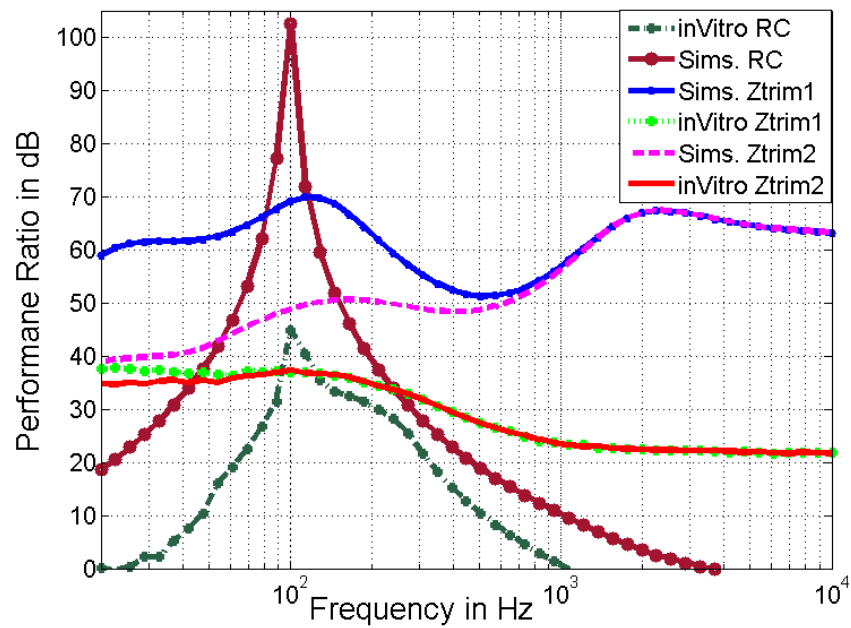


Fig 3.13 Performance ratio of compensation circuits in EMG minimisation. Simple RC trim shows peak at 100Hz as it was nulled for that frequency, giving an improvement of 102dB(sims.) and about 46dB (invitro). At 100Hz, Ztrim1, 3 stage RC ladder compensation circuit gives a performance of about 70dB in sims. in contrast to about 50dB with Ztrim2 in simulations. Invitro verification resulted in about 38dB improvement with Ztrim1 in contrast to about 36dB with Ztrim2. None of the compensation circuit falls below 20dB.

3.5.3.5 Sensitivity Analysis of R and C in the Compensation Circuit

Sensitivity analysis shown in fig. 3.14, displays the degree of EMG minimisation achieved, by choosing a certain combination of Rx and Cx in 3 stage RC compensation circuit. This is shown as a specific achieved transimpedance on each contour line in the graph. As only, first R and C in the network are varied, this analysis also shows the effects on EMG minimisation if they move off their optimal values, which can also help in selecting a range for both R and C with less tolerance for reliable performance. The sharpest gradients are observed for the capacitor values, but they improve after 1uF and not sensitive around its optimum value of 2uF. Hence, this unsymmetrical trend indicates that a reliable range of Cx can be considered above 1uF, after which the divergence from the minimum are increasing much more gradually. Anything below 1uF can be unreliable due to low tolerance and high sensitivity. Similarly, resistance, Rx is indicating to have negligible effect after about 18Ω in achieving a certain minimum. Hence, the safe components range in 3-stage RC ladder compensation circuit can be considered above 1uF and 18Ω. However, this will result in a large size capacitor that requires scaling or off-chip installation to the implant.

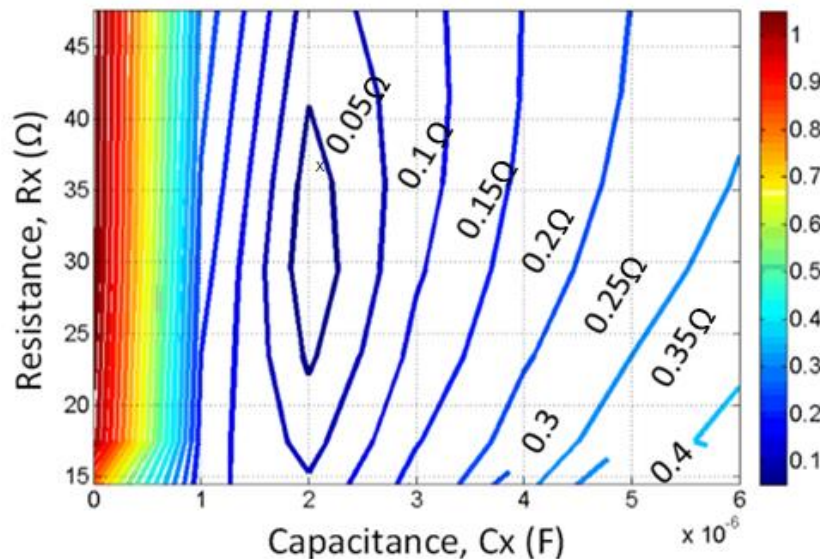


Fig. 3.14. Sensitivity analysis, to check robustness of Rx and Cx parameters in 3-stage RC compensation circuit in achieving a certain EMG minimum. Transimpedance values obtained for each combination are shown on the contour lines. The suitable range for Cx is beyond 1uF and for resistors below 18Ω, after which differences from the minimum rise much more gradually.

3.5.4 Discussion of the Experimental Results

The equivalent circuit model of the tripolar book electrode shown in fig. 3.5 by using electrode impedance measurement can replicate experimental results of the book electrode to an outstanding level (fig 3.8). A high degree correlation between the invitro and simulated results of the uncompensated tripolar book electrode is very important as circuit parameters of the Ztrim compensation circuits are first deduced from the simulations and then tested with the book electrode in invitro testing for EMG minimisation. Hence, any change between them will also affect the results obtained during the saline measurements. From results it can be seen that small discrepancies were observed between the simulations and invitro verifications, in spite of the highly correlated matching observed both for the individual electrode impedances and uncompensated book electrode. This could be because of the two simplifications we used. First, it might not be possible to accurately model a CPE element with simple 3-stage RC ladder network for a wider frequency bandwidth, as a trade off between the simplicity and efficiency of the CPE model was expected. Second, the ratios used between the parameters of the compensation circuit are the ones that were obtained in individual electrode impedance measurements. This ensured CPE conversion as observed in the results but as explained in [168] using a constant number is distinctly a simple representation of the recursive relations that was used in the method. However, despite of these limitations the EMG both in simulations and saline measurements was seen to be minimised to a good standard that is close to the null in the entire frequency bandwidth, along with the benefit of implementing resistor banks and switched capacitors for changing impedance, if required further to improve EMG minimisation.

Ideally, the book electrode should be balanced with the use of Ztrim compensation circuit with it, giving a zero EMG (transimpedance) output. However, it was observed that our proposed simple 3 stage and 2 stage RC ladder networks are not able to completely remove EMG, but they are capable of minimising interference linearly to a good degree, in the entire frequency band of interest, especially where EMG and ENG spectrum overlap. In a book electrode

with about 20% imbalance and 1Ω introduced EMG interference, 3-stage RC ladder network reduced it about 37 times in simulations and about 8 times in the saline measurements, giving EMG minimisation improvement of 97% 86% respectively. In terms of performance ratio, it means that the uncompensated book electrode gave 70dB improvement of EMG minimisation in simulations when it was compensated in contrast to about 38dB improvement observed in invitro results. On the contrary, 2 stage RC compensation circuit offers the benefit of less lumped components and hence even simpler Ztrim compensation circuit to be used with implant in terms of noise performance, power requirements and implantation space restrictions. However, it is still an approximation of the CPE and hence might not be suitable to be used for high degree EMG minimisation at lower frequencies as shown in the results. At frequencies beyond, 1kHz the response of both ladder networks become similar in EMG minimisation. When observed at a lower frequency of 100Hz, 2 stage RC ladder compensation circuit also reduced EMG from 1Ω by a factor of about 14 in simulations and 7 in saline measurements, giving an improvement of about 93% and 85% of EMG reduction respectively. In terms of performance ratio, this means an improvement of about 50 dB in simulations when book electrode was compensated in contrast to about 36 dB improvement observed in invitro verifications. In vivo-testing of using 2 stage RC ladder network as a compensation circuit can further reveal if it can be used even at lower frequencies for EMG minimisation to a level from where an unaffected ENG signal could be recorded for further processing. Similarly, results obtained in EMG minimisation using simple RC circuit are encouraging but this technique is not useful in neural signal recording as EMG can only be nullified at the spot frequency rather than in the entire frequency band of interest.

Saline measurements of EMG minimisation using compensation circuits are also sensitive to experimental conditions. It was observed that the electrode book immersed in the electrolyte in the T-shaped Perspex tank was sensitive even to the slight movement of the wires and connections in the tank during experiment. The slight change in the amount and quality of electrolyte was also affecting the results, where a conductivity of 15.95m/S was to kept constant during the measurements. Another considerable factor to be taken into account was the time

duration between the measurements of uncompensated and compensated book electrode setup, in which experimental conditions were to be kept constant. This is because after taking measurements of the imbalanced book electrode, circuit parameters to be used with the compensation circuits were derived from the simulations which could be a time-consuming process. Even a little change in the uncompensated output during this time could cause a significant difference in the EMG minimization results when tested with compensation circuits. There will also be noise added to the saline measurements from external sources. However, this all can be improved by improving the experimental setup. Thus, it is expected that improvement in the design of the current experimental setup will help in further minimization of EMG in invitro verifications with results more matching to the ones obtained in simulations.

Apart from the interference from external sources that could be improved, interference will also be added from the lumped components of the compensation circuit, that is needed to be calculated to check its effect on the quality of neural signal to be recorded. In 3-stage RC compensation circuit, the first resistor ($\sim 35\Omega$) being dominant contributes a small thermal noise of about $0.8 \text{ nV}/\sqrt{\text{Hz}}$. On the other hand, the larger capacitor values are expected to shorten the resistors even at smaller frequencies, making insignificant noise addition to the EMG source. However, the large necessary capacitor values might need some scaling (discussed later) if they are to be used as on-chip to the implant and other methods need to be deduced to use small circuit parameters in the compensation circuit without compromising on the simplicity of the design.

Nonetheless, the novel technique of minimising EMG in the entire frequency band of interest, with the use of proposed simple 3 stage and 2 stage RC ladder compensation circuits is very encouraging, with EMG minimisation up to about 85% in a 20% imbalanced book electrode. The linear minimisation of EMG in the bandwidth without requiring any re-adjustment to the component values is very appealing in making the process even simpler, while the uncomplexity of the compensation circuit may be helpful in using it as an on-chip to the implant with appropriate parameter values, for the interference reduction.

3.6 Possible Ways of Optimising Ztrim Component Parameters

The compensation circuit component values obtained in EMG minimisation show the use of large capacitors, in micro Farad range that are not suitable to use as on-chip with the implant. On the contrary, IC implementation of the resistors ($\sim 3.4\text{K}\Omega$ max. in our case) is possible due to smaller layout area they take. In terms of using compensation circuits with an implant, there are two possible ways of using capacitors which are discussed as follows.

3.6.1 Off- Chip Installation

The proposed compensation circuit is a mixture of R and C lumped components and for smaller capacitors it offers the benefit of using it on-the chip with an implant, hence simplifying the design in terms of size and power requirements. For larger capacitors, we can consider using compensation off the chip in some protective casing and connection to the tripolar cuff can be made via wireless connection transmission techniques. The idea of using Ztrim off the chip is already introduced in the first chapter (section 1.3). Where off-chip installation of Ztrim complicates the system design by increasing size and power requirements, it also offers the benefit of making our proposed EMG minimisation technique universal. Approximate interference near device implantation site can be measured from surface electrodes and multiple readings can be recorded to improve its accuracy. Based on this data, compensation circuit parameters can be obtained for minimising this EMG interference. As only the first R and C parameters in Ztrim are varied while rest being linked to them in ratios, for an off chip Ztrim installation benefit is the tweaking facility available outside the implant to further adjust EMG minimisation. This scenario also offers the benefit of using same implant for all patients and just changing the Ztrim compensation circuit externally. To what extent this possibility is feasible for reliable neural signal recording can be confirmed through invivo verifications.

3.6.2 Ztrim Impedance Scaling

The other way is to scale down the size of capacitors so that they can be used as on-chip with an implant. Impedance convertors can be used to achieve smaller equivalent capacitors for Ztrim, at the expense of increasing system complexity due to use of another amplifier along with resistors for each capacitor to be scaled. It could be advantageous to see the effect of scaling down capacitors on EMG minimisation in compensation circuit, as follows.

The 3-stage RC ladder compensation circuit can be decomposed into three simple RC low pass filters; the output of one form the input of the other in front (fig. 3.15). Since there are three low pass filter in series, each filter can be studied alone. In low pass filter, the cut off frequency is inversely proportional to the product of resistor and capacitor thus, if we want to scale down the size of capacitor, the size of resistor will have to increase in order to keep the overall characteristics of the filter same. For example, for capacitors to convert from μF range to pF range, capacitance must be multiplied by a factor of 10^{-5} and hence resistance by 10^5 . So in our compensation circuit, scaling of capacitor in the first branch of ladder from 2 μF to 20pF, the corresponding resistor required will be 3.55 M Ω rather than 35.5 Ω used. This was tested by scaling down the capacitor values and hence scaling up the resistor values in 3 stage RC ladder compensation circuit and comparing the results with the output of the original(unscaled) compensation circuit in minimizing EMG. Results are shown in

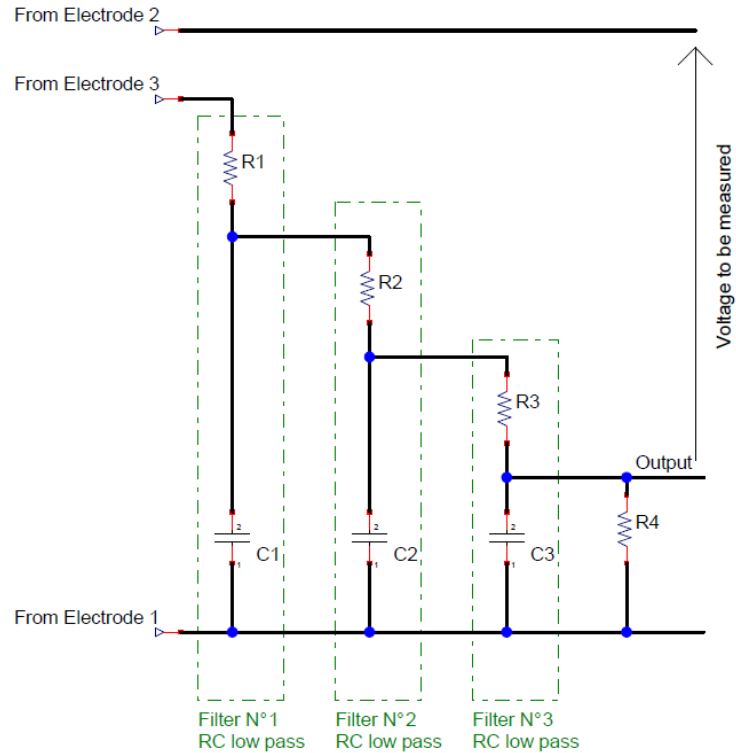


Fig. 3.15 The 3-stage RC compensation circuit that can also be seen as 3 low pass RC filters attached to another.

fig 3.16, that shows that output in transimpedance (magnitude and phase) is same for the scaled and unscaled compensation circuits, hence confirming that if capacitors are scaled down, then resistors are needed to be scaled up. Increasing size of resistors in the compensation circuit means a little increase in the chip size along with more noise contribution from larger resistors to EMG source. There is a fair chance that increasing the size of the resistors to this extent (mega and tera range) will contaminate the ENG signal further, thus requiring new values for the compensation circuit parameters for further EMG minimisation (complicating the process).

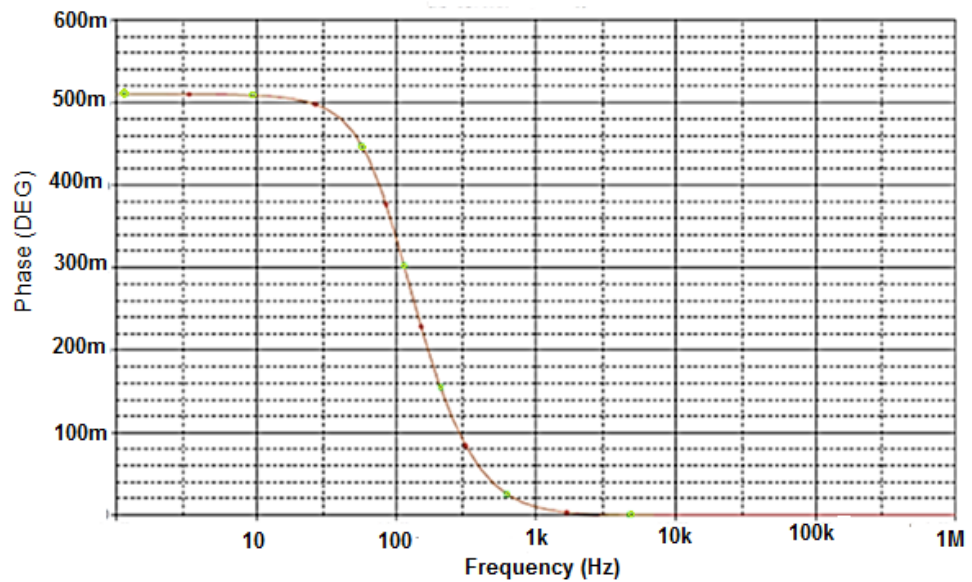
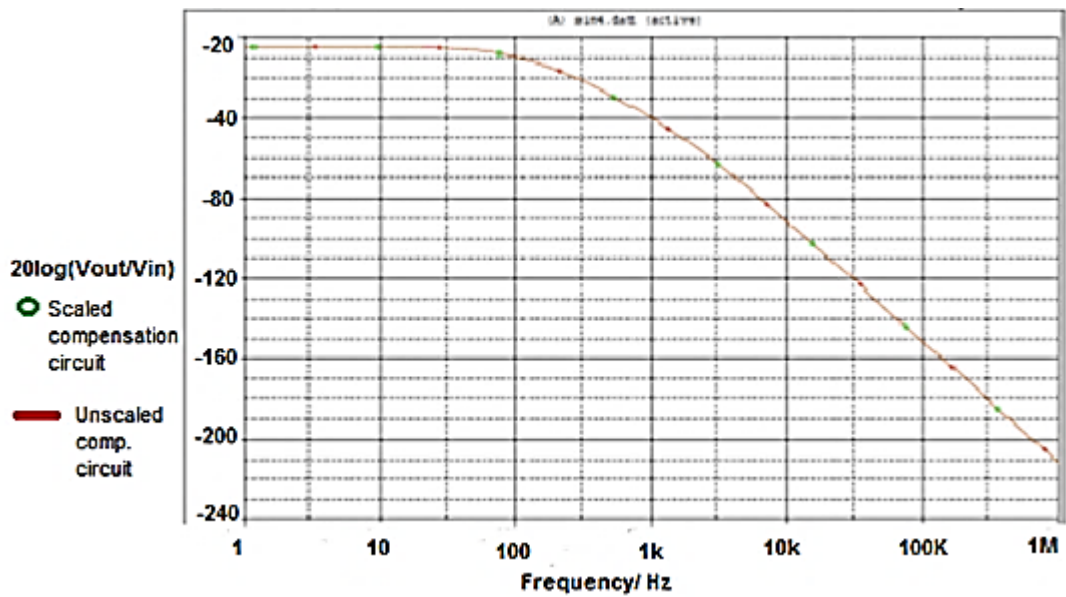


Fig. 3.16 Graphs showing magnitude and phase comparison of the original unscaled 3 stage RC compensation circuit with its scaled version, when resistors were scaled up by the same value when capacitors were scaled down.

Another possible idea is proposed in appendix A, in which capacitor values of the Ztrim compensation circuit can be fixed to appropriate values and corresponding resistor values required can be found through calculation for EMG minimisation. This can also omit the requirement of using simulations to find Ztrim

compensation circuit parameters, along with using less power and space in the implant. However, the proposed idea is naïve and requires invitro verifications along with more simulations.

3.7 Noise due to compensation circuit

The neural signal is embedded behind the EMG interference and any more significant noise added to the system can further contaminate the signal. Hence, it is important to estimate the noise added to EMG source due to the use of Ztrim compensation circuit with the book electrode. However, at this stage it was only tested in silico and further work in future is required for invitro and invivo verifications.

Compensation circuit used is a passive RC ladder network in which the thermal noise contribution, which is the significant one is mainly from the use of resistors. This noise was calculated in the simulations for a frequency bandwidth of interest to observe the noise contribution by each component of the passive network. For 3 stage RC compensation circuit, the noise contributions are listed in table 3.3, giving a total thermal noise contribution of about 16.7nV/sqrt Hz, with most contribution by the first resistor in the network. Conversely, large capacitors do not make significant noise contribution as they shorten the resistors even at the lower frequencies.

TABLE 3.3
NOISE CONTRIBUTIONS BY THE RESISTORS OF THE COMP. CIRCUIT

Parameter	Noise Contribution (nV/sqrt (Hz))	% of Total
35.5 Ohm	0.76	82.30
365.4 Ohm	2.45	14.45
2.26k Ohm	6.1	2.19
3.38k Ohm	7.46	1.07

Noise spectral density was also calculated in simulations, to see noise power in the frequency bandwidth of interest using 1V AC signal. Function of this circuit

was unity and the input and output referred noise were the same. This was done to see the noise distribution in the frequency domain. Results in fig. 3.17 shows that at lower frequencies noise power is higher but as the frequency increases it becomes almost negligible at frequencies beyond 1kHz. This was expected as it means that capacitors are becoming short circuit at higher frequencies hence, smoothing out the current flow and reduction in noise.

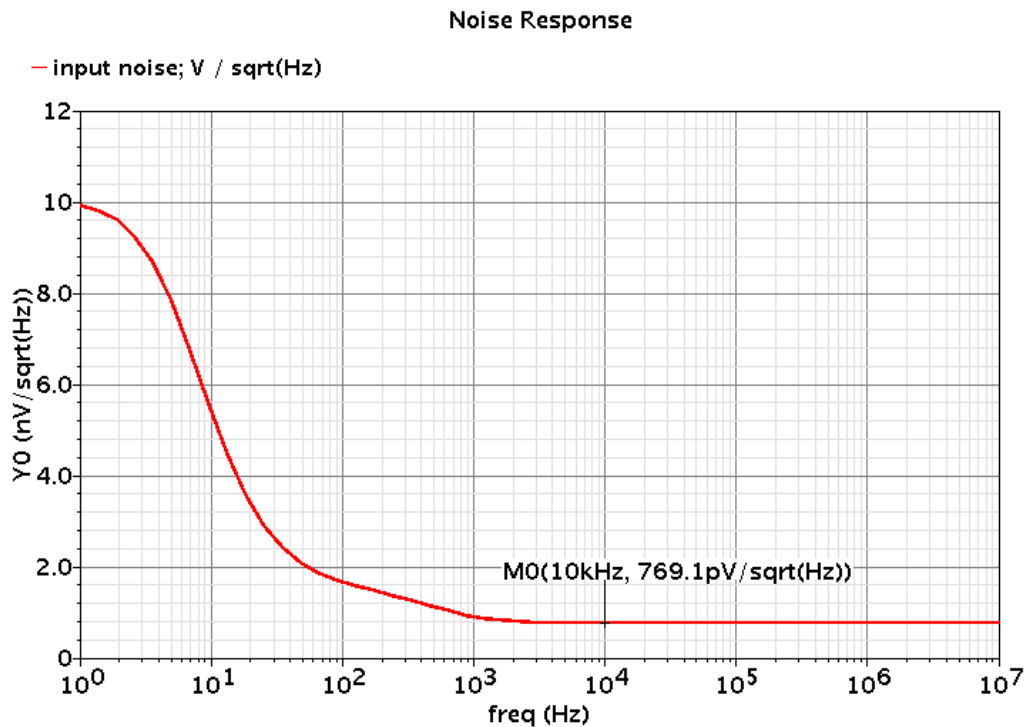


Fig 3.17 Noise response of a 3- stage compensation circuit observed over a longer frequency range, it is evident that noise contribution is more at lower frequencies and almost negligible at higher frequencies.

Although not verified in invitro conditions, simulation results show that noise added from the 3-stage RC compensation circuit is not much. Total contribution is about 17nV/sqrt (Hz) and most contribution is from the first resistor being 0.76nV/sqrt (Hz). Results are encouraging as ENG signal is in microvolt range and noise added from the compensation circuit seems to be lower than ENG magnitude. However, further noise analysis in invitro and in invivo verifications are required to confirm the results obtained in simulations.

3.8 Summary

The analogy between the tripolar cuff and the Wheatstone Bridge is helpful in minimizing EMG interference by trying to balance it using electrode-electrolyte interface impedance (CPE) as a Ztrim compensation circuit with either end of its outer electrodes. EMG is significantly reduced at the spot frequency using simple passive components R and C as a compensation circuit. It is not linearly neutralized as interface impedance is of complex nature and does not behave like simple RC. Proposed simple 3-stage RC ladder network in this work is capable of mimicking CPE behaviour to an extent then when used as a Ztrim compensation circuit, minimised EMG interference linearly in the entire frequency bandwidth of interest (500-10kHz). Even simpler 2-stage RC ladder network as a compensation circuit is also capable of minimising interference linearly just like 3-stage RC at the higher frequencies beyond 1k Hz. Results look encouraging as atleast three-quarters of the imbalance in the book electrode is removed using the proposed compensation networks. The larger values of capacitors in the compensation circuit can either be scaled down using impedance convertors or can be used as an off-chip to the implant, however both techniques will increase the system complexity in terms of space and power requirements. Off-chip installation of capacitors can give an additional benefit of tweaking resistor and capacitor values to further improve EMG minimisation. Better solution can be found by fixing capacitor values to an appropriate number and finding corresponding resistor value that results in EMG minimisation like it was observed in simulations using global optimisation procedure. Noise contributed to EMG source by compensation circuit is less, however further work is required to do its analysis in invitro verifications. Nonetheless, a novel technique of minimising EMG interference with less passive elements has been proposed in this chapter that can be further improved for better EMG minimisation.

CHAPTER FOUR

Conclusion and Future Work

4.1 Summary

In this work a novel technique of reducing EMG interference linearly in the entire frequency bandwidth of interest is presented by using simple 3 and 2 stage RC ladder networks. The compensation circuits are used with the imbalanced book electrode to balance it, where balancing it completely means the removal of EMG interference that appears at the amplifier input. The reliable neural ENG signal can then be recorded, which was embedded behind the interference spectrum, to be used in neuroprosthesis devices for restoring lost motor functional activities of an individual, for example bladder control implant that was considered in this work.

Chapter 1 introduces the reader with the tragedy of the spinal cord injury and its effect on the life of victims. Motivation behind the work is explained along with the aims of this project. It finishes with the main contributions being done in reaching the aims of the project. Chapter 2 provides a literature review about the physiology and anatomy of the human nervous system and how it gets affected after an injury. Focusing on neuroprosthesis and functional electrical stimulation, it discusses different electrodes that can be used to record ENG signal from the peripheral nerves and choice of cuff electrodes to be used in the current task. It then explains different amplifier configurations that can be used with tripolar cuff to record a clean neural signal along with the benefits and drawbacks of the arrangement with respect to the neuroprosthesis implant.

Chapter 3 begins with an introduction of another amplifier configuration that has further benefits as compared to other configurations, to record ENG signal using less power, complexity and space. It is called modified quasi tripole, mQT, in

which tripolar cuff electrode is considered as a bridge and balancing it with a compensation circuit results in the removal of EMG interference at its output. It also introduces the reader with the electrode-electrolyte interface complexities in neural signal recording. 3 simple compensation circuits are then proposed for EMG minimisation in cuff electrode. When simple RC was used as a compensation circuit, it was observed that although simpler in arrangement, but interference was only removed at the spot frequency and not in the entire frequency band of interest. It was important to neutralize the EMG interference at all frequencies because the frequency range for neural signal detection was selected to be between 500Hz to 10k Hz. This confirmed that impedance profile is of complex nature and simple RC cannot be used to model that impedance for bridge balancing. The complex electrode-electrolyte nature can be effectively modelled by CPE, where different complex models of CPE are available we proposed a simple representation of CPE using only 3 stage RC ladder network by making some assumptions about capacitive and resistive paths at the interface. Although, a trade-off between quality and complexity was selected, yet individual electrode impedance models showed that this representation of CPE is effective in replicating results observed in invitro arrangements. A tripolar book electrode equivalent circuit was generated using electrode impedance models to derive compensation circuit parameters in simulations. In simulations, optimisation was used and only first R and C in ladder networks were varied, while the rest were connected to them in ratios. Simulation results showed outstanding EMG reduction linearly in the entire frequency bandwidth rather than at one spot frequency. 2 stage RC ladder compensation circuit was proposed by realising a possible redundant stage in even 3 stage RC ladder network, hence simplifying the topology further. Invitro verifications confirmed that both 3 stage and 2 stage RC ladder network when used with about 20% imbalanced electrode reduced EMG linearly by a minimum factor of 6, leaving about 3% imbalance in the book. The saline results are expected to be improved further by improving the setup for invitro testing. 3 stage RC ladder compensation circuit gives an invitro EMG reduction improvement of about 86% (50 dB) in contrast to about 85% (36dB) for 2 stage RC ladder compensation circuit. The response of EMG minimisation for both compensation circuits become similar at higher frequencies

beyond 1 kHz. Sensitivity analysis performed on first R and C components of compensation circuit showed component ranges that could be considered for EMG minimisation with reliable ENG recording.

Nonetheless, the results obtained with simple RC compensation circuits are encouraging. However, large capacitor values in the compensation circuits require consideration in terms of using them with an implant. Such large values of capacitors cannot be used as on chip with an implant due to their sizes. Hence, compensation circuit can either be used off chip to the implant offering the benefit of tweaking R and C as well, if required for better EMG reduction or capacitors can be scaled down using impedance inverters. This will result in smaller capacitors but bigger resistors and more amplifiers and resistors in the design. Both suggested ways will also increase system complexity in terms of power, space and even noise. It will be more suitable if another technique is tested in which capacitor values can be selected and based on the topology of our compensation circuit, corresponding resistor values are deduced, using a relation to minimise EMG linearly as was observed in simulation results. Finally, resistors in the compensation circuit are the source of further noise that required examination. Noise analysis in simulation were performed on 3 stage RC compensation circuit that confirmed that noise added with the use of our proposed compensation circuit is in nV range and likely will not contaminate ENG signal which is in μV range.

4.2 Future work recommendations

The proposed 3-stage and 2-stage RC compensation circuits are capable of minimising EMG interference linearly in the entire frequency of interest, however further work is required to improve and confirm its performance. Invitro testing involves noise analysis to be performed on the book electrode with compensation circuit to observe the amount of noise it will be adding to the EMG source and if its noise is below ENG spectrum as observed in the simulation or not. At this stage, noise was only calculated in silico and due to time constraints invitro measurements were not made, which should be done later as a future

recommended work. However, the noise calculation is only for the compensation circuit that we used, and it will be different for a compensation circuit with different circuit parameters. Hence, it is advisable to make a noise sensitivity chart for range of parameter values that can be used in the compensation circuit without contaminating the ENG signal.

The design of a low power, small size, high gain and negligible noise amplifier in the adaptive mQT was out of scope of this project but in the future, this needs to be done to complete the design of a neural recording system and to test it in *in vivo* preparation using proposed compensation circuits to record reliable neural signal. As, large capacitor values of the compensation circuit cannot be used as an on-chip to the implant, so it is advisable to use them as an off chip and test it under *in vivo* arrangements for EMG minimisation. Using impedance convertors, on-chip use of compensation circuit can also be observed as a future work and both possible ways of using them with an implant can be compared for best selection.

Finally, another idea of finding RC parameters of compensation circuit is presented in appendix section. The equation was found in trying to find a mathematical connection between the book electrode and the compensation circuit that forces the interferences close to null in a linear pattern. This mathematical relationship was derived by using regression analysis and limiting theorem, supported by the simulation results. However, it is in its early stages and work can be carried forward by improving this mathematical relation and checking its effectiveness in EMG minimisation under experimental conditions, as if it works our proposed compensation circuits can be possibly used an on-chip to the implant without requiring any additional circuitry for parameters scaling.

Appendix A

Ztrim Parameters Deduction using a Mathematical Relation

Introduction

In chapter 3 the technique of minimizing EMG interference was introduced using simple RC compensation circuits with cuff electrode. The 3 and 2 stage RC compensation circuits were able to minimize EMG interference linearly in the frequency band of interest. Although this method was simpler and used few electrical components to minimise the interference, but not only the Ztrim component values were unrealistic to be used as an on-chip to the implant but Ztrim parameters were also found a lengthy optimisation procedure in simulations. In optimisation method, a range of values for the components is first

defined and then the results are collected at each frequency until the closest result to the set result is obtained. In our case the set result was null. Component values obtained from optimisation when used in invitro resulted in satisfactory EMG minimisation but if the transimpedance (EMG) output of book electrode changes then the new set of values would also be required for the compensation circuit for EMG minimisation, involving a lengthy simulation process. Hence, another approach of finding Ztrim circuit parameters can be helpful that can be used to find unknown components in a less amount of time and ease.

In this section, a universal relation is proposed that can be used to find the unknown components of the Ztrim RC compensation circuits. The relation is first tested with the 3-stage RC compensation circuit as 2-stage is simply making the last RC combination of the 3-stage network redundant. At first, the circuit analysis is presented in finding a relationship between the tripolar cuff electrode and the Ztrim compensation circuit that forces the EMG interference close to null. This approach is then tested with a series of assumptions on the optimization and experimental results obtained in chapter 3. Based on the results obtained, a relationship is derived in which by setting one component value constant (R or C) and setting output close to zero, other unknown components can be derived. The solution presented is not a full and final solution and further work is required to check its ability in minimizing EMG interference, explained later in the section.

Analyzation of Book Electrode with Ztrim Circuit using Representative Model

A mathematical relation is required that forces the output from the book electrode close to null by using 3- stage RC compensation circuit. In order to make the process simpler, the whole circuit of book electrode with compensation circuit can be divided into 2 parts. In this chapter 'Circuit 1' is referred to the book electrode model and 'circuit 2' is referred to the Ztrim RC compensation circuit. The structural topology of circuit 1 and circuit 2 are similar, as 3-stage RC

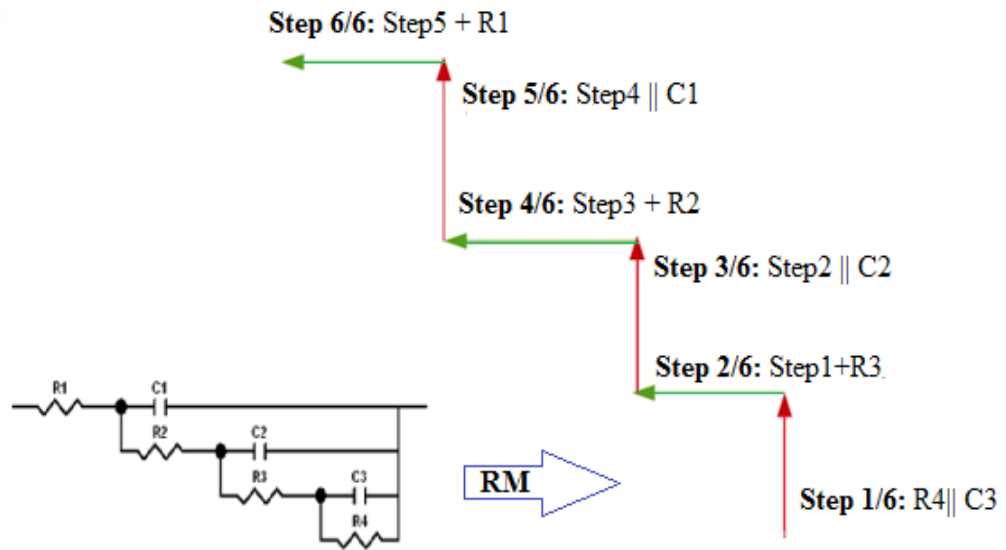


Fig. A Approach considered to build a representative model (RM) of circuit 1(book electrode) using its electrode impedance model

compensation circuit's topology is exactly the same as that of one of the electrode rings of the book electrode (mimicking interface impedance). Thus, first representative model labelled RM of circuit 1 is created that is used to derive the representative model RM for circuit 2 when viewed in the complexity of the whole circuit (fig. A.). The assumption is made that if the representative model correlates well with the output of the tripolar cuff electrode alone then it can be used to calculate the mathematical relationship linking the two circuits together that forces the output close to zero. Any compiler can be used to estimate the output of the unit shown in fig. A., which, is also the topology of 3-stage RC compensation circuit and one ring of the tripolar cuff electrode model. Here, Liberty Basic, version 4.5.1., was used to calculate the output of such RC ladder network at frequencies from 20Hz to 10 kHz. Any compiler including Matlab can be used to calculate the output impedances of the tripolar cuff electrode with and without compensation circuit but this compiler is only used because of its user ease and low cost. Detailed programming code can be seen at the end of appendix and some snippets are shown here for the reader's understanding. It should also be noted that user can change the component values according to the requirement,

however here only first electrode of the book electrode (labelled unit) is considered to make the RM of the circuit 1 and if that is not enough it will be evident in the correlation results of representative and real model of the book electrode, shown later in the results.

Table 4.1. Component values used in calculating the impedance output of the unit. Resistors R_x , $R_{end1,2}$, and $R_{t1,2}$ are taken from the tripolar cuff electrode model that can also be changed if required.

Table X: Values used to create Representative Model
[params]
$R_{end1} = 54 : R_{end2} = 64 : R_{t1} = 22 : R_{t2} = 9.6 : R_x = 4.17 : \dim R_{bar}(4)$
$R_{bar}(4) = 3380 : R_{bar}(3) = 2260 : R_{bar}(2) = 365.4 : R_{bar}(1) = 35.5$
$C_{bar1} = 0.000002 : C_{bar2} = 0.000002 : C_{bar3} = 0.000124$

The representative model (RM) of the book electrode, circuit 1 is then constructed as shown in fig. B.

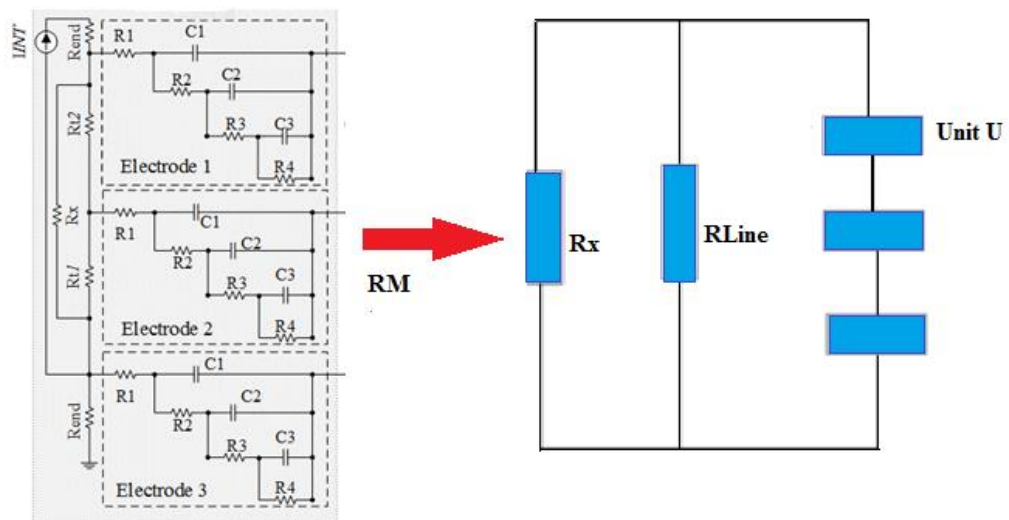


Fig. B. The representative model of book electrode, created using the unit circuit shown in fig. A. where R_{line} is the combined resistance of R_{end} , R_{t1} and R_{t2} . Each unit U represents one ring of tripolar cuff electrode.

Looking into the RC ladder network circuit shown in fig. 4.1., we see that R_4 is parallel to C_3 , which are then in series with R_3 , solution of which is in parallel to C_2 which, again is in series with R_2 and so on. Hence, using that, impedance of the unit is calculated in the compiler from which the effective impedance, Z_{eff} of the RM of circuit 1 from fig B., can be calculated as follows.

$$Z_{\text{eff}} = \frac{\frac{U}{3} \left(\frac{R_x R_{\text{line}}}{R_x + R_{\text{line}}} \right)}{\frac{U}{3} + \left(\frac{R_x R_{\text{line}}}{R_x + R_{\text{line}}} \right)}$$

$$Z_{\text{eff}} = \frac{U \cdot R_x \cdot R_{\text{line}}}{U(R_{\text{line}} + R_x) + 3 \cdot R_x \cdot R_{\text{line}}} \quad (1)$$

where,

$$R_{\text{line}} = R_{\text{end1}} + R_{\text{t1}} + R_{\text{t2}} + R_{\text{end2}}$$

and,

$$U = \frac{\left(\left(\frac{R_4 \cdot XC_3}{R_4 + XC_3} + R_3 \right) \cdot XC_2 \right)}{\frac{R_4 \cdot XC_3}{R_4 + XC_3} + R_3 + XC_2} + R_2 \cdot XC_1}{\frac{\left(\frac{R_4 \cdot XC_3}{R_4 + XC_3} + R_3 \right) \cdot XC_2}{\frac{R_4 \cdot XC_3}{R_4 + XC_3} + R_3 + XC_2} + R_2 + XC_1} + R_1 \quad (2)$$

Table Y: Calculate RM Impedance of Book Electrode

```
[Zeff]
Rline = Rend1 + Rt2 + Rt1 + Rend2
a = Rx : b = Rline : gosub [parallelCombineR]
a = result : b = U : gosub [parallelCombineR]
Zeff = result
RETURN
```

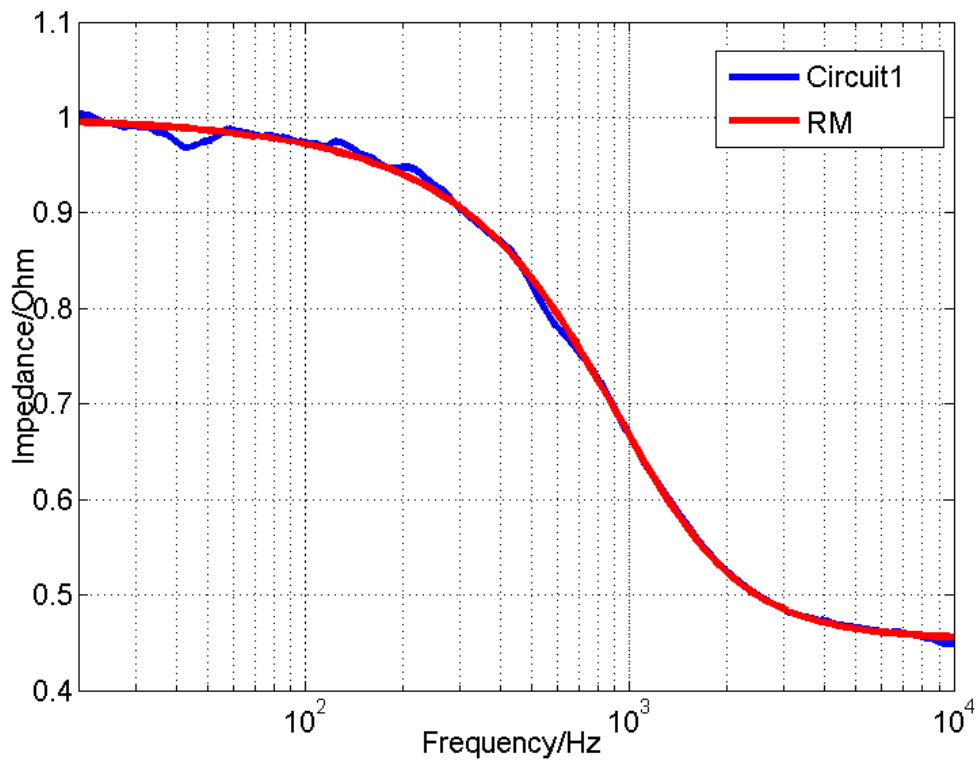


Fig. C. Figure showing comparison of the results obtained by building representative model of circuit 1 (book electrode) with experimental results obtained in the lab as in chapter 3.

The equations above are used in the compiler to calculate the approximate impedance output of circuit 1 in the frequency range of 20Hz to 10 kHz and to see its correlation with the experimental results of the book electrode without any compensation circuit, as shown in fig. C. We can see that shapes of both graphs are almost identical, with RM model lying on top of the non-compensated book electrode, indicating that the approximation made in building the model is acceptable and it can now be used in finding a relation between circuit 1 and

circuit 2 that neutralises the impedance output close to zero. For further testing of RM model, regression statistics is also performed that is shown in the next section of this chapter.

Regression analysis of the representative model RM

The regression analysis can be used to see the relation of the independent variable with respect to the dependent variable. The independent variable here is the RM of circuit 1 and dependent variable is the real data of the non-compensated book electrode, circuit 1. In order to see the correlation between the two variables, the regression statistics is performed using the Curve Expert Professional version 2.6.4 and choosing the 4-parameter non-linear Dr Hill Regression dose-response model that uses Hill equation is shown in table 4 and its correlation is shown in fig. 4.4. This model was chosen only because it uses Hill equation to fit non-linear data on the experimental results with accuracy. The purpose of performing regression analysis is three-fold.

- 1- To prove that it is reliable in terms of showing good correlation with the results of the experimentally tested circuit 1.
- 2- To prove the underlying assumption for designing the RM for the 3-stage compensation circuit, circuit 2.
- 3- To provide a conversion formula for mapping impedance values obtained from representative model to the real values from which mathematical relation of finding component values of the compensation circuit can be derived.

Table Z Dr-Hill Regression model used for regression analysis of RM

Overview

Name	DR-Hill
Kind	Regression
Family	Dose-Response Models
Equation	$y = \alpha + \theta x^\eta / (\kappa^\eta + x^\eta)$
# of Indep. Vars	1
Standard Error	0.005838
Correlation Coeff. (r)	0.999643
Coeff. of Determination (r²)	0.999286
DOF	96
AICC	-1026.506690

Parameters

	Value	Std Err	Range (95% confidence)
alpha	0.451174	0.001781	0.447638 to 0.454711
theta	0.603940	0.005129	0.593759 to 0.614121
eta	28.898416	0.487567	27.930603 to 29.866229
kappa	3.741869	0.002223	3.737456 to 3.746282

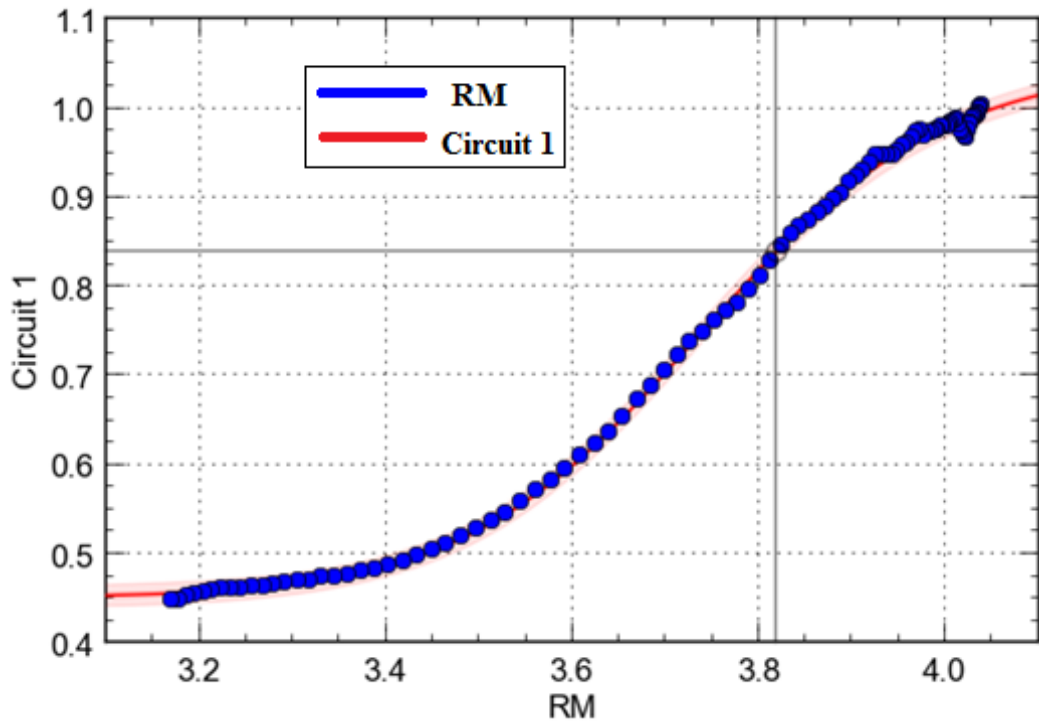


Fig. D Regression analysis plot showing correlation between RM of circuit one (x-axis) and real data values of circuit 1 (y-axis)

Dr-Hill Regression (dose-response model) was used the relation to perform regression analysis that is shown in table Z, along with the values of the coefficients resulted after successful regression analysis. The conversion formula purpose is to provide with a way of converting RM output to real output, so that if a problem is modelled with RM, we can convert the output to the real form.

$$Converted = 0.451 + \frac{0.6039 \times RM^{28.89}}{3.741^{28.89} + RM^{28.89}} \quad (3)$$

Where 28.89=eta from Hill equation (table Z).

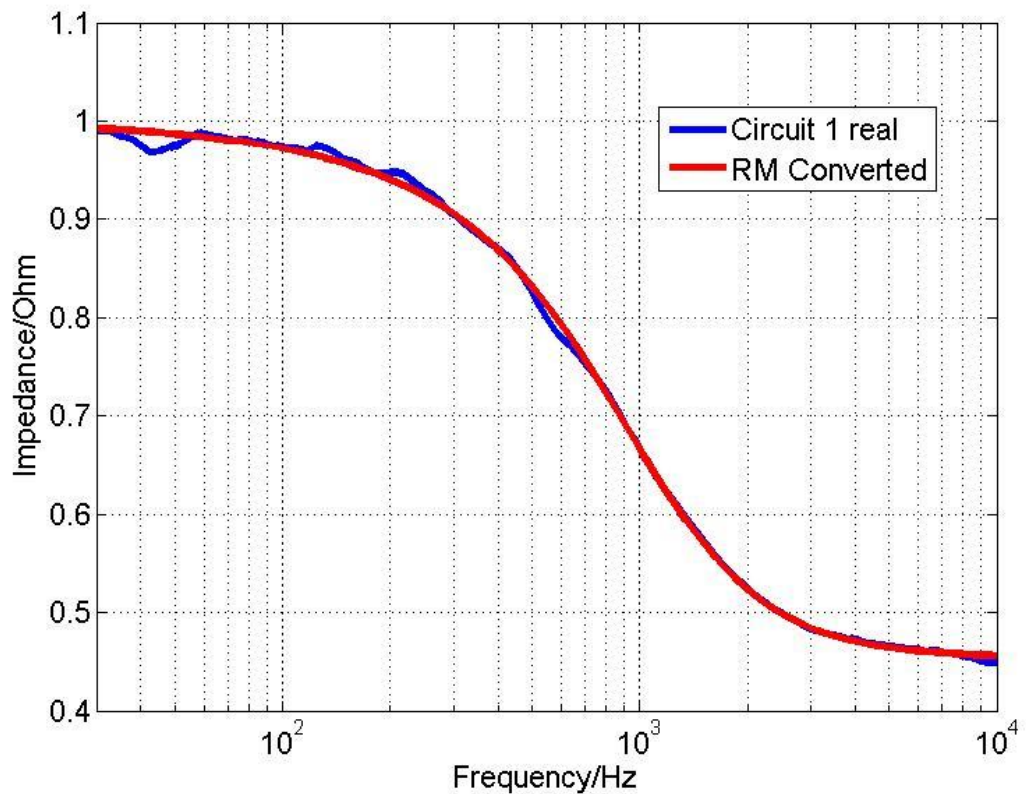


Fig. E. Comparison between RM converted of circuit 1 to the real experimental values of circuit 1

The comparison between the conversion from RM results and experimental results of circuit 1 is also performed to further examine how realistic the assumptions set before performing regression analysis are about the RM model of circuit 1 built so far, as shown in fig. E, that shows a close fitting of RM converted data on the experimental data. A high correlation of about 99.96% was also observed in the regression analysis done on the RM model created for the tripolar cuff model and its experimental data (fig. D). Results from both figures confirms that RM as designed for circuit 1 is a suitable representative model for the tripolar cuff electrode without compensation circuit and can be used further to derive the RM for circuit 2 and universal relation for neutralising interferences. The unit, U (impedance model of one electrode), that was used to represent one electrode ring of the tripolar cuff electrode and the resistor network (R_x , R_{line})

which together make up the RM of circuit 1 are valid for the acceptable approximation for RM which the approximate output of the uncompensated tripolar cuff electrode and it also proves the other assumptions that follow on the basis of RM and the unit, U are valid in the context of RM and the unit, U.

Mathematical relation between Circuit 1 and Circuit 2

Now that it is confirmed that RM model designed for the tripolar cuff electrode without compensation circuit is acceptable, focus is shifted towards the results when circuit 1 and 2 both are connected together using RM. From previous chapters we know that when both circuits are connected together EMG interference is neutralised but instead of using optimisation techniques a mathematical relation is tried to find what exists between the two circuits that forces the output close to zero.

Previously calculations were shown to find approximate impedance Z_{eff} of circuit 1 by taking in account U. If n extra unit of U are added in parallel to RM of circuit 1 (fig. F), the new overall approximate impedance can be calculated as,

$$Z_{\text{new}} = \frac{U \cdot Z_{\text{eff}}}{U + n \cdot Z_{\text{eff}}} \quad (4)$$

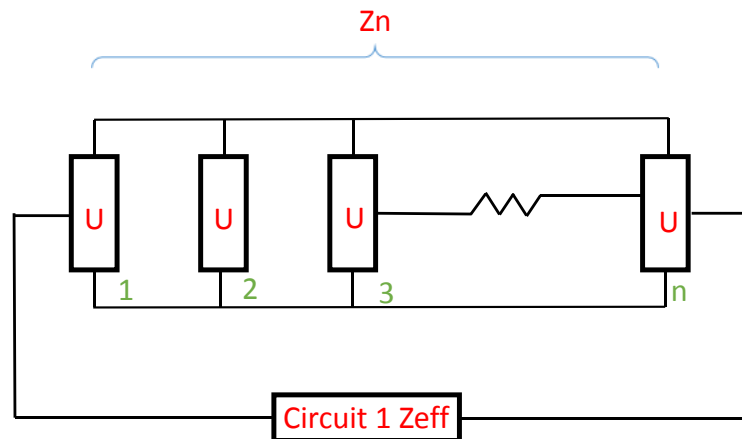


Fig. F connecting 'n' units in parallel to RM of Circuit 1 to create limiting relation for new overall impedance, Z_n . See equation 4.

If n is zero then new impedance is equal to the impedance of the circuit without compensation circuit but if n increases, Z_{new} approaches to zero, which is also wanted as a solution to neutralize EMG interference. Hence, the limiting value can be given by,

$$Z_{limit} = \frac{U}{n} \rightarrow 0 \quad (n \rightarrow \infty)$$

Dr-Hill regression model used on RM of circuit 1 uses the fixed limit of $0.451(\alpha)$ in the results (table 4) according to its equation. Therefore, *limit refactoring* needs to be applied to adjust the Z_{new} function as shown below.

Let $n_1 = 0.451$ and $n_2 = 0$, as we need the EMG neutralised output from the tripolar cuff with the compensation circuit, which is 0 in ideal circumstances.

From equation 4, let,

$$Limit_1 = \frac{A}{B + n_1 \cdot C}$$

and

$$Limit_2 = \frac{A}{B + n_2 \cdot C}$$

where $A = Z_{eff}$ of circuit 1, $B =$ unit impedance U used in circuit 1 and n is the number of units parallel to circuit 1. Rearranging the above equations we get,

$$n_1 = \frac{A - Limit_1 \cdot B}{Limit_1 \cdot C}$$

$$n_2 = \frac{A - Limit_2 \cdot B}{Limit_2 \cdot C}$$

In order to get the output 0 when any circuit is attached to circuit 1 in parallel, a multiplier is required that forces our current limit (0.451) to our new limit (0). 0 is only achieved theoretically in ideal conditions and under real conditions EMG minimisation close to null, much below the ENG signal is observed as shown in the previous chapter. Hence instead of using 0 in the calculations that will give an output of 0, any value close to null can be used. Here $1\text{m}\Omega$ is used as an example, about $30\text{m}\Omega$ was observed in the EMG minimisation during the experimental results using global optimisation procedure.

$$n_2 = multiplier(k) n_1$$

$$multiplier(k) = \frac{n_2}{n_1} = \left(\frac{A - Limit_2 \cdot B}{A - Limit_1 \cdot B} \right) \cdot \left(\frac{Limit_1}{Limit_2} \right)$$

Since the limits are generally less than 1,

$$\left(\frac{A - Limit_2 \cdot B}{A - Limit_1 \cdot B} \right) \approx 1$$

$$multiplier(k) = \frac{n_2}{n_1} = \left(\frac{Limit_1}{Limit_2} \right) = \frac{0.451}{0.001} = 451$$

The 451 is just showing the number of turns before reaching the required output. It is there because we selected the output ourselves to be 1mΩ and pushed the limit of 0.451 to 0.001. So for example, for an output of 30mΩ, limit of 0.451 is needed to be divided by number 15.033. Hence, by putting this in the Z_{new} relation, the mathematical relation that gives the total impedance closed to null when the 3-stage compensation circuit, Circuit 2(n=1) is added to the tripolar cuff, Circuit 1 can be derived as,

$$Z_{new} = \frac{U \cdot Z_{eff}}{U + 451n \cdot Z_{eff}} \quad (5)$$

This equation is then tested in the compiler by putting n= 1 that is one unit attached as a compensation circuit and it was observed that just by attaching a single unit to circuit 1, the output goes to an average of 1mΩ linearly in the frequency band of interest. This was the output needed in this calculation and the trend is also similar to the results being observed during the experimental testing of the 3 stage compensation circuit with book electrode using the global optimisation method in simulations described in chapter 3.

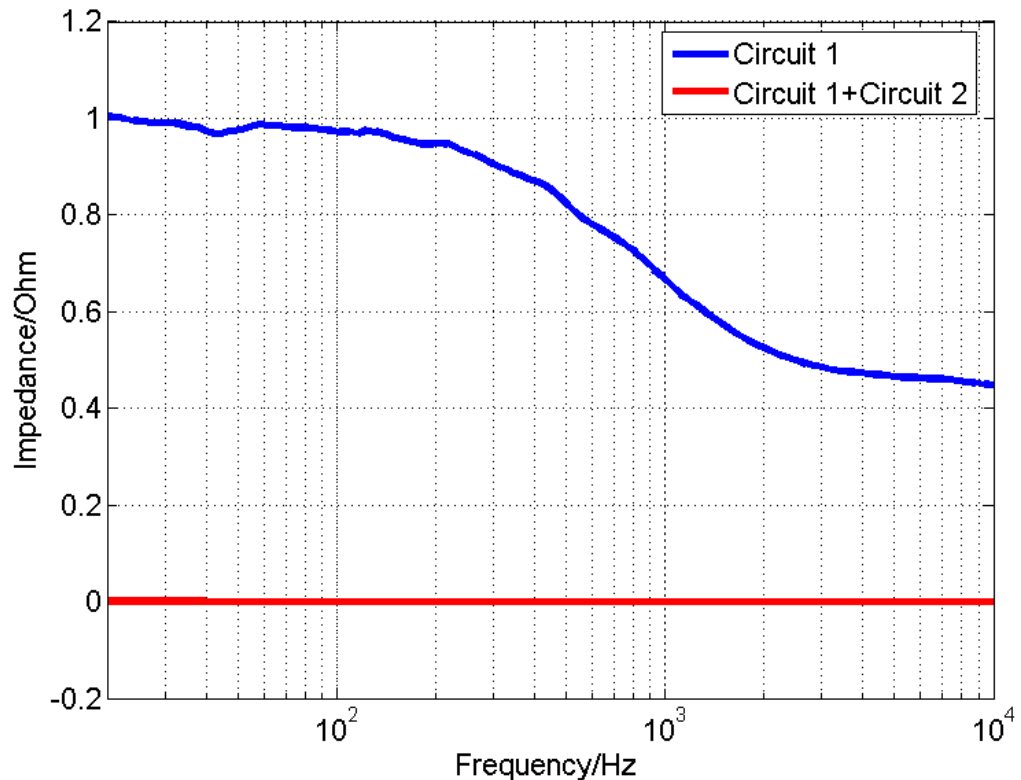


Fig. G Output results of Z_{new} when circuit 2, compensation circuit is attached to circuit 1. It shows that when only one unit is attached it forces the output close to null. Also, output response of circuit 1 and 2 is not a flat line but ranging between $1.6\text{m}\Omega$ to $1\text{m}\Omega$, with becoming constant at higher frequencies

Thus, from equation (5) and equation (2) the unknown components of the 3-stage RC ladder network can be found by fixing either of the component, resistor or capacitor in the relationship and finding the other unknown (fig H). In equation (5) by setting out the output impedance close to null or desired value and by using Z_{eff} of circuit 1 either from the programming code given or any other relevant method, output impedance of circuit 2 (named U) required to reach to that output in the equation can be found. Once this is known, equation (2) can be used to find either resistor or capacitor by fixing one of them. Both Z_{eff} and U can be calculated fairly quickly and easily by using the programming provided in the abstract A for frequency range of 20 to 10k Hz. Only component values of the tripolar cuff electrode need to be updated in the code if and when required for the calculation.

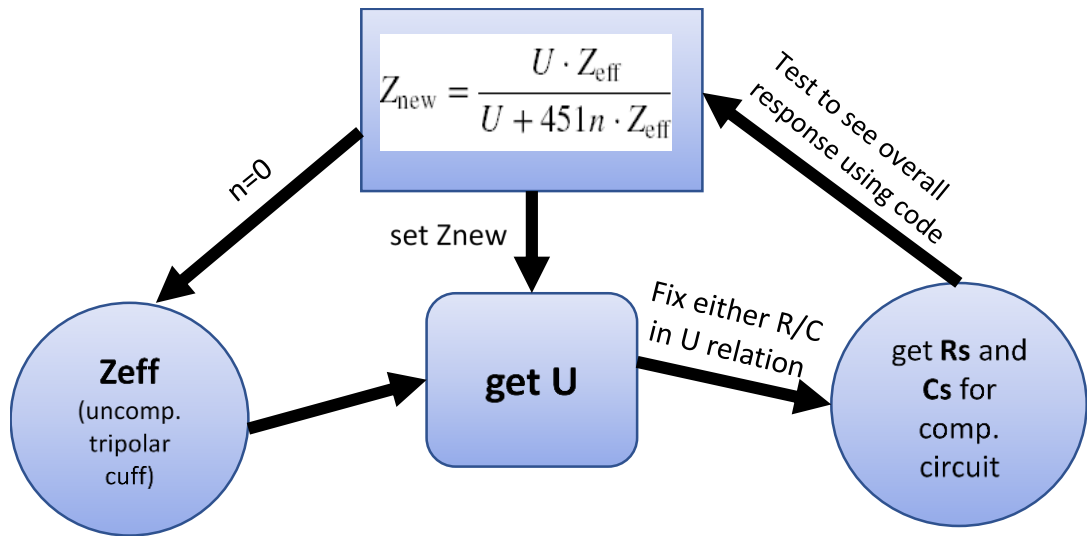


Fig H Block diagram showing the steps that can be taken to calculate the circuit parameters of the compensation circuit required in bringing the output of the tripolar cuff closer to null for EMG minimisation

Discussion and Analysis

There could be several methods of finding the electrical components of a compensation circuit to be used with the tripolar cuff electrode for EMG neutralisation, but two methods have been considered in this work. Where global optimisation is one method of finding the unknown components, it suffers from few major problems. Most importantly, it is a complicated and lengthy process which is not user friendly and the component values it provides are not always realistic to be used with the real implant. Moreover, if the capacitor values obtained are in microfarad range then it further complicates the process of having the need of multipliers to use the equivalent smaller size capacitors at the expense of increasing the size requirements and also power requirements due to increase in the size of the resistors.

In this section another proposal of a mathematical relation is presented that can be possibly used to find the unknown components of the 3-stage compensation circuit. It should be noted that the mathematical relation provided in this chapter (equation 5) is obtained through one approach and any other approach can also be used in finding the unknown components of the compensation circuit instead of using the lengthy global optimisation process presented in the previous chapter. There are further improvements that can be applied on this relation, which will be highlighted later in the chapter.

The mathematical relation in equation 5 was found by taking the problem in the black box. As, it is known that the output of a tripolar cuff electrode suffers from the EMG interference thus, in order to extract an unaffected ENG signal, this interference has to be ideally removed or suppressed much below the required signal. Where it was seen that the simple RC network is able to remove EMG interference at the spot frequency, it is shown in the previous chapters that simple 3 and 2 stage RC ladder compensation circuits minimise the EMG interference almost linearly in the entire frequency range of interest, independent of the frequency. Hence, the purpose of the compensation circuit is always to bring the output close to null linearly in the frequency band of interest, which in our case is between 500 – 10k Hz. Thus, the output from the tripolar cuff along with the topology of the compensation was known but mathematical relationship that forces the output close to null, linearly in the frequency band of interest was missing that was tried to be found using the black box approach Hence, the procedure started with the set of assumptions by keeping in record that if they don't go with the required results then they will be discarded and procedure shall be revised. However, as can be seen in the graph (fig C) obtained that the set assumptions worked out satisfactorily with the expected results, the output of circuit 1/tripolar cuff electrode alone matches satisfactorily to the results obtained in the lab. Impedance modelling of a tripolar cuff electrode gives its equivalent circuit model as explained in detail in chapter 3 using a simple EC lab software. Same circuit model has been used in this chapter deriving the new mathematical relations, however any electrode model can be used to calculate its output and its corresponding component values can be updated in the programming code

provided in the appendix A. However, this might not always be needed as it can be easily and quickly seen on the impedance spectrometer as well. Similarly, next Dr- Hill Regression model was used to perform regression analysis to confirm the correlation of the output of uncompensated tripolar cuff electrode with its corresponding lab results (fig. D) and most importantly to design a new representative model to map output impedance values to the experimental data (fig. E). This can may be replaced as well if required with even a better model. However, in the current work, this was taken forward for the derivation of the relation. The mathematical relationship between tripolar cuff electrode and the compensation circuit is then found using the limiting theorem. It was used due to the assumption set that if more compensation circuits are used in parallel to the tripolar cuff, output shall reduce and eventually falls to zero but as in the current problem only 1 need to be used to force the output to the null hence a limit needs to be applied. Equation 5 clearly shows this relation. If number of units to be attached with the tripolar cuff is zero then the relationship reduces to only Z_{eff} , which is the output of the uncompensated tripolar cuff and can be found from the program as well. The figure 451 in the equation is due to the regression model used, it's the fixed value of α in the Hill-equation. As it has a limit of 0.451 and the output from the tripolar cuff was set to $1m\Omega$, 451 was achieved. For a different output, this would be a different number and it can easily be updated in the code without affecting the functionality of the circuit. This, however needs further investigation and it might be possible that either a different regression model with a different limit (ideally close to as null as possible) is tested or a different mathematical relationship independent of the regression model is derived. Nonetheless, it does not affect the functionality of the circuit and this relationship when used in the programming code for an output response of $1m\Omega$, resulted in a linear EMG minimisation in the frequency band of interest, fig. G. By deciding a desired output, Z_{new} , the value of the multiplier can be updated in the equation 5 and as the output of uncompensated tripolar cuff, Z_{eff} is known, the required output of the compensation circuit, U can be found. Once, this output is known, one parameter either resistor or capacitor in the impedance relation of U (equation 2) can be fixed to find the other unknown. Resistor being frequency independent would be easier to find by fixing the value of the capacitor. It is

expected that any one frequency in the bandwidth of range of interest can be used to find the components of the compensation circuits as, frequency dependence was observed in the output responses of the cuff. This however, needs further testing which can be done either by computing the output of the compensation circuit at all frequencies or by finding the components at few fixed frequencies and noticing if they came out to be the same parameters. The new approximated component parameters of the compensation circuit can also be quickly tested with the programming code (appendix 1) to see the output response of cuff with respect to EMG minimisation for neural signal recording.

Summary

Thus, at this stage, a mathematical relationship has been proposed by using one approach that can be used to find the unknown components of the compensation circuit when attached with any tripolar cuff. However further work is required in may be improving the relationship and most importantly testing it in invitro and invivo conditions with different tripolar cuff to see its effectiveness in minimising the EMG interference.

[Programming code for estimation of response from tripolar cuff and compensation circuits]

```
rem circuit analysis - final code
```

```
rem Revision Date - November 9, 2017
```

```
rem Author: Sabeeka Zehra
```

```
'THIS IS WHERE WE FETCH THE FREQUENCY DATA
```

```
[data]'this process [data] scans the freq file and writes the values into memory
```

```
dim agent$(0,0)
```

```
files "", "*. **", agent$(
```

```
path$ = agent$(0,2)+agent$(0,3)
```

```

file$ = path$+"freq.txt" : open file$ for append as #f : #f "" ; : close #f
open file$ for input as #f
data$ = input$(#f, lof(#f)) : count = lof(#f)
close #f
data$ = mid$(data$, 1, len(data$) - 1)
data$ = chr$(10)+data$
dim x(count) : dim y(count)
x = 0 : y = 0
for node = 1 to len(data$)
node$ = mid$(data$,node,1)
if node$ = chr$(10) then x = x + 1 : x(x) = node
if node$ = chr$(13) then y = y + 1 : y(y) = node
next node
nodes = x : dim freq(nodes)
for use = 1 to nodes
freq(use) = val(mid$(data$,x(use)+1, y(use) - x(use) - 1))
next use

```

'THIS IS WHERE WE SET PARAMETER VALUES

[params] ' these are parameter settings for the unit(use dashboard to make changes)

Rend1 = 54 : Rend2 = 64 : Rt1 = 22 : Rt2 = 9.6 : Rx = 4.17 : dim Rbar(4)

Rbar(4) = 3380 : Rbar(3) = 2260 : Rbar(2) = 365.4 : Rbar(1) = 35.5

dim Cbar(3) : Cbar(3) = 0.000124 : Cbar(2) = 0.000002 : Cbar(1) = 0.000002

units = 1 : multiplier = 451 'set unit to 0 and multiplier to 1 to only get circuit 1 output

'and set unit =1 and multiplier= 451 to get circuit output along with the circuit 2

goto [solve]

'THIS IS WHERE EQUATION ARE CALLED FOR CALCULATIONS

[seriesCombineRC]

result = $(y^2 + z^2)^{0.5}$

RETURN

[seriesCombineR]

result = $y + z$

RETURN

[parallelCombineRC]

result = $(a*b)/((a^2 + b^2)^{0.5})$

RETURN

[parallelCombineR]

result = $(a*b)/(a+b)$

RETURN

'THIS IS THE CONVERSION EQUATION FROM RM TO ACTUAL

[DRtransform]

limit = 0.451/multiplier 'limit re-factoring applied

$y = \text{limit} + ((0.6039*(x^{28.89}))/((3.741^{28.89} + x^{28.89}))$

RETURN

'THIS IS WHERE WE CALCULATE THE CIRCUIT 2 IMPEDANCE

[UImpedance]

$x = 1/(2*3.14*freq*Cbar(3))$

a = Rbar(4) : b = x : gosub [parallelCombineRC]'step 1 in U calculation

$x = 1/(2*3.14*freq*Cbar(2))$

a = result + Rbar(3) : b = x : gosub [parallelCombineRC]'steps 2 and 3 in U calculation

$x = 1/(2*3.14*freq*Cbar(1))$

a = result + Rbar(2) : b = x : gosub [parallelCombineRC]'steps 4 and 5 in U calculation

```

impedance = result + Rbar(1)

RETURN

'THIS IS WHERE WE CALCULATE CIRCUIT 1/TRIPOLAR CUFF ALONE IMPEDANCE

[Zeff]

Rline = Rend1 + Rt2 + Rt1 + Rend2

a = Rx : b = Rline : gosub [parallelCombineR]

a = result : b = U : gosub [parallelCombineR]'combination of that result with U (net impedance of
3 Units = impedance/3)

Zeff = result

RETURN

'THIS IS THE SOLVER THAT CALCULATES TOTAL IMPEDANCE OUTPUT

[solve]

for node = 1 to nodes 'looping process for dynamic total impedance calculation over all
frequency values

freq = freq(node)'dynamic frequency selection from stored values in memory (from freq.txt file)

gosub [UImpedance] 'update value of U for new frequency

U = impedance/3 'calculate net impedance for 3 units in circuit 1

gosub [Zeff]'fetch circuit 1 impedance

for add = 1 to units*multiplier 'batch process to add new units of circuit2 to circuit1

Zeff = (Zeff*impedance)/(Zeff + impedance)'Z(new) updated for new impedance input

next add

x = Zeff : gosub [DRtransform]'conversion process from RM value to actual value

Zeff = y : print Zeff 'result display

next node 'repeat this process

END

```

References

- [1] National spinal cord injury statistical center (NSCISC), "Spinal cord injury facts and figures at a glance," available at: <https://www.nscisc.uab.edu>, last accessed: April 2018.
- [2] International Spinal Research Trust, "The Facts", Available at: <https://www.spinal-research.org/>, last accessed January 2018.
- [3] Spinal research centre, "annual review", available on <https://www.spinal-research.org/>, last accessed March 2018.
- [4] National Cancer Institute, "SEER training modules", available on <https://training.seer.cancer.gov/>, last accessed Aug 2017.
- [5] National institute of neurological disorders and stroke, available on <https://www.ninds.nih.gov/>, last accessed on Feb 2017.
- [6] Eck. C./F., "Spinal cord injury: levels, treatment, symptoms, recovery", spinal cord injury treatments and rehabilitation centre, from <https://www.medicinenet.com/>, last accessed March 2018.
- [7] Ando. T et al., "Improved functional recovery of injured spinal cords by efficient siRNA delivery using photomechanical waves", pp. 159-163, 1st International Symposium on Access Spaces (ISAS), Yokohama, 2011,
- [8] Chikuda. H, Yasunaga. H, Takeshita. K, Horiguchi. H, Kawaguchi. H, Ohe. K, Fushimi. K, Tanaka. S, "Mortality and morbidity after high-dose methylprednisolone treatment in patients with acute cervical spinal cord injury: a propensity-matched analysis using a nationwide administrative database", Emergency medical journal, Feb 2013.
- [9] Evaniew. et al., "Methylprednisolone for the treatment of patients with acute spinal cord snjuries: A propensity score-matched cohort study from a canadian multi-center spinal cord injuryRegistry", vol. 32, no. 21, pp. 1674–1683. Nov 2015.
- [10] Khan.K. H, Souter. M.J, "Challenging Topics in Neuroanesthesia and Neurocritical Care",pp. 83-95, 1st edition, Springer, Tehran, 2017.
- [11] Korse. N. S, Veldman. A. B, Peul. W. C, Lankamp. V, "The long-term outcome of micturition, defecation and sexual function after spinal surgery for cauda equina syndrome", vol. 12, April 2017.
- [12] McDonald. J. W, Becker. D, Huettner. J, (2013- pp. 273-738). Handbook of stem cells, second edition, department of neurology, Nashville, USA, 2013.
- [13] Yarkony. G. M, "Spinal cord injury: Medical Management and Rehabilitation", Rehabilitation institute of Chicago, Chicago, 1994.
- [14] Mayo Clinic, "Spinal cord injury", available on <https://www.mayoclinic.org/diseases-conditions/spinal-cord-injury/symptoms-causes/syc-20377890>, last accessed on May, 2016.
- [15] Villines. Z, "The Top 10 Causes of Spinal Cord Injuries", from <https://www.spinalcord.com>, last accessed on February 08, 2016.
- [16] Norenberg. M. D, Smith. J, Marcillo. A, "The Pathology of Human Spinal Cord Injury: Defining the Problems", vol. 21, No. 4, 8 Jul 2004.

- [17] Anwar. M. A, Tuqa S, Ali H. E, "Inflammogenesis of Secondary Spinal Cord Injury." *Frontiers in Cellular Neuroscience* 10 (2016), vol 98., PMC. Web., 30 Apr. 2018.
- [18] Spinal cord.com, "Complete vs incomplete spinal cord injuries", available on <https://www.spinalcord.com/blog/complete-vs.-incomplete-spinal-cord-injuries>, last accessed on May 2016.
- [19] Mcdonald, J. W., "Repairing the damaged spinal cord", *Sci Am* 281, pp. 64-73, 1999.
- [20] David. G, David. D, Britney. T, Ashraf. G "Functional electrical stimulation therapies after spinal cord injury", *Neurorehabilitation*, vol. 28, pp. 231-48, 2011.
- [21] Lynch. C. L, Popovic. M. R, "Functional Electrical Stimulation", in *IEEE control systems*, vol. 28 no. 2 April 2008.
- [22] M.R. Popovic, T.A. Thrasher, V. Zivanovic, J. Takaki, and V. Hajek, "Neuroprosthesis for restoring reaching and grasping functions in severe hemiplegic patients," *Neuromod.*, vol. 8, no. 1, pp. 60–74, 2005.
- [23] Adamczyk, M.M, and Crago, P.E, "Simulated feedforward neural network coordination of hand grasp and wrist angle in a neuroprosthesis," *IEEE Trans. Biomed. Eng.*, vol. 8, no. 3, pp. 297–304, 2000.
- [24] Matjacic, Z and Bajd, T., "Arm-free paraplegic standing—Part II: Experimental results," *IEEE Trans. Rehab. Eng.*, vol. 6, no. 2, pp. 139–150, 1998.
- [25] Holderbaum, W., Hunt, K.J., and Gollee, H., "H[∞] robust control design for unsupported paraplegic standing: Experimental evaluation," *Control Eng. Practice*, vol. 10, pp. 1211–1222, 2002.
- [26] Donaldson, N., Perkins, T.A., Fitzwater, R., Wood, D.E., and Middleton, F., "FES cycling may promote recovery of leg function after incomplete spinal cord injury," *Spinal Cord*, vol. 38, no. 11, pp. 680–682, 2000.
- [27] Demchak, T.J., Linderman, J.K., Mysiw, W.J., Jackson, R., Suun, J., and Devor, S.T., "Effects of functional electrical stimulation cycle ergometry training on lower limb musculature in acute SCI individuals," *J. Sports Science Med.*, vol. 4, no. 3, pp. 263–271, 2005.
- [28] Collinger, J. L., Foldes, S., Bruns, T. M., Wodlinger, B., Gaunt, R., & Weber, D. J., "Neuroprosthetic technology for individuals with spinal cord injury. *The journal of spinal cord medicine*, 36(4), 258-72, 2013.
- [29] Baer, G.A., Talonen P.P., Shneerson J.M., Exner G., Wells F.C., "Phrenic nerve stimulation for central ventilatory failure with bipolar and four-pole electrode systems.", *Pacing Clin Electrophysiol* ; 13(8):1061-72, Aug, 1990.
- [30] Brindley GS, Polkey CE, Rushton DN., "Sacral anterior root stimulators for bladder control in paraplegia." *Paraplegia*. 20:365–81, Dec. 1982.
- [31] Haugland M., and Sinkjaer T., "Interfacing the body's own sensing receptors into neural prosthesis devices," *Technol. Health Care*, vol. 7, no. 6, pp. 393-399, January 1999b.
- [32] Kirkham A. P. S., Knight S. L., Craggs M. D., Casey A. T. M., and Shah P. J. R., "Neuromodulation through sacral nerve roots 2 to 4 with a Finetech-Brindley sacral posterior and anterior root stimulator," *Spinal Cord*, vol. 40, no. 6, pp. 272-281, June 2002.

- [33] Brindley G. S., Polkey C. E., Rushton D. N., and Cardozo L., "Sacral anterior root stimulators for bladder control in paraplegia: the first 50 cases," *J. Neurol. Neurosurg. Psychiatry*, vol. 49, no. 10, pp. 1104-1114, October 1986.
- [34] Boyer S., Sawan M., Abdel-Gawad M., Robin S., and Elhilali M. M., "Implantable selective stimulator to improve bladder voiding: design and chronic experiments in dogs," *IEEE Trans. Rehab. Eng.*, vol. 8, no. 4, pp. 464-470, December 2000.
- [35] Brindley G. S., Polkey C. E., and Rushton D. N., "Sacral anterior root stimulators for bladder control in paraplegia," *Paraplegia*, vol. 20, pp. 365-381, 1982.
- [36] Brindley G. S., "The first 500 patients with sacral anterior root stimulator implants: general description," *Paraplegia*, vol. 32, no. 12, pp. 795-805, December 1994.
- [37] Jezernik S., Wen J. G., Rijkhoff N. J. M., Djurhuus J. C., and Sinkjaer T., "Analysis of bladder related nerve cuff electrode recordings from preganglionic pelvic nerve and sacral roots in pigs," *J. Urol.*, vol. 163, no. 4, pp. 1309-1314, April 2000.
- [38] Stein R. B., Charles D., Davis L., Jhamandas J., Mannard A., and Nichols T. R., "Principles underlying new methods for chronic neural recording," *Le J. Can. des Sciences Neurologiques*, vol. 2, pp. 235-244, 1975.
- [39] Stein. R. B, Nichols. T. R, Jahamandas. J, Davis. L, Charles. D, "Stable long-term recordings from cat peripheral nerves", *Brain Research*, vol. 128. Pp. 21-38, 1977.
- [40] Haugland M. K., and Hoffer J. A., "Artifact-free sensory nerve signals obtained from cuff electrodes during functional electrical stimulation of nearby muscles," *IEEE Trans. Rehab. Eng.*, vol. 2, no. 1, pp. 37-40, March 1994.
- [41] Hoffer J. A., Marks W. B., and Rymer W. Z., "Nerve fibre activity during normal movements," *Proc. Annu. Society for Neuroscience Meeting*, vol. 4, p. 300, 1974.
- [42] Armstrong, R.D. and Burnham, Richard, "The effect of roughness on the impedance of the interface between a solid electrolyte and a blocking electrode." *Journal of Electroanalytical Chemistry and Interfacial Electrochemistry*, vol. 72, pp. 257-266, 1976.
- [43] Bryden. A. M, Kilgore. K. L, Kirsch. R. F, Memberg. W. D, Peckham. P. H, Keith. M. W, "An implanted neuroprosthesis for high tetraplegia", *Top Spinal Cord Inj Rehabil.*, vol. 10, pp. 38-52, 2005.
- [44] Normann. R. A, Fernandez. E, "Clinical applications of penetrating neural interfaces and Utah Electrode Array technologies", vol. 13, December 2016.
- [45] Andreasen. L. N, Struijk. J. J, "Artefact reduction with alternative cuff configurations", *IEEE Trans. Biomed. Eng.*, vol. 50, no. 10, pp. 1160-1166, October 2003.
- [46] Struijk J. J., and Thomsen M., "Tripolar nerve cuff recording: stimulus artifact, EMG, and the recorded nerve signal," *IEEE Eng. Med. and Biol.*, vol. 2, pp. 1105-1106, September 1995.
- [47] Struijk J. J., Thomsen M., Larsen J. O., and Sinkjaer T., "Cuff electrodes for long-term recording of natural sensory information," *IEEE Eng. Med. and Biol.*, vol. 18, no. 3, pp. 91-98, May/June 1999.

- [48] Kurstjens G. A. M, Borau A., Rodriguez A., Rijkhoff N. J. M., and Sinkjaer T., "Intraoperative recording of electroneurographic signals from cuff electrodes on extradural sacral roots in spinal cord injured patients," *J. Urol.*, vol. 174, no. 4 Pt-1, pp. 1482-1487, October 2005.
- [49] Pachnis, I., Demosthenous, A., and Donaldson, N., "Passive neutralization of myoelectric interference from neural recording tripoles.," *IEEE transactions on bio-medical engineering*, vol. 54, no. 6 Pt 1, pp. 1067–74, Jun. 2007.
- [50] Pachnis, I., Demosthenous, A., and Donaldson, N., "Towards an adaptive modified quasi-tripole amplifier configuration for EMG neutralization in neural recording tripoles.," in *ISCAS 2010 – 2010 IEEE International Symposium on Circuits and Systems*, pp. 3144–3147, 2010.
- [51] Donaldson N., Perkins T., Pachnis I., Vanhoest A., and Demosthenous A., "Design of an implant for preventing incontinence after spinal cord injury," *Artif. Organs*, vol. 32, no. 8, pp. 586-591, August 2008.
- [52] Demosthenous, A., Pachnis, I., Jiang, D., and Donaldson, N., "An Integrated Amplifier with Passive Neutralization of Myoelectric Interference from Neural Recording Tripoles," in *IEEE Sensors Journal*, vol. 13, no. 9, pp. 3236-3248, Sept. 2013.
- [53] Brindely. G. S, "Electrode array for making long-lasting electrical connections to spinal roots", *J. Physiol.*, vol. 222, no. 2, p. 135, 1972.
- [54] Ottoson. D., (1983 pp. 33-77). *Physiology of the Nervous System*. Basignstoke, U.K., Palgrave Macmillan.
- [55] Amerman E.C., 2016. *Human Anatomy & Physiology*, Cambridge, Pearson.
- [56] Mathers L. H., "The Peripheral Nervous System: Structure, Function, and Clinical Correlations, Wokingham, U.K.: Addison-Wesley, 1985.
- [57] Mittal. P, Gupta. R, Mittal. A, Mittal. K, "MRI findings in a case of spinal cord Wallerian degeneration following trauma", *PMC US national library medicine* Vol. 21, 2016.
- [58] Khan Academy, "Organ Systems", available on <https://www.khanacademy.org/test-prep/mcat/organ-systems>, last accessed on April, 2008.
- [59] Inner Body, "Nervous System", available on, <http://www.innerbody.com/image/nervov.html>, last accessed March 2018.
- [60] Lumen Boundless Biology, "How neurons communicate", available on, <https://courses.lumenlearning.com/boundless-biology/chapter/how-neurons-communicate/>, last accessed April, 2018
- [61] Zipursky. et al., "Molecular Cell Biology.", 4th edition, W. H. Freeman, New York, 2000.
- [62] DuBois M.I, "Action Potential: Biophysical and Cellular Context, Initiation, Phases, and Propagation", Nova publishers, New York, 2010.
- [63] Susuki. K, "Myelin: A specialized membrane for cell communication", *nature education*, vol. 3, pp. 59, 2014.
- [64] Meng. E, "Technologies to Interface with the Brain for Recording and Stimulation", *Biomedical and Electrical Engineering, Frontiers of Engineering, National Academy of Engineering*, www.naefrontiers.org, last accessed on Dec, 2018.

- [65] Vanhoestenbergh A., "Implanted devices: improved methods for nerve root stimulation," Ph.D. dissertation, Dept. of Medical Physics and Bioeng., University College London, London, U.K.: 2007.
- [66] Keynes R. D., Aidley D. J., Huang C. L., Nerve and Muscle, Chapter 2, pp. 12, 4th ed., London, U.K.: Cambridge University Press, 2001.
- [67] Davis. L. E., King. M. K., and Schultz. J. L., "Fundamentals of Neurologic Disease", Chapter 10, pp. 101-103, New York, U.S.A. :Demos Medical Publishing Inc., 2005.
- [68] Diagram taken from Wikipedia: the free encyclopaedia, "Action Potential," available at: https://www.cs.mcgill.ca/~rwest/wikispeedia/wpcd/wp/a/Action_potential.htm, last accessed: Dec 2018.
- [69] Tsintou. M, Dalamagkas. K, Seifalian. A. M, "Advances in regenerative therapies for spinal cord injury: a biomaterials approach", Neural Regen Res. 726–742, 10 May 2015.
- [70] Bauchet. L, Lonjon. N, Perrin. F. E, Gilbert. C, Privat. A, Fattal. C, "Strategies for spinal cord repair after injury", a review of the literature and information. Ann Phys Rehabil Med., vol. 52, pp. 330–351, 2009.
- [71] Bullock, R., Nathoo, "N. Injury and cell function. in: P.L. Reilly, R. Bullock (Eds.) Head injury", pp. 113-119, London, Hodder Education, 2005.
- [72] Mittal. P, Gupta. R, Mittal. A, Mittal. K, "MRI findings in a case of spinal cord Wallerian degeneration following trauma", PMC US national library medicine Vol. 21, 2016.
- [73] Stroncek J. D, Reichert W. M, Overview of Wound Healing in Different Tissue Types. In: Reichert WM, editor. Indwelling Neural Implants: Strategies for Contending with the In Vivo Environment. Boca Raton (FL), CRC Press/Taylor & Francis., 2008.
- [74] Okutan. Et al., "Immunomodulation of acute experimental spinal cord injury with human immunoglobulin", pp. 549-553, G. J Clin Neurosci Off J Neurosurg Soc Australas, vol 16, 2009.
- [75] Rabinowitz et.al,"Urgent Surgical Decompression Compared to Methylprednisolone for the Treatment of Acute Spinal Cord Injury", pp. 2260-2268, Spine, vol. 33, 2008.
- [76] Armstrong. R. D, Burnham. R. Agnew W. F., and McCreery D. B., Neural Prostheses: Fundamental Studies, PP. 10-57, London, U.K.: Prentice-Hall, 1992.
- [77] Borton. D, Micera. S, Jdel. R. M and Courtine. G, "Personalized neuroprosthetics", Science translational medicine, vol. 5, pp. 210, November 2013.
- [78] Blana. D, Hincapie. J. G, Chadwick. E. K, Kirsch. R. F, "A musculoskeletal model of the upper extremity for use in the development of neuroprosthetic systems", Journal of Biomechanics., vol. 41, issue 8, pp. 1714-1721, 2008.
- [79] Stein R. B., Peckham P. H., and Popovic D. P., Neural Prostheses: Replacing Motor Function After Disease or Disability, New York, U.S.: Oxford University Press, 1992.
- [80] Becker. D, Sadowsky. C. L and McDonald. J. W, "Restoring function after spinal cord injury", The Lancet Neurology, vol. 9, no. 1, p 1-15, January 2003.

- [81] Dietz. V, Nef. T, Rymer. W. Z, *Neurorehabilitation Technology*, pp. 517-526, 2nd edition, Springer, London, U.K., 2010.
- [82] Cooper. R. A, Ohnabe. H, Hobson. D. A., "An Introduction to Rehabilitation Engineering", pp. 162-168, CRC Press, 2010
- [83] Kilgore. K., "Implantable Neuroprostheses for Restoring Function", Woodhand publishing series in biomaterials, 1st edition, 2015.
- [84] Peckham P. H., and Knutson J. S., "Functional electrical stimulation for neuromuscular applications," *Annu. Rev. Biomed. Eng.*, vol. 7, pp. 327-360, 2005.
- [85] Yan. T, Hui-Chan. C. W. Y, Li. L. S. W, "Functional electrical stimulation improves motor recovery of the lower extremity and walking ability of subjects with first acute stroke: a randomized placebo-controlled trial", *Stroke*, vol. 36, pp.80-85. Jan 2005.
- [86] Wikipedia: the free encyclopaedia, "Functional Electrical Stimulation," available at: https://en.wikipedia.org/wiki/Functional_electrical_stimulation, and 'Spinal Cord Injury' https://en.wikipedia.org/wiki/spinal_cord_injury, last accessed: April 2018.
- [87] Gorman. P, Peckham. P, Selzer. M, Clarke. S, Cohen. L, Kwakkel. G, & Miller. R, (2014 pp.120-134). *Neural Repair and Rehabilitation; Functional electrical stimulation in neurorehabilitation*, Cambridge, Cambridge University Press 2014.
- [88] Cleveland FES centre, "The Cleveland FES Center's freehand system", available on <http://fescenter.org/>, last accessed April, 2018
- [89] Hampson. R. E, Gerhardt. G. A, Marmarelis. V, Song. D, Opris. I, Santos. L, Berger. T. W, Deadwyler. S. A, "Facilitation and restoration of cognitive function in primate prefrontal cortex by a neuroprosthesis that utilizes minicolumn-specific neural firing", vol. 9, no. 5, September 2012.
- [90] Shendkar. C, Lenka. P. K, Biswas. A, Kumar. R and Mahadevappa. M, "Design and development of a low-cost biphasic charge-balanced functional electric stimulator and its clinical validation," in *Healthcare Technology Letters*, vol. 2, no. 5, pp. 129-134, October 2015.
- [91] Boncompagni. S., "Severe muscle atrophy due to spinal cord injury can be reversed in complete absence of peripheral nerves", *European Journal Translational Myology - Basic Applied Myology*, vol. 22, pp. 161-200, 2012.
- [92] de Boer. R, Borntraeger. A, Knight. A. M, Hebert-Blouin. M. N, Spinner. R. J, Malessy. M. J, Yaszemski. M. J, Windebank. A. J, "Short- and long-term peripheral nerve regeneration using a poly-lactic-co-glycolic-acid scaffold containing nerve growth factor and glial cell line-derived neurotrophic factor releasing microspheres", *J. Biomed. Mater. Res. A*, vol. 100, pp. 2139–2146, 2012.
- [93] Lynch. C. L and Popovic. M. R, "A Comparison of Closed-Loop Control Algorithms for Regulating Electrically Stimulated Knee Movements in Individuals with Spinal Cord Injury," in *IEEE Transactions on Neural Systems and Rehabilitation Engineering*, vol. 20, no. 4, pp. 539-548, July 2012.[94] Rahal M., Winter J., Taylor J., and Donaldson N., "Application of closed-loop control in the reduction of interference in nerve cuff recordings," *IEEE Proc. ICECS*, vol. 2, pp. 1039-1042, September 1999.

- [95] Popovic D. B., Stein R. B., Jovanovic K. Lj., Dai R., Kostov A., and Armstrong W. W., "Sensory nerve recording for closed-loop control to restore motor functions," *IEEE Trans. Biomed. Eng.*, vol. 40, no. 10, pp. 1024-1031, October 1993.
- [96] Webster J. G., *Medical Instrumentation: Application and Design*, pp. 137-220, 4th ed. London, U.K.: John Wiley & Sons, 2010.
- [97] McAdams E. T., *Bioelectrodes Ch.*, *Encyclopedia of Medical Devices and Instrumentation*, 2nd ed., edited by Webster J. G., London, U.K.: John Wiley & Sons, 2006.
- [98] Rushton. D.N., "Functional Electrical Stimulation", *Physiol Meas.*, vol 18, no.4, pp. 241–275, November 1997.
- [99] Naples G. G., Mortimer J. T., Scheiner A., and Sweeney J. D., "A spiral nerve cuff electrode for peripheral nerve stimulation," *IEEE Trans. Biomed. Eng.*, vol. 35, no. 11, pp. 905-916, November 19
- [100] Marsolais. E. B., and Kobetic. R., "Implantation techniques and experience with percutaneous intramuscular electrodes in the lower extremities.", *J. Rehab. Res. Dev.*, vol 23, pp.1-8, 1986.
- [101] Haugland M., "A flexible method for fabrication of nerve cuff electrodes," *Proc. IEEE Eng. Med. and Biol. Soc.*, vol. 1, pp. 359-360, November 1996.
- [102] Sahin M., Durand D. M., and Haxhiu M. A., "Whole nerve recordings with the spiral nerve cuff electrode," *Proc. IEEE Eng. Med. and Biol. Soc.*, vol. 1, pp. 372-373, November 1994.
- [103] International Industry Society in Advanced Rehabilitation Technology, "Principles of new technologies", IISART education material, pp. 34, 2015.
- [104] Kallesoe K., Hoffer J. A., Strange K., and Valenzuela I., "Implantable cuff having improved closure," U.S. Patent No. 5.487.756, 1996.
- [105] Kaplan T., and Gray L. J., "Effect of disorder on a fractal model for the ac response of a rough interface," *Phys. Rev. B*, vol. 32, no. 11, pp. 7360-7366, December 1985.
- [106] Nikolic Z. M., Popovic D. B., Stein R. B., and Kenwell Z., "Instrumentation for ENG and EMG recordings in FES systems," *IEEE. Trans. Biomed. Eng.*, vol. 41, no. 7, pp. 703- 706, July 1994.
- [107] Blana. D, Hincapie. J. G, Chadwick. E. K and Kirsch. R. F, "Selection of muscle and nerve-cuff electrodes for neuroprostheses using customizable musculoskeletal model", *J Rehabil Res Dev.*; 50: 395–40, 2013.
- [108] J. Ungar, Ira & Thomas Mortimer, J & Sweeney, James, "Generation of unidirectional propagating action potentials using a monopolar electrode cuff. *Annals of Biomedical Engineering*, vol. 14, pp. 437-450, 1986.
- [109] Triantis I. F., "An adaptive amplifier for cuff imbalance correction and interference reduction in nerve signal recording," Ph.D. dissertation, Dept. of Electronic and Electrical Eng., University College London, London, U.K.: 2005a.

- [110] Rahal M., Taylor J., and Donaldson N., "The effect of nerve cuff geometry on interference reduction: a study by computer modelling," *IEEE Trans. Biomed. Eng.*, vol. 47, no. 1, pp. 136-138, January 2000a.
- [111] Pflaum C., Riso R. R., and Wiesspeiner G., "Performance of alternative amplifier configurations for tripolar nerve cuff recorded ENG," *Proc. IEEE Eng. Med. and Biol.*, vol. 1, pp. 375-376, 1996.
- [112] Triantis I. F., Demosthenous A., and Donaldson N., "On cuff imbalance and tripolar ENG amplifier configurations," *IEEE Trans. Biomed. Eng.*, vol. 52, no. 2, pp. 314-320, February 2005b.
- [113] Triantis I. F., and Demosthenous A., "The effect of interference source proximity on cuff imbalance," *IEEE Trans. Biomed. Eng.*, vol. 53, no. 2, pp. 354-357, February 2006.
- [114] C. Eder, S.S. Zehra, M. Zamani and A. Demosthenous, "Suitable compensation circuits for on-chip interference reduction in neural tripolar recordings," 2013 IEEE 20th International Conference on Electronics, Circuits, and Systems (ICECS), pp. 241-244, December 2013.
- [115] Rahal M., Winter J., Taylor J., and Donaldson N., "An improved configuration for the reduction of EMG in electrode cuff recordings: a theoretical approach," *IEEE Trans. Biomed. Eng.*, vol. 47, no. 9, pp. 1281-1284, September 2000b.
- [116] Rahal M., "Optimisation of nerve cuff electrode recordings for functional electrical stimulation applications," Ph.D. dissertation, Dept. of Electronic and Electrical Eng., University College London, London, U.K.: 2000c.
- [117] Pachnis I., Demosthenous A., and Rahal M., "Adaptive EMG neutralization using the modified QT," *IEEE Proc. ISCAS*, pp. 2941-2944, May 2008.
- [118] Demosthenous A., Taylor J., Triantis I. F., Rieger R., and Donaldson N., "Design of an adaptive interference reduction system for nerve-cuff electrode recording," *IEEE Trans. Circuits Syst. I: Fundamental Theory and Applications*, vol. 51, no. 4, pp. 629- 639, April 2004.
- [119] Demosthenous A., and Triantis I. F., "An adaptive ENG amplifier for tripolar cuff electrodes," *IEEE JSSC*, vol. 40, no. 2, pp. 412-421, February 2005.
- [120] Akay. M, "Handbook of neural engineering", Chapter 34, pp. 560-564, Institute of electrical and electronics engineer, Inc., 2007.
- [121] Triantis I. F., Demosthenous A., Donaldson N., and Struijk J. J., "Experimental assessment of imbalance conditions in a tripolar cuff for ENG recordings," *Proc. IEEE Eng. Med. and Biol.*, pp. 380-383, March 2003.
- [122] Cirmirakis D., Demosthenous A., and Donaldson N., "Comparison of methods for interference neutralisation in tripolar nerve recording cuffs," *IEEE Proc. ISCAS*, pp. 3465-3468, August 2010. Craggs M., and McFarlane J., "Physiological society symposium: the physiology and pathophysiology of the lower urinary tract," *Exper. Physiol.*, vol. 84, pp. 149-160, 1999.
- [123] Riso. R, Pflaum. C, "Performance of alternative amplifier configurations for tripolar nerve cuff recorded ENG", presented at the Proc. IEEE-EMBS Annu. Meeting, Amsterdam, The Netherlands, Oct. 31-Nov. 4, 1996.

- [124] Pflaum C., Riso R. R., and Wiesspeiner G., "An improved nerve cuff recording configuration for FES feedback control system that utilise natural sensors," Proc. IFESS, pp. 407–410, 1995.
- [125] Upshaw B., and Sinkjaer T., "Digital signal processing algorithms for the detection of afferent nerve activity recorded from cuff electrodes," IEEE Trans. Rehab. Eng., vol. 6, no. 2, pp. 172-181, June 1998.
- [126] Demosthenous A., Jiang D., Pachnis I., Liu X., Rahal M., and Donaldson N., "A programmable ENG amplifier with passive EMG neutralization for FES applications," IEEE Proc. ISCAS, pp. 1552-1555, May 2008.
- [127] Andreasen. L. N, Struijk. J. J, "Signal strength versus cuff length in nerve cuff electrode recordings", IEEE Trans. Biomed. Eng., vol. 49, no. 9, pp. 1045-1050, September 2002.
- [128] Rajagopalan V., Cruz A.-V., and Popovic D. B., "Control of functional electrical stimulation for walking and standing of hemiplegics," IEEE EUROCON, vol. 1, pp. 48-51, November 2005. Rammelt U., and Reinhard G., "On the applicability of a constant phase element (CPE) to the estimation of roughness of solid metal electrodes," Electrochimica Acta, vol. 35, no. 6, pp. 1045-1049, 1990.
- [129] Andreasen. L. N, Jensen. W, Veltink. P. H and Struijk. J. J, "Natural Sensory Feedback for Control of Standing", 18th Ann. Int. Conf. of the IEEE Eng. in Med. and Biol. Soc., 1996.
- [130] Andreasen L. N. S., Struijk J. J., and Lawrence S., "Measurement of the performance of nerve cuff electrodes for recording," Med. and Biol. Eng. and Comput., vol. 38, pp. 447-453, 2000.
- [131] Andreasen L. N. S., Struijk J. J., and Haugland M., "An artificial nerve fiber for evaluation of nerve cuff electrodes," Proc. IEEE Eng. Med. and Biol., vol. 5, pp. 1997- 1999, 1997.
- [132] Mirtaheri, P., Grimnes, S., and Martinsen, G., "Electrode Polarization Impedance in Weak NaCl Aqueous Solutions", IEEE transactions on Biomedical Engineering, vol. 52, no. 12, pp. 2093-2099, Dec. 2005.
- [133] Geddes, L. A., da Costa, C. P. and Wise, G., "The impedance of stainless-steel electrodes.", Medical and Biological Engineering and Computing, vol. 9, no. 5, pp. 511-521, 1971.
- [134] D. Jaron, S. A. Briller, H. P. Schwan and D. B. Geselowitz, "Nonlinearity of Cardiac Pacemaker Electrodes," in IEEE Transactions on Biomedical Engineering, vol. BME-16, no. 2, pp. 132-138, April 1969.
- [135] Ragheb, T. and Geddes, L. A., "The polarization impedance of common electrode metals operated at low current density.", Annals of Biomedical Engineering., vol. 19, no.2, pp. 151-163, March 1991.
- [136] Merrill, D.R., Bikson, M., and Jefferys, J. G. R., "Electrical stimulation of excitable tissue: design of efficacious and safe protocols.", Journal of Neuroscience Methods, vol. 14, no.2, pp. 171-198, 2005.
- [137] Helmholtz. V, "Ueber einige gesetze der vertheilung elektrischer strome in korperlichen leitern mit anwendung auf die thierischelektrischen versuche", Ann Phys., vol .89, pp. 211–33, 1853.

- [138] Guoy G., "Constitution of the electric charge at the surface of an electrolyte." *J Physique*, vol. 9, pp. 457–67, 1910.
- [139] Chapman, D.L., "A contribution to the theory of electrocapillarity.", *Philos Mag*, vol.25, pp. 475-481, 1913.
- [140] Stern O., "Zur theorie der elektrolytischen doppelschicht.", *Z Elektrochem*, vol. 30, pp.508–516., 1924.
- [141] Grahame, D.C., "The electrical double layer and the theory of electrocapillarity.", *Chem Rev.*, vol. 41, pp. 441-501, 1947.
- [142] Pollak V., "An equivalent diagram for the interface impedance of metal needle electrodes," *Med. and Biol. Eng.*, vol. 12, no. 4, pp. 454-459, July 1974a.
- [143] McAdams E. T., and Jossinet J., "Tissue impedance: a historical overview," *Physiol. Meas.*, vol. 16, pp. A1-A13, 1995a.
- [144] Pollak. V., "Computation of the impedance characteristic of metal electrodes for biological investigations", *Med and Biol. Eng.*, pp. 460-464, July 1974.
- [145] Scheider. W., "Theory of the frequency dispersion of electrode polarization. Topology of networks with fractional power frequency dependence, " *J. Phys. Chem.*, vol. 79, no. 2, pp. 127-136, January 1975.
- [146] Freeborn, Todd & Maundy, Brent & Elwakil, Ahmed, "Numerical extraction of Cole-Cole impedance parameters from step response. Nonlinear Theory and Its Applications.", *IEICE*, vol. 2, pp. 548-561, 2011.
- [147] E. Warburg, "Ueber das Verhalten sogenannter unpolarisbarer Elektroden gegen Wechselstrom," *Annalen der Physik und Chemie*, vol. 67, pp. 493–499, 1899.
- [148] J. E. B. Randles, "Kinetics of rapid electrode reactions," *Discussions Faraday Soc.*, vol. 1, pp. 11–19, 1947.
- [149] Onaral B., and Schwan H. P., "Linear and nonlinear properties of platinum electrode polarisation. Part 1: frequency dependence at very low frequencies," *Med. and Biol. Eng. & Comp.*, vol. 20, pp. 299-306, May 1982.
- [150] Pachnis I, "Neutralisation of myoelectric interference from recorded nerve signals using models of the electrode impedance", PhD thesis, Department of electronic & electrical engineering, UCL, 2010.
- [151] Pachnis I., Demosthenous A., and Donaldson N., "Realization of constant phase element in metallic electrodes for interference reduction in neural recording tripoles," *IFMBE Proceedings 25/IX WC*, pp. 353-357, September 2009b.
- [152] Roy S. C. D., and Sheno B. A., "Distributed and lumped RC realization of a constant argument impedance," *J. Franklin Inst.*, vol. 282, no. 5, pp. 318-329, November 1966.
- [153] Pajkossy T., "Impedance of rough capacitive electrodes," *J. Electroanal. Chem.*, vol. 364, pp. 111-125, 1994.

- [154] Wang J. C., "Realizations of generalized Warburg impedance with RC ladder networks and transmission lines," *J. Electrochem. Soc.*, vol. 134, no. 8, pp. 1915-1920, August 1987.
- [155] Hsu C. H., Mansfeld. F., "Concerning the conversion of the constant phase element parameter Y_0 into a capacitance," *Corrosion*, vol. 57, no. 9, pp. 747-748, 2001.
- [156] Franks W., Schenker I., Schmutz P., and Hierlemann A., "Impedance characterization and modeling of electrodes for biomedical applications," *IEEE Trans. Biomed. Eng.*, vol. 52, no. 7, pp. 1295-1302, July 2005.
- [157] Donaldson N. de N., Zhou L., Perkins T. A., Munih M., Haugland M., and Sinkjaer T., "Implantable telemeter for long-term electroneurographic recordings in animals and humans," *Med. Biol. Eng. Comput.*, vol. 41, no. 6, pp. 654-664, 2003.
- [158] Zehra S and Demosthenous A., "Simple Compensation Circuits Realisation for Interference Reduction in the Entire Band of Neural Tripolar Recordings," *IEEE 37th Annual International Conference of Engineering in Medicine and Biology Society EMBC*, August 2015.
- [159] Polasek. K. H, Hoyen. H. A, Keith. M. W, Tyler. D. J, "Stimulation stability and selectivity of chronically implanted multicontact nerve cuff electrodes in the human upper extremity", Vol. 17, no. 5, Oct. 2009.
- [160] A. Demosthenous, I. Pachnis, D. Jiang and N. Donaldson, "An Integrated Amplifier With Passive Neutralization of Myoelectric Interference From Neural Recording Tripoles," in *IEEE Sensors Journal*, vol. 13, no. 9, pp. 3236-3248, Sept. 2013.
- [161] P. Kassanos, I. F. Triantis and A. Demosthenous, "A CMOS Magnitude/Phase Measurement Chip for Impedance Spectroscopy," in *IEEE Sensors Journal*, vol. 13, no. 6, pp. 2229-2236, June 2013.
- [162] Kotnik. T, Kramar. P, Pucihar. G, Miklavcic. D and Tarek. M, "Cell membrane electroporation- Part 1: The phenomenon," in *IEEE Electrical Insulation Magazine*, vol. 28, no. 5, pp. 14-23, September-October 2012.
- [163] C. Eder, S.S. Zehra, M. Zamani and A. Demosthenous, "Suitable compensation circuits for on-chip interference reduction in neural tripolar recordings," *2013 IEEE 20th International Conference on Electronics, Circuits, and Systems (ICECS)*, pp. 241-244, December 2013.
- [164] DeCarlo R. A., and Lin P.-M., Ch. 10, *Linear Circuit Analysis: Time Domain, Phasor, and Laplace Transform Approaches*, 2nd ed. Oxford, U.K.: Oxford University Press, 2001.
- [165] Grimnes, Sverre, Martinson, Orjan Grottem, "Bioimpedance and bioelectricity basics, s.1.: Academic Press, 2000.
- [166] Duck F. A., *Physical Properties of Tissue – A Comprehensive Reference Book*, London, U.K.: Academic Press, 1990.
- [167] Pachnis I., Demosthenous A., and Donaldson N., "Interference reduction techniques in neural recording tripoles: an overview," *IEEE Proc. PRIME*, pp. 332-335, July 2009a.
- [168] S.C. Dutta Roy, "Constant argument immittance realization by a distributed rc network.", *IEEE Trans Circuits Syst*, vol. CAS-21, no.5, pp. 655-658, 1974.
- [169] Sedra A. S., and Smith K. C., *Microelectronic Circuits*, 3rd ed., London, U.K.: Saunders College Publishing, 1991.

